AD-A112 114 MICHIGAN UNIV ANN ARBOR COOLEY ELECTRONICS LAB F/G 9/3
PN MATCHED FILTERS IN ADAPTIVE ARRAYS.(U)
SEP 81 M P RISTENBATT, T G BIRDSALL DAAG29-79-C-0220
UNCLASSIFIED 017818-F ARO-17104.1-A-EL NL

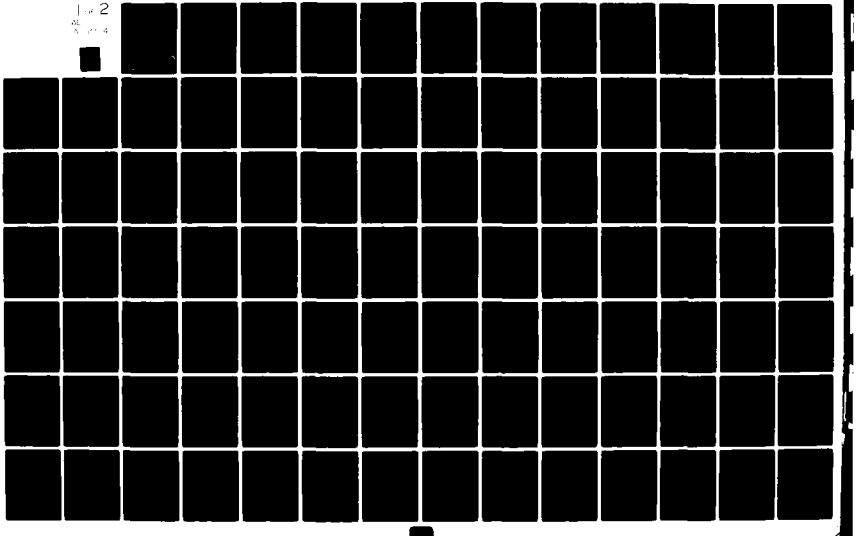

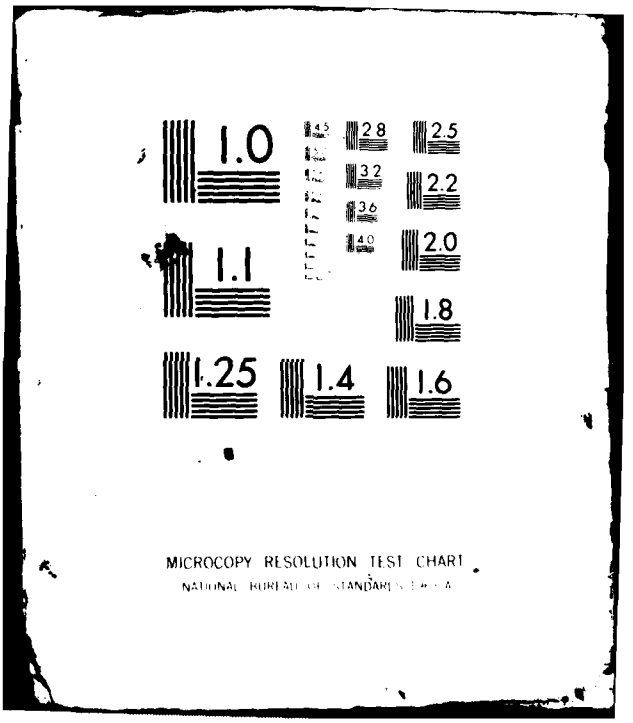
1.0
1.1
1.25
1.4
1.6
2.8
3.2
3.6
4.0
2.5
2.2
2.0
1.8
MICROCOPY RESOLUTION TEST CHART

PN MATCHED FILTERS IN ADAPTIVE ARRAYS

Final Report

M. P. Ristenbatt
T. G. Birdsall
E. Holland-Moritz

September 1981

U. S. Army Research Office
and
U. S. Army Combat Surveillance and
Target Acquisition Laboratory, DELC-I

DAAG29-79-C-0220

Cooley Electronics Laboratory
Department of Electrical and Computer Engineering
The University of Michigan
Ann Arbor, Michigan 48109

Approved for Public Release;
Distribution Unlimited.

The view, opinions, and/or findings contained in this report are those of the authors and should not be contrued as an official Department of the Army position, policy, or desision, unless so designated by other documentation.

Abstract and Summary

This report describes and evaluates a new way to combine the two interference-resistant techniques of pseudo-noise (PN) spread spectrum and adaptive (antenna) arrays. Each element in the array feeds a separate PN matched filter, and the sampled-matrix-inversion (SMI) algorithm is used on the matched-filter outputs, along with multiple steering vectors corresponding to apriori beams. The SMI calculation is done on a sliding-window basis, where the noise covariance matrix is estimated using matched filter output samples that precede the "current-sample," and the resulting multiple optimum weights, computed by matrix inversion multiplied by the multiple steering vectors, are applied to the current sample. The number of samples used in the covariance matrix estimation is at least twice the number of antenna elements.

The evaluation of this PN matched filter plus adaptive array technique was done by using a 4-element linear array and: 1) straightforward matrix calculations; 2) a computer computation of output signal-to-noise ratio; SNR_o, versus angle when the theoretically correct noise covariance matrix was used; and 3) a computer simulation/demonstration that estimated the noise covariance matrix from computer-generated interference samples.

It was found that, as expected, the separation of interference-only samples from interference-plus-signal samples,

afforded by the pulse-compression nature of the matched filter, permits full combined processing gain (PN plus adaptive array) from the outset, in the acquisition mode. We confirmed that the noise covariance matrix estimate requires using only sample sizes on the order of twice the number of elements for 3 db loss from optimum.

We used, as a theoretical performance measure, the output SNR_o as a function of angle, assuming the steering vector points in the direction of the "current angle." Realizing this performance in practice would require a (slightly) different steering vector for each (say) degree. In the effort here we demonstrate that one need only use about 4 steering vectors to achieve near-optimum SNR_o for the entire range of angles.

Thus, a near-optimum combined processing has been effected which can be viewed as sliding-window in both the time axis and in the spatial domain (due to the multiple steering vectors). The theoretical computer computations, which used the ideal covariance matrix, were used to portray SNR_o versus angle for a variety of single and multiple interferer conditions, for a single signal. The computer simulation/demonstration documented the performance for two single-interferer examples, and one two-interferer example.

These results indicate that using the method evolved here, along with the 4 parallel steering vectors, may likely be the best way to combine PN waveform processing and adaptive array processing. The advantages are: 1) the combination does not

initially (before sync) attempt to null the signal, but offers immediately the full combined processing gain; 2) the response to either signal turn-on or interferer variation is near instantaneous, and does not depend on loop time-constants; 3) there is no constraining relation between interferer size and time-response, as there is for a closed-loop system, and 4) there is no "great race" problem between modem synchronization and array nulling, as there is when a PN reference is used in a closed-loop; and 5) the technique here should be more resistant to specific and determined interferer attacks (such as blinking). It is recommended that this method be further pursued, to further develop and document its advantages.

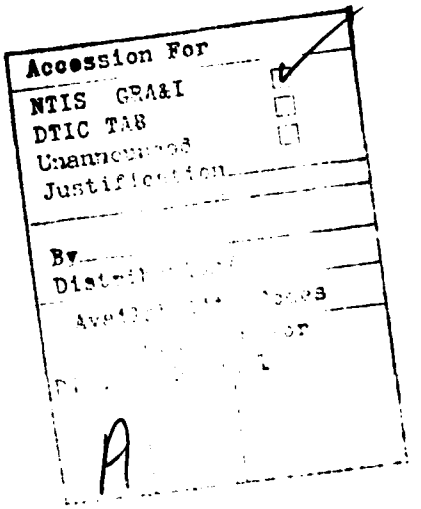

Foreward

The authors wish to acknowledge the technical conversations with Steven Bleier of the U. S. Army Combat Surveillance and Target Acquisition Laboratory, and John Graniero of the Air Force Rome Air Development Center (RADC).

Also, the extensive software for the simulation/demonstration described in Sec. 6 was written by Shang-Min Juang. We appreciate his dedicated efforts in supporting this work.

TABLE OF CONTENTS

LIST OF ILLUSTRATIONS

LIST OF ILLUSTRATIONS (Cont.)

LIST OF ILLUSTRATIONS (Cont.)

LIST OF ILLUSTRATIONS (Cont.)

LIST OF ILLUSTRATIONS (Cont.)

LIST OF ILLUSTRATIONS (Cont.)

LIST OF ILLUSTRATIONS (Cont.)

LIST OF ILLUSTRATIONS (Cont.)

PN MATCHED FILTERS IN ADAPTIVE ARRAYS

1. Introduction

The overall objective in this effort is to achieve more effective and robust arrangements for combining spread spectrum and spatial processing gain in ECCM communication systems. We assume here that the spread spectrum is pseudo-noise (PN), and investigate the potential of using identical PN matched filters at each antenna element, followed by a spatial nulling algorithm. Thus, a significant feature of the approach here is that the waveform processing, and hence, temporal processing gain, precede the spatial processing. The spatial processing most suitable for this approach is some form of direct matrix inversion; we have used the straight-forward sampled matrix inversion (SMI) for this effort.

2. Background

Two techniques for providing interference[1]-resistant communications against either unintentional or intentional interference are spectrum spreading and antenna gain. The antenna gain here refers to the gain in the desired-signal direction viz-a-viz the gain in the interferer direction. In many communication applications either the terminals themselves

---

1. Interference refers to any man-made electro-magnetic signal, as distinguished from nature's ubiquitous Gaussian noise (WGN). It is any signal from a point source (plane wave) which is not correlated with the desired PN signal.

or the interferers move in physical space in an unpredictable manner, so that the antenna gain must be adaptive, using adaptive arrays.

The essential idea in spectrum-spreading is to disperse the intended signal over a frequency-space that is large relative to that required by the information data rate, which permits a temporal signal processing advantage against any interference (jamming or RFI) that is subject to electronic amplification limitations[1] and is not correlated with the PN signal. The adaptive array reduces the antenna gain in the direction of the interference in such a way as to maximize the SNR for the desired signal.

Past interference-resistant communications have usually used spread-spectrum (utilizing waveform or temporal processing). More recently, adaptive antenna techniques (utilizing spatial processing) have been combined with spread spectrum to provide increased, and more robust, interference-resistance. Combining the two techniques offers the potential of realizing the sum (in db) of the two processing gains against either the intentional or unintentional interferences.

If frequency-hopping (FH) is the spread-spectrum technique, then the antenna array is "adapted" in a step-by-step fashion, slightly ahead of the frequency-hop path. If pseudo-noise (PN) is the spread spectrum technique, then the

---

1. There is no temporal processing gain against white Gaussion noise (WGN), such as receiver noise, because the noise is already present at all frequencies. Increasing signal bandwidth then also increases the total noise received in the signal bandwidth. Any interference subject to electronic amplication is limited by the power dissipation capability of electronic devices; in this case the total interference from any given source is fixed. Increasing signal bandwidth then allows the intended receiver to reject a longer fraction of the interference power from such a source.

antenna is adapted on either a time-continuous or a sampled basis corresponding to the symbol rate of the digital transmission.

The fundamental operations of an adaptive antenna (alone) are depicted in Fig. 1. Signals received in each

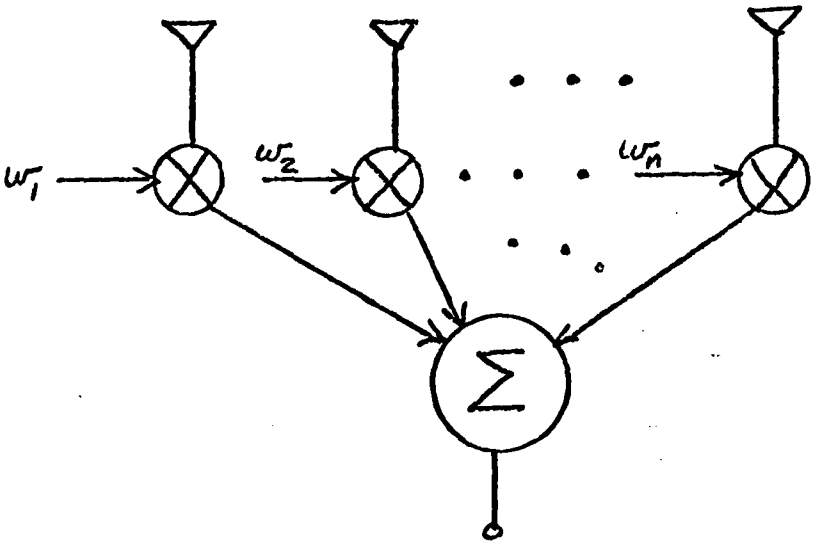

Figure 1. Generic Adaptive Array

element channel are weighted by a complex coefficient and summed together to form the output of the array. Temporarily assume that only interference[1] sources are present, so that any ensuing receiver deals with directional interference power (which is to be nulled) plus ordinary receiver thermal noise. It is useful to describe the desired element weighting (complex) vector in terms of the "covariance matrix" of the impinging noise and interfering signals, plus a possible steering-vector.

---

1. Although many adaptive arrays are intended to operate against jammers, the algorithms adapted work equally-well against unintentional interference that may be present, including other friendly users. Therefore, we will use the general term interference, rather than jammer, throughout this report.

It is the intent of the covariance matrix to describe in systematic form all of the information about the interference environment (see Ref. 1.) Let the covariance matrix M have elements (m_{kl})

$$M = (m_{kl}) \tag{1}$$

The element value, m_{kl}, is the expected value of the product of the (complex envelope representation) noise received (jamming plus receiver noise) by the kth and lth antenna elements:

$$m_{kl} = E(m_k^* m_l) \tag{2}$$

This implements the definition of covariance (see any communications textbook), and physically represents the crosspower in the envelopes of the two interference signals. Thus, m_{kl} is the cross-power in the envelopes of antenna elements k and element l. These element values clearly contain directional interference information since any RF delay-pattern set up by the point-source and antenna array configuration determine the averaged cross-product of each element-pair. In these terms, a weight-vector which will theoretically yield the best signal-to-interference ratio for a single (desired) signal case is given by:

$$MW = \mu S^* \tag{3}$$

where: M = covariance matrix of the interference

μ = arbitrary nonzero complex constant

S^* = complex conjugate of the desired-signal vector (from the array), i.e., a steering vector.

W = complex weight vector

For radar cases, the S vector for electronically-steered arrays is essentially a beam-steering-vector. For communication cases, where the direction of the desired signal is not known a priori, the S vector may either correspond to an omnidirectional pattern, or to a hypothesized desired signal direction. In either case, the optimum weight vector can be written as:[1]

$$W = \mu M^{-1} S^* \tag{4}$$

It is useful to describe any adaptive antenna processing in terms of its handling of the matrix-inversion contained in Eq. 4. It is fundamental to distinguish between open-loop and closed-loop implementation approaches, which are depicted in Fig. 2. Two basic approaches are: 1) implement Eq. 4 directly by sampling the observed M matrix, and inverting the observed matrix (shown in Fig. 2(a)); 2) form a servomechanism-like closed loop, and use a processing-algorithm in that loop (shown in Fig. 2(b)).

The open-loop technique is called sampled-matrix inversion (SMI), and is, of course, a digital processing technique. This method, since it is open-loop, requires relatively high arithmetic precision to obtain good results. To obtain an accurate estimate of the covariance matrix, it has been found (Ref. 9) that at least 2K such sample matrices should be calculated and averaged for the estimated covariance matrix.[2] (K is the number of elements.) Also, the covariance samples should be obtained when no desired signals

1. M^{-1} is the inverse of M. It will exist if ambient noise is present. It is often close to singular with strong interferen
2. This assumes a known steering vector. In actual operation a somewhat larger number of samples may be needed (Ref. 11).

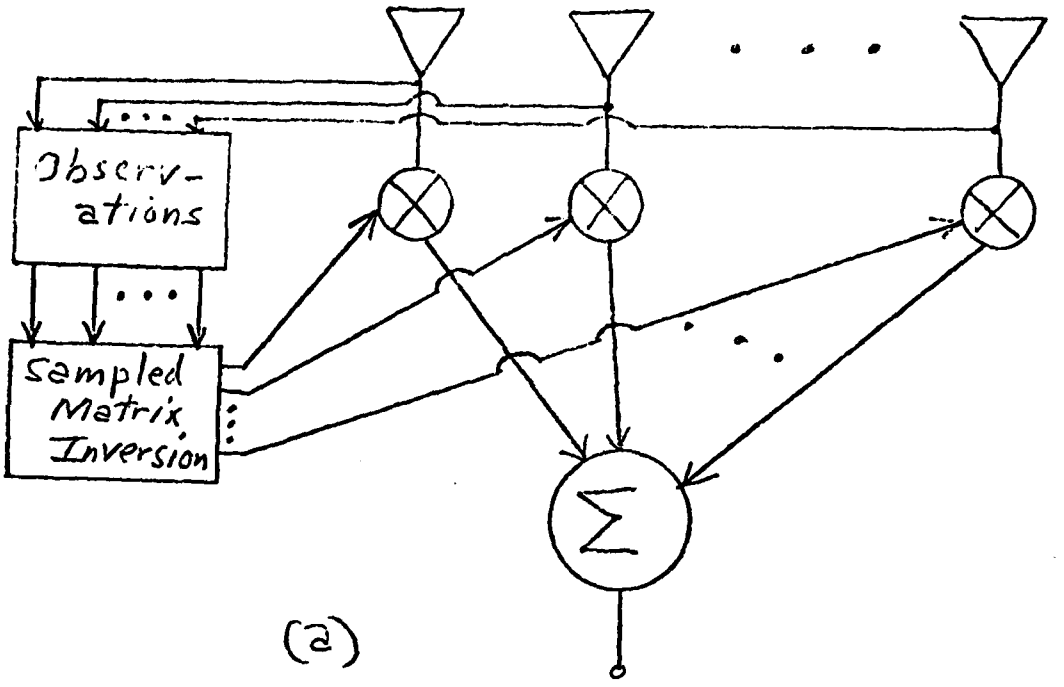

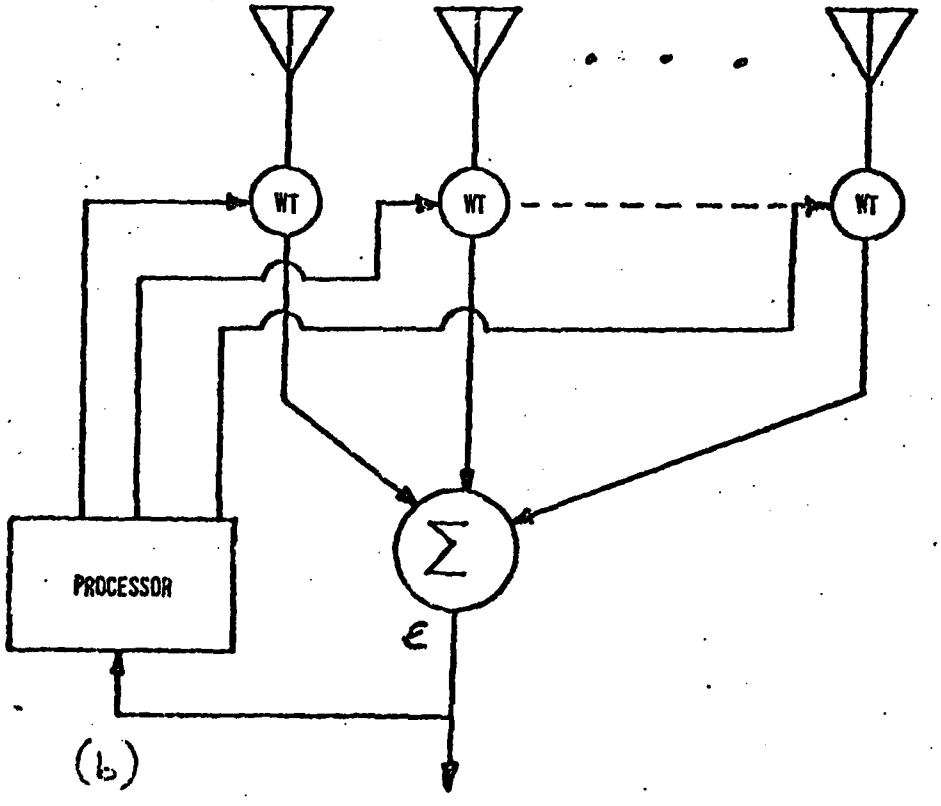

Fig. 2. Adaptive Receiving Antennas: a) open-loop; b) closed-loop

are present. Otherwise the array gain in the desired signal directions will also be reduced.

The advantages of the algorithm are: (1) It gives a clearly specified algorithm which is optimal for any assumed noise environment; (2) the response to a change in noise environment can be very fast. The fundamental limitation in response time is the time required to obtain the independent samples for the covariance matrix.

The closed-loop (servo-like) arrangement in Fig. 2(b) has been popular in radar work, and has been the starting point for communication applications. Such a closed-loop arrangement has the self-adaptive properties inherent in any servo-like loop. It can be shown (Ref. 1) that the feedback rule that maximizes the signal-to-interference ratio is the "least mean square (LMS)" algorithm. In effect, the loop attempts to adapt to the situation where the feedback "error" signal is zero. Physically, the loop attempts to place a (relative) null on every point source in its field of view by adjusting the antenna weights so that the signal output, after combining, is a least-mean-square best fit to a stored copy of the expected signal waveform (zero, if ambient noise is neglected). The stronger the signal, the deeper the null. Such a (loop) antenna continuously adjusts its own pattern by means of feedback as it operates.

It is interesting to note that the asymptotic values of the complex weights, with the LMS algorithm, are exactly the covariance matrix (M) values given in Eq. 4. Thus the

theoretical underpinnings of the open-loop (SMI) and the closed-loop (LMS) are the same. However, their actual implementation, especially when combining with waveform (spread spectrum) processing, and their response to jammers differ substantially (as we shall see). Also we may note that both implementations attempt to "spatially whiten"; that is, reduce gain the direction of point sources so that all directions appear to have a noise level equal to the ambient noise level.

Thus far, the closed-loop version has been pursued when combining PN spread spectrum with adaptive antennas. A procedure of particular interest has been using the "Widrow LMS processor" with a PN signal as the reference signal. Fig. 3 shows a basic arrangement (Ref. 2) where a PN signal forms the reference signal. When the PN code is synchronized, the desired signal part of the array output passes through the code-reference loop without change, but the modem data can be extracted as shown. The first mixer removes the PN code so that the signal will pass through the data bandwidth filter, the limiter fixes the amplitude, and the second mixer puts the code back on. In this way, the PN code prevents the adaptive array from attempting to null the intended signal. Rather, nulls are placed on any interference source which are uncorrelated with the reference signal. Note that the PN modem involved is of the active-correlator type. In Ref. 3 the same basic technique is used except that now multiple delays are used with each antenna element so as to implement better wideband null steering.

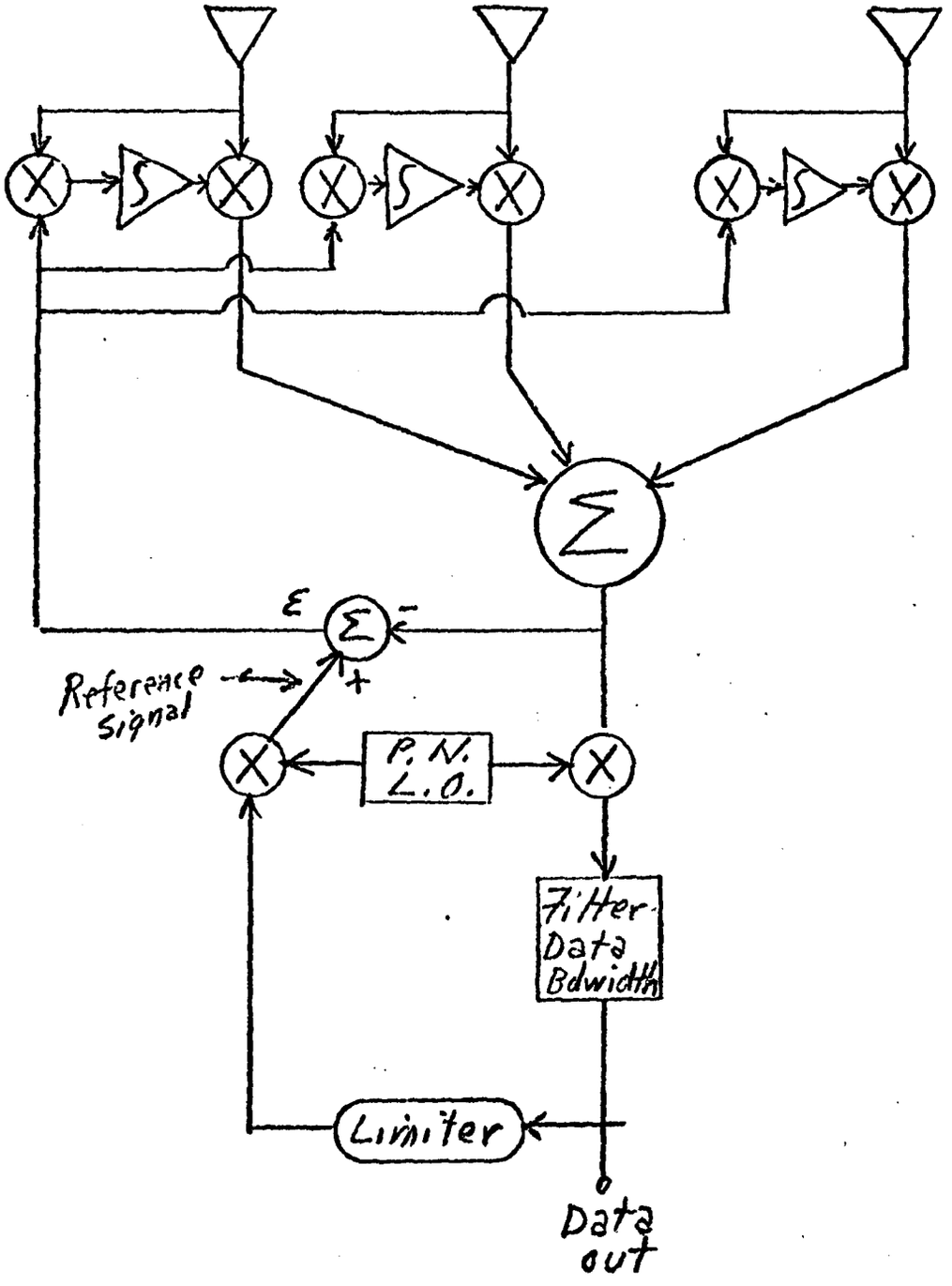

Fig. 3. Closed-Loop Processor for PN, Using LMS Processor

Two significant aspects of the arrangement in Fig. 3 are: 1) the spatial processing precedes the waveform of temporal (spread spectrum) processing; and 2) the architecture is that of a closed loop, with the PN modem arranged to form the "known signal" reference for the loop so that the intended signal is not nulled.

An alternative to the closed-loop approach of Fig. 3 was suggested in Ref. 4, and uses an active PN correlator ahead of the adaptive array processing, as depicted in Fig. 4. This arrangement, in its basic form, is an open-loop technique and hence suggests the use of direct Sampled Matrix Inversion (SMI). As noted, significant aspects of any such open-loop technique are: 1) it is inherently digital, requiring both sampling and quantizing; 2) it can react instantaneously as opposed to exhibiting a transient response.

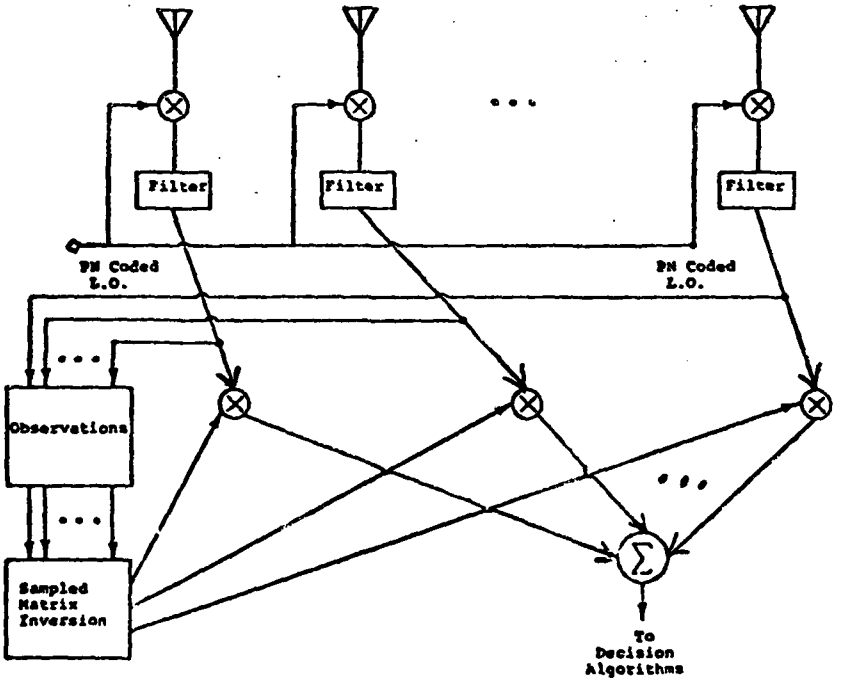

Fig. 4. Open loop PN technique using Direct Samples Matrix Inversion

A recent report[1] (Ref. 5) includes a steady-state investigation of the arrangement shown in Fig. 4, and uses the descriptive terms "code-stripping" to describe this arrangement. We will discuss this further in the next section.

In Ref. 6 the SMI algorithm is evaluated for use with a frequency-hopping spread spectrum temporal processing. In that case the receiver can estimate the noise covariance matrix one step ahead of the frequency-hopping pattern, and apply the calculated weights of the signal-present subsequent interval. As noted, the interest here is in cases where PN is the spread spectrum technique.

3. PN Matched Filters Preceding SMI Array Processing

In Ref. 7 we proposed using PN matched filters at each antenna element, and envisaged using multiple (time-delayed) samples at the output of each matched filter to feed a (then as yet) undetermined null-forming and beam-forming processing. In the early stages of this effort we realized that direct SMI was an appropriate spatial processing for processing samples of the matched filter outputs.

A filter matched to a maximal length (see Ref. 8) PN sequence has the unique feature that, assuming that two full periods of the sequence are transmitted,[2] the output exhibits ideal "pulse compression." That is, all the energy from a single period of the received (noiseless) sequence appears at a single peak, and the preceding samples values

---

1. The work reported in Ref. 5 was conducted during the same period as the work of this report.
2. One can avoid the need for 2 periods, using specially-constructed matched filters. This implementation aspect is beyond the scope of this study.

(at independent times) can be arranged to be zero. The idealized time description of sampled values of the matched filter output, assuming no noise is present, is sketched in Fig. 5. Note that if the phase modulation used is slightly less than 180°, the signal output will be exactly zero between signal peaks.

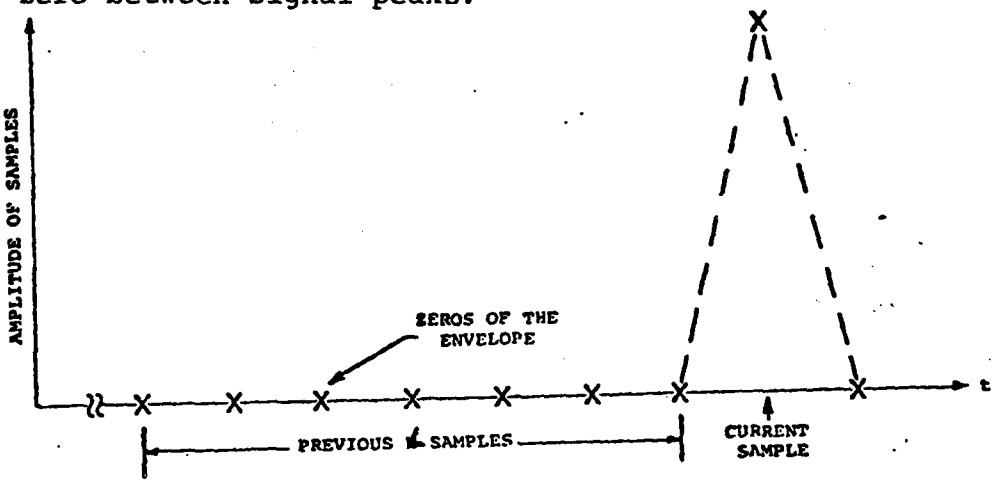

Fig. 5. Sampled Envelope Values of Signal Autocorrelation

This pulse compression feature of the K matched filter suggests that the SMI algorithm is sensibly applied to the K matched filter outputs in the following way. Assume momentarily that the (signal) matched position is the "current sample" value. Then the immediately preceding (to the left) independent samples must contain noise-only. About 2K preceding samples from each of the K matched filter outputs are used to estimate the noise covariance matrix. The optimum weights are computed by inverting this matrix and multiplying by an apriori beam steering vector, to be described. These K complex values are then used to weight the K "current-sample" values. The process just described can be operated in a sliding-window

fashion, so that this procedure is suitable for the acquisition mode, where the filter "matched position" is not known apriori but must be determined by an ensuing threshold-crossing algorithm.

The significant point to be made here is that the pulse compression nature of the matched filter output permits separating signal plus noise samples from noise-only samples, while still allowing use of a continuous signal. Furthermore, the noise samples used are a subset of those that occured during the signal-epoch corresponding to the matched filter length.

Thus the algorithm pursued in this effort is pictured schematically in Fig. 6. In addition to using a sliding-window in the time axis (or temporal domain), we use an equivalent feature in the spatial domain consisting of using multiple apriori beams (or steering vectors). These apriori beams mean that, in the absence of any point-source interferers, multiple beams will be formed with the multiple elements of the array. The number and orientation of such beams are decided in advance, and do not vary with the interference scenario. When combined with adaptive processing, the use of multiple apriori beams amounts to performing multiple weight-calculations, which results in multiple output time-tracks. That particular processing which has a beam placed in the general direction of the intended signal should experience the highest spatial processing gain, from among the multiple processsings.

Thus, with the understanding that the samples used for the covariance matrix are separate from the samples to

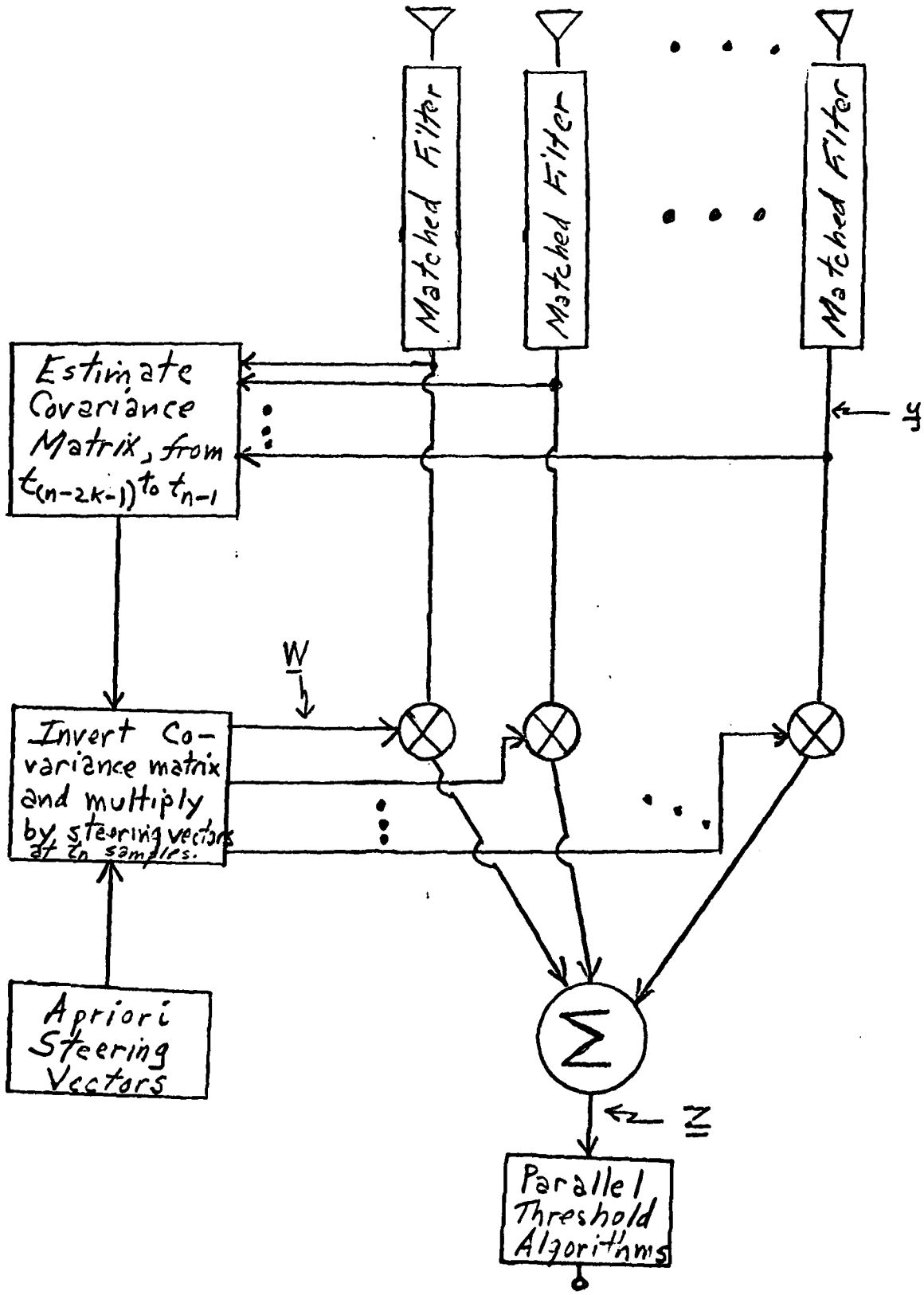

Fig. 6. PN Matched Filters followed by SMI.

which the computed weights are applied, we can write:

$$\underline{W}_{\ell} = (\hat{M})^{-1} S^{*}_{k\ell} \tag{5}$$

where: $\underline{W}_{\ell}$ = the estimated optimum weight vector for the ℓth apriori-beam
$\hat{M}$ = K by K covariance matrix, estimated by 2K samples from $\underline{t}_{n-1}$ to $\underline{t}_{n-2K-1}$
$S^{*}_{k\ell}$ = a K by ℓ matrix that represents ℓ different apriori beams or "beamformers."

If one multiplies the current samples, $\underline{t}_n$, by the ℓ weight vectors, one obtains ℓ outputs, $\underline{Z}_{\ell}$, which is a vector having one element for each apriori beam:

$$\underline{Z}_{\ell} = \underline{Y}\underline{W}_{\ell} \tag{6}$$

where: $\underline{Z}_{\ell}$ = ℓ^{th} output of SMI processing
$\underline{Y}$ = output of K matched filters

4. Theoretical Performance Evaluation

Here we assume a linear array of K elements, with element spacings d, as sketched in Fig. 7.

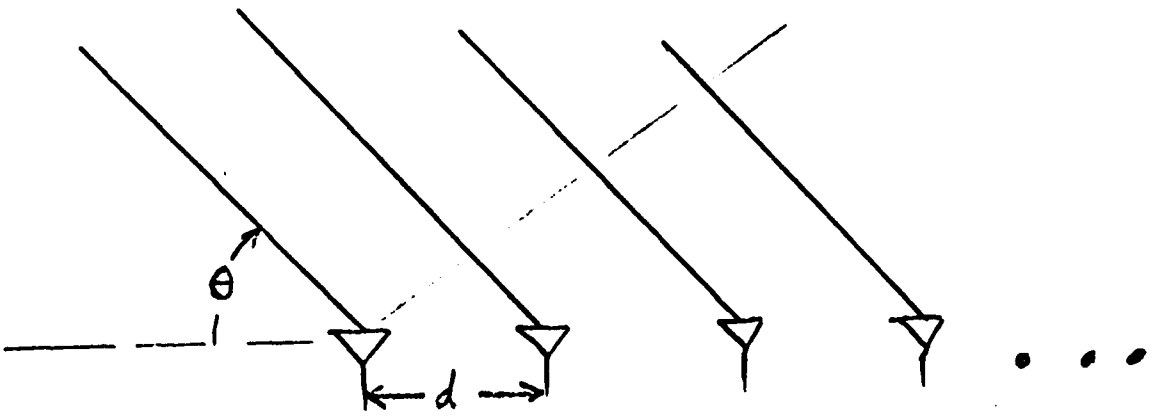

Fig. 7. Linear Array of K Elements.

4.1 Array Performance Measure

To begin, we consider only one interferer, at electrical angle θ'. The array performance measure used here is the output signal to noise ratio when the beamformer is pointed in the direction of the unit signal, at angle θ'. We normalize so that the total received ambient noise is 1.

With the single interferer, a normalized theoretical covariance matrix can be shown (see App. A) to be:

$$M = N_a I + N_I R_\theta \tag{7}$$

where: N_a = ambient (mean-square) power per antenna element.
I = identity matrix
N_I = interference (mean square) power per antenna element.

$$R_\theta = V_\theta V_\theta^{*T} = \frac{1}{K} \left| e^{j(\text{Row}-\text{Col})\theta} \right|$$

$$V_\theta = \frac{1}{\sqrt{K}} \begin{vmatrix} 1 \\ e^{-j\theta} \\ e^{-2j\theta} \\ \vdots \\ e^{-(K-1)j\theta} \end{vmatrix}$$

$\theta = \frac{2\pi f d}{c} \cos\alpha'$ = electrical phase shift in radians between elements separated by a distance d, for a plane wave arriving at an angle α' degrees with respect to the line of the array.

Then the inverted covariance matrix is:

$$M^{-1} = \frac{1}{N_a}\left(I - \frac{N_I}{N_a + N_I} R_\theta \right) \tag{7a}$$

It is germane to ask what interferer bandwidth implications arise from writing the receiver voltage vector, V_θ, in terms of a plane-wave at a given RF frequency. This technique essentially assumes that the envelope of the

arriving interference is the same, for all elements of the array. This will certainly be true for any narrowband interferer, and will be approximately true for random PN-coded interferers and Gaussian matched-spectrum interferers. In the following, we will be implying that the interferers are either random-coded PN or Gaussian matched-spectrum.

Note that a random-coded PN interference signal can be treated, for many purposes, as approximately a piecewise CW signal, since, for the vast majority of the time axis, each element in the array is seeing the same "chip."

From classical theory (see App. A), and using the above-described procedure for forming multiple weights by using multiple steering vectors, the weights for a steering angle, θ', are:

$$W_{\theta'} = (M^{-1})\ V_{\theta'} \tag{8}$$

where: $W_{\theta'}$ = optimum weights, using an apriori beam in the direction θ'.
$V_{\theta'}$ = same vector as before, except θ' replaces θ

The resulting normalized beam point pattern for a signal from direction ϕ is:

$$W_{\theta}^{*T} V_{\phi} \tag{9}$$

where: $\phi = 2\ f\frac{d}{c} \cos \beta$

β = any physical angle, in degrees, between the signal source and the line of the array.

Since we have chosen to evaluate the performance, in any given direction β, as the magnitude of the beam-pattern when the

apriori beam (steering vector) points in that direction (the $\Theta' = \phi$), the output power due to the signal in that same direction is:

$$P_{o\phi} = M^{-1}V_\phi \; {}^{*T}V_\phi = {}^{*T}V_\phi \, M^{-1} \, {}^{*T}V_\phi = {}^{*T}V_\phi \, M^{-1}V_\phi \qquad (10)$$

where: $P_{o\phi}$ = output power, due to interference, in direction ϕ.

We can now note that the output SNR equals $P_{o\phi}$ since: 1) the output signal power, for electrical direction ϕ, is $P_{o\phi}^2$, and 2) the output noise power for electrical direction ϕ is $P_{o\phi}$. Hence, the on-beam output SNR is simply $P_{o\phi}$.

Equation (10) implies that the noise output power, for a given angle, is not constant, but is a function of the steering direction. To achieve the same SNR gain, but have spatial whitening (which is a superior model concept) one lets:

$$W = \frac{(M^{-1}V_\phi)^*}{P_{o\phi}} = \frac{(M^{-1}V_\phi)^*}{V_\phi^{*T}M^{-1}V_\phi} \qquad (11)$$

Then, let $\underline{Z}$ represent the output:

$$Z = W_\phi^T y \qquad (12)$$

In noise alone:

$$E\{\,|Z|^2\,\} = 1 \qquad (13)$$

for all straight angles,

and in unit signal, on-beam:

$$E\{Z\} = \frac{(M^{-1}V_\phi)^{*T}V_\phi}{P_{o\phi}} = P_{o\phi} \qquad (14)$$

and $$|E(Z)|^2 = P_{o\phi} \qquad (15)$$

This is the output signal for unit input power per element. Since output noise is normalized to 1, it is also the output SNR when the steering vector is in the direction of the desired signal.

In the case of a single interference, in addition to ambient, the $P_{o\phi}$ can be reduced to a single equation (see App. A), and appears as:

$$P_{o\phi} = \frac{1}{N_a} - \frac{N_1}{N_a(N_a+N_1)}\left[\frac{\sin K\pi \frac{fd}{c}(\cos\alpha - \cos\alpha_\tau)}{K \sin \pi \frac{fd}{c}(\cos\alpha - \cos\alpha_\tau)}\right]^2 \quad (16)$$

For a signal power, S, per element and an array of K elements, this becomes:

$$SNR_{out} = K\left(\frac{S}{N_a}\right)\left[1 - \frac{N_{I/S}}{\frac{N_I}{S}+\frac{N_a}{S}}\left[\frac{\sin K\pi \frac{fd}{c}(\cos\alpha - \cos\alpha_\tau)}{K \sin\pi\frac{fd}{c}(\cos\alpha - \cos\alpha_\tau)}\right]^2\right] \quad (17a)$$

where: $\frac{S}{N_a}$ = Received ambient $\frac{S}{N_a}$ per element (omnidirectional)

$\frac{N_I}{S}$ = Received directional interference to signal ratio per antenna element (omnidirectional)

α = angle between line to interference and line of the array[1] in radians

α_τ = angle between line to desired signal and line of the array in radians

The squared term on the right will be recognized as the $sinc^2$ periodic sampling function which is small for all angles except when the denominator is zero. Then $sinc^2 = 1$ and the output

---

1. Note: This differs from the more usual case where angles are measured from the array normal. $\alpha = \frac{\pi}{2} - \gamma$ where γ is the angle from normal.

becomes $SNR_{out} \approx K \frac{S}{N_I+N_a}$. This happens, for example, whenever $\cos\alpha = \cos\alpha_\tau$. One example is when the signal and interference come from the same direction ($\alpha = \alpha_\tau$). The interference is suppressed completely whenever $\sin(K\pi \frac{fd}{c} \cos\alpha - \cos\alpha_\tau) = 0$, while $\sin \pi \frac{fd}{c} (\cos\alpha - \cos\alpha_\tau) \neq 0$. The important feature of the equation is that in practical cases, the interference is almost completely suppressed almost everywhere except in the immediate direction of the interference.

A series of selected examples for this single-interferer case are collected in Ref. 12.

In general, one can note that:

$$M = E(YY^*) = \sum_n |i_n(t)|^2 V(\theta_n) V^*(\theta_n) + N_a I_k \qquad (17)$$

where we have assumed independence of interferers so that all expected values for cross-product terms are zero.

Where: $i_n(t)$ = interference time waveform from n^{th} interferer

$V(\theta_n)$ = voltage vector received, at angle θ_n, from n^{th} interferer

$N_a I_K$ = covariance matrix of ambient noise.

We found no single expression which can relate theoretical SNR performance to angle for the multiple interferer case, so we resorted to using a computer computation, the results of which is now described.

4.2 Theoretical Computer Computations

A computer program, in BASIC language, was written to be run on our own CEL Line 8 minicomputer. The intent of this

program was to find the theoretical predicted results for the algorithm and linear array being used here for general cases, where more than one interferer is present.

Therefore, the theoretical covariance matrix was used; this was formed, after the interferer directions and powers are stated, by deterministrative computation, using the usual trigonometric relations.

The first program, CMAT4, assumes that an infinite number of steering vectors are available, since the SNR versus angle ϕ always assumes that the steering vector is in the direction of the intended signal no matter what signal direction is chosen. A four-element half-wavelength spaced linear array is assumed. The user specifies the power and direction of each directional interference, and the ambient power. The matrix inversion is accomplished by using elementary row operations. The CMAT4 computes the dot-product performance measure for 0 to 180 degrees in 10 degree steps, then allows the user the option of selecting a different signal direction range or stop, or re-cycling for a new interference description.

It must be emphasized that, in the results here, the covariance matrix was not obtained by an estimate using the incoming samples, but rather was formed by initially stating the interferer directions and powers, and then using trigometric plane-wave relations to deterministically find the covariance matrix.

Note that an operational communication system does not know either the noise covariance matrix or the exact direction from which a desired signal is, or will be arriving. It must estimate the covariance matrix from a set of noise samples. It can choose that one of the set of steering vectors which maximizes the SNR for its approximate covariance matrix, but this generally is not exactly the correct steering vector for the actual signal.

In this section, we compute the exact optimum SNR based on the known parameters. In the next sections, we will estimate how close an actual system working with finite numbers of noise samples can come to this optimum performance.

Here we discuss the SNR performance data for numerous examples. In the next section we discuss the antennae power patterns which are obtainable from the programs. The SNR in db is displayed as a function of signal direction for the optimum case where the steering angle is pointed in the signal direction. As noted in Sec. 4.1, the analysis and computation here applies accurately to narrowband interferer cases, and approximately to both random-coded PN and Gaussian spectrum-matched interferers.

On these curves S/N_a is the S/N_a observed at the output of each of the 4 matched PN filters when only ambient noise is present. $N_{I/S}$ is the $N_{I/S}$ observed at the output of each of the matched PN filters. The output $(S/N)_o$ is the actual output signal to noise ratio.

In Fig. 8 the ambient noise at the output of each matched PN filter is assumed to give an ambient $\frac{S}{N_a}$ of 10 db. In the absence of all jammers the performance would be +16 db in all receiving directions, as shown by the dotted line. The presence of a 30 db N_I/S interferer at +45° (measured counter-clockwise from the + x axis), results in the decrease in $\left(\frac{S}{N}\right)_o$ shown for signals near +45°. Since the ambient is much smaller than the interferer, the minium $(S/N)_o$ is essentially that due to the interferer, -30 db. Example: S = 1 Watt N_I = 1 KW N_a = 0.1 Watt. $\frac{S}{N_a+N_I} \approx$ 30 db. The interferer carrier is assumed to be at the desired signal frequency. If the interferer shifts frequency, his angular position will appear to shift. If he shifts very much, part of his signal may fall outside of the signal bandwidth.

In Fig. 9 a second 30 db N_I interferer is added at +120° to the 30 db N_I jammer shown in Fig. 8. A second minimum appears as expected. These interferers are far enough apart so that for most angles of signal the received noise level is essentially the ambient level, and $(S/N)_o$ = +16 db. A third interferer could be added, say at 0° without changing the $S/N)_o$ for the existing lobes very much. However, if 2 or more jammers are close together, a wider combined minimum is formed, as in Fig. 10.

In Fig. 10 three $N_{I/S}$ = 30 db interferers are at 72°, 90°, and 108°. The ambient $\frac{S}{N_a}$ is still +10 db at each filter or +16 db at the array output. This could only represent 3 separate interferers, each at the given angle with each interfering transmitter using a different random PN sequence with the carriers all at the signal carrier frequency. It could also represent 3 Gaussian spectrum-matched interferers.

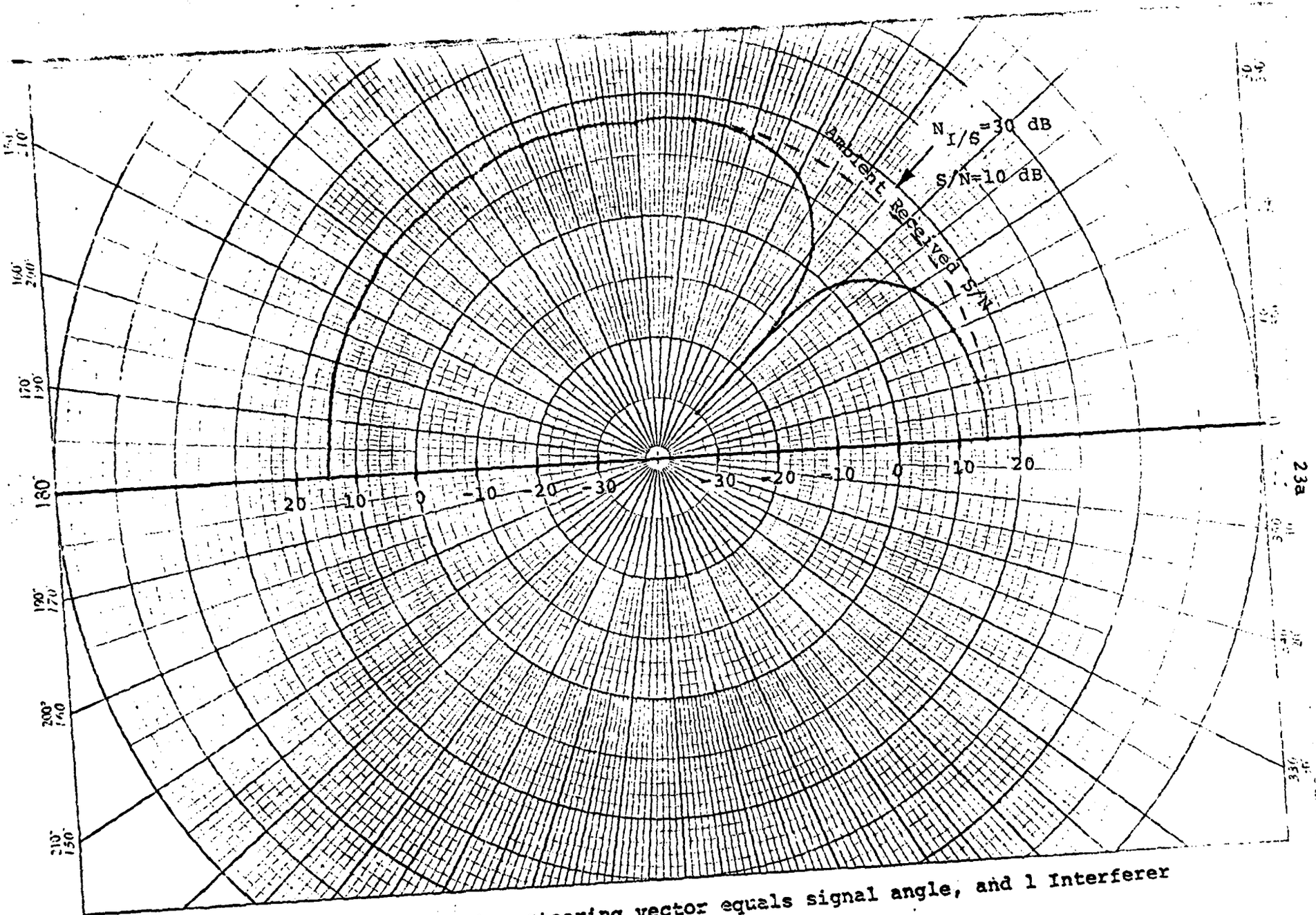

Fig. 8. SNR_o versus angle when steering vector equals signal angle, and 1 Interferer at 45°, with $N_I = 10^3$W; N_a = .1 W; S = 1W.

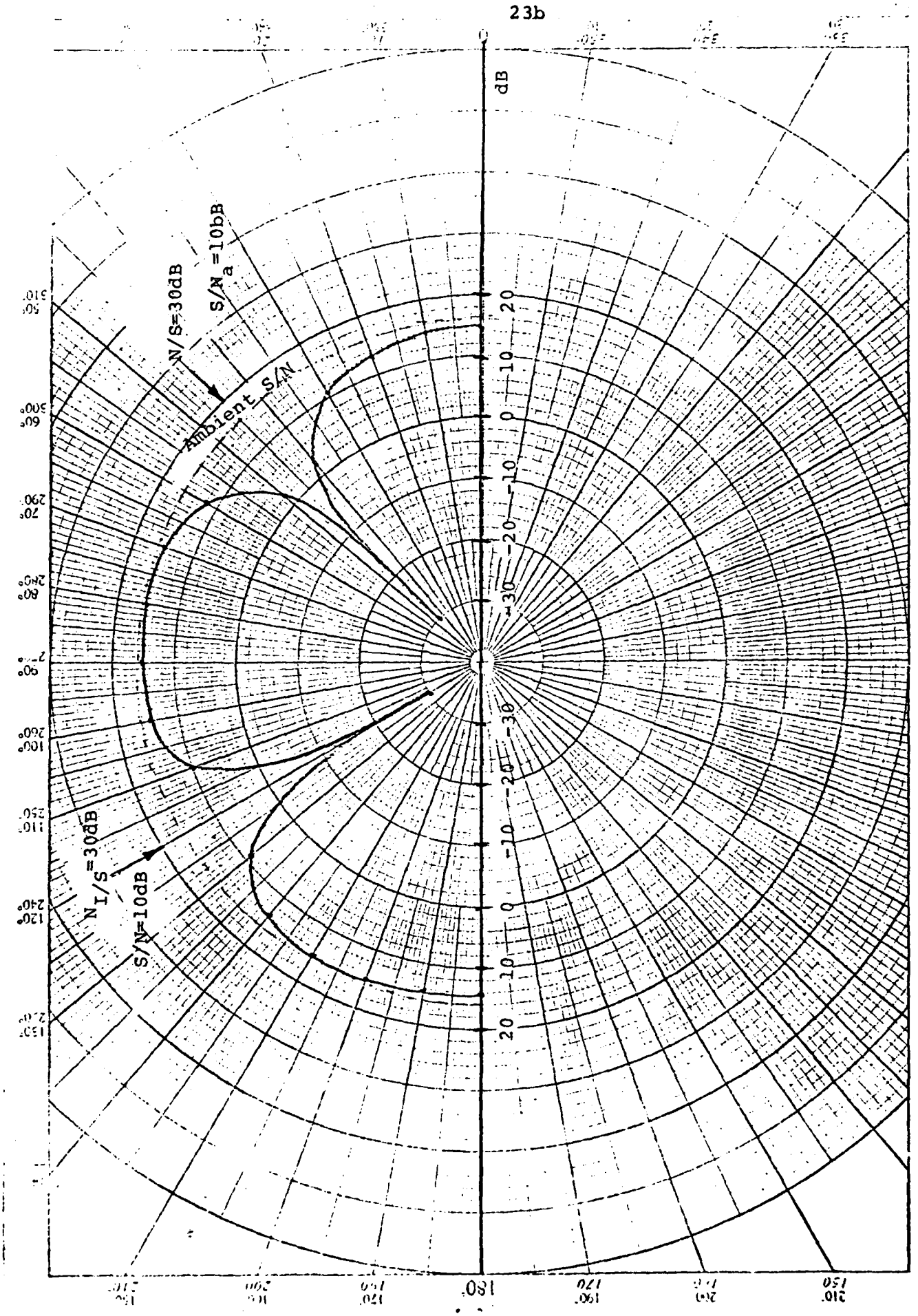

Fig. 9. SNR_o versus angle when steering vector equals signal angle, with 2 Interferers, each with $N_I = 10^3$W, one at 20°, one at 45°; N_a = .1W, S = 1W.

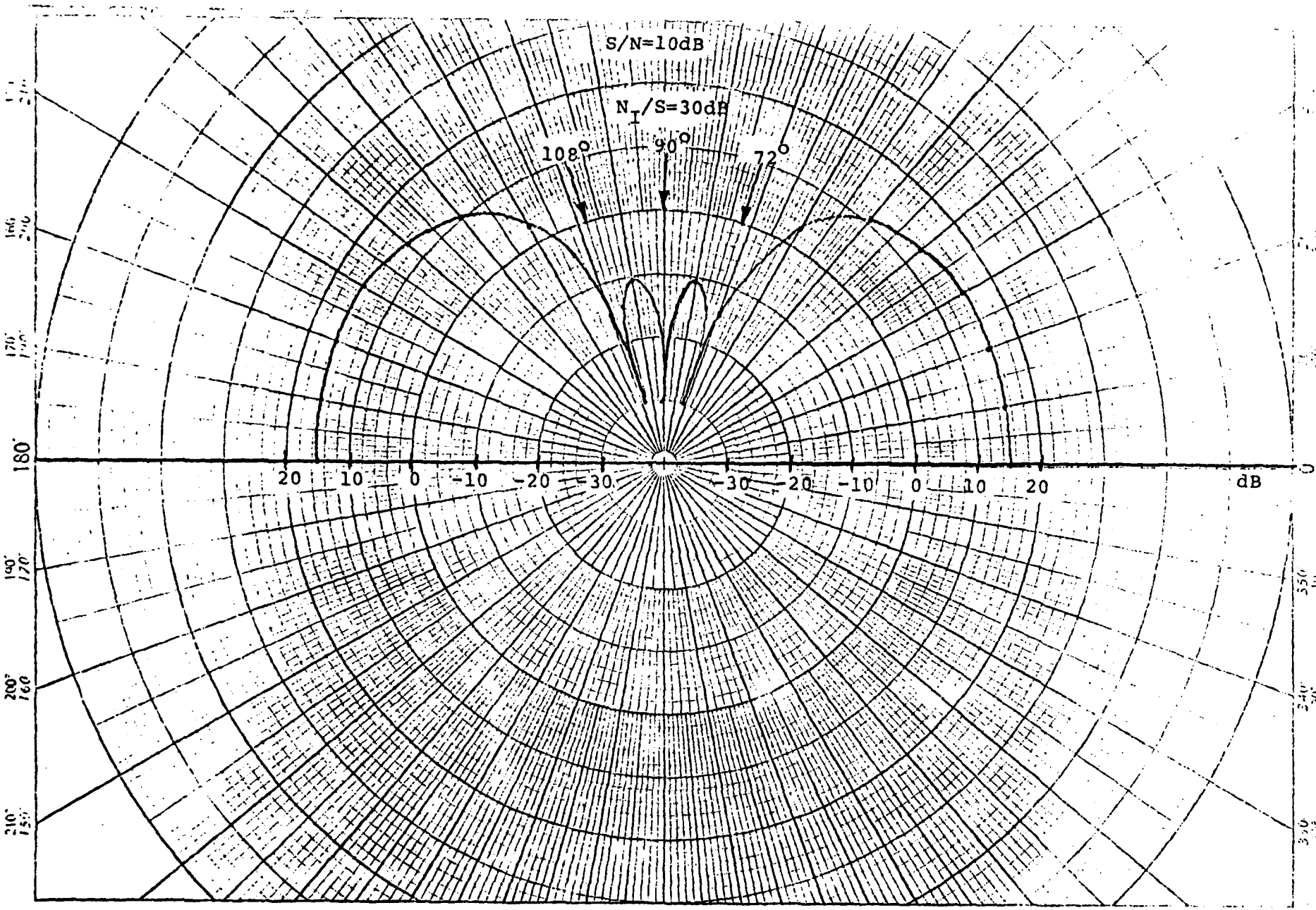

Fig. 10. SNR_o versus angle when steering vector equals signal angle, with 3 Interferers, each with $N_I = 10^3$W, at angles 72°, 90°, 108°; N_a = .1W; S = 1W.

In Fig. 11 we again have 3 interferers close to each other, but they are not symmetric about 90°. Note that the minimum SNR values are not affected even in this case, (all -30 db), but the range of angles where the received SNR is within 5 db of the ambient, (+16 db), is much reduced.

Also in this case it is theoretically possible for a single interferer at one of the 3 angles to transmit 3 frequencies simultaneously, with the frequencies chosen so that the phase shifts between adjacent elements match those for the assumed geometry shown for 3 interferers. The adaptive algorithm described cannot distinguish between these two cases. The amount of shift required in Fig. 11 would probably move the shifted frequencies out of practical receiver bandwidths. But smaller shifts must be considered as a possible jamming threat.

Note that if the interferer were frequency hopping between the 3 frequencies a covariance matrix based on observations over an extended time interval, as required by some adaptive narrow band algorithms, would contain all three frequency contributions. However, our measurements, where the covariance matrix is based on wideband observations taken within a short-time interval, might see one frequency at a time and shift the array weights to track the apparent change in interferer position.

In Fig. 12 the performance of the 4 element array changes completely as one increases the number of jammers from 3 interferers to 4 interferers.

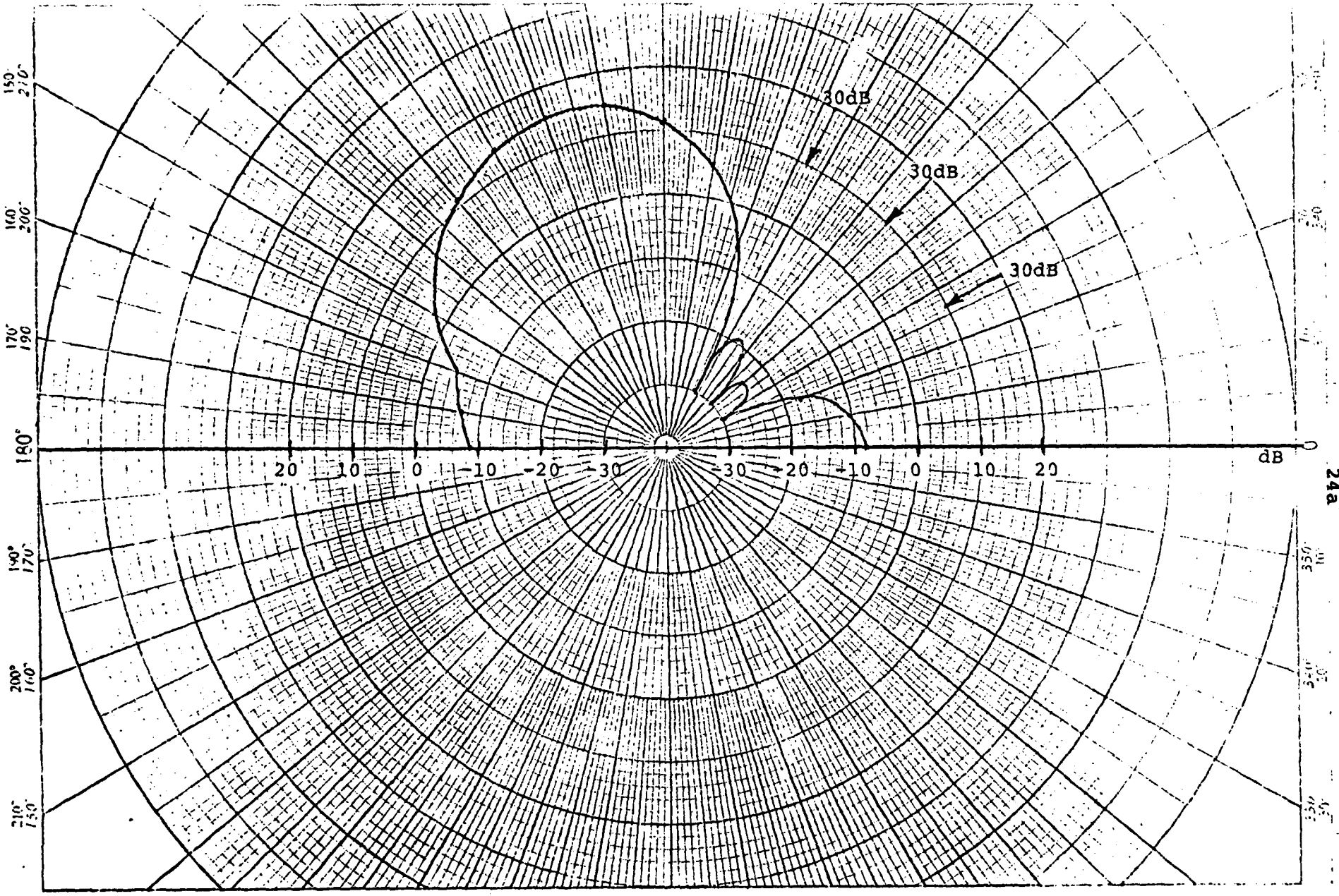

Fig. 11. SNR_o versus angle when steering vector equals signal angle, with 3 Interferers, each with $N_I = 10^3 W$, at angles 27°, 45°, 63°; N_a = .1W; S = 1W.

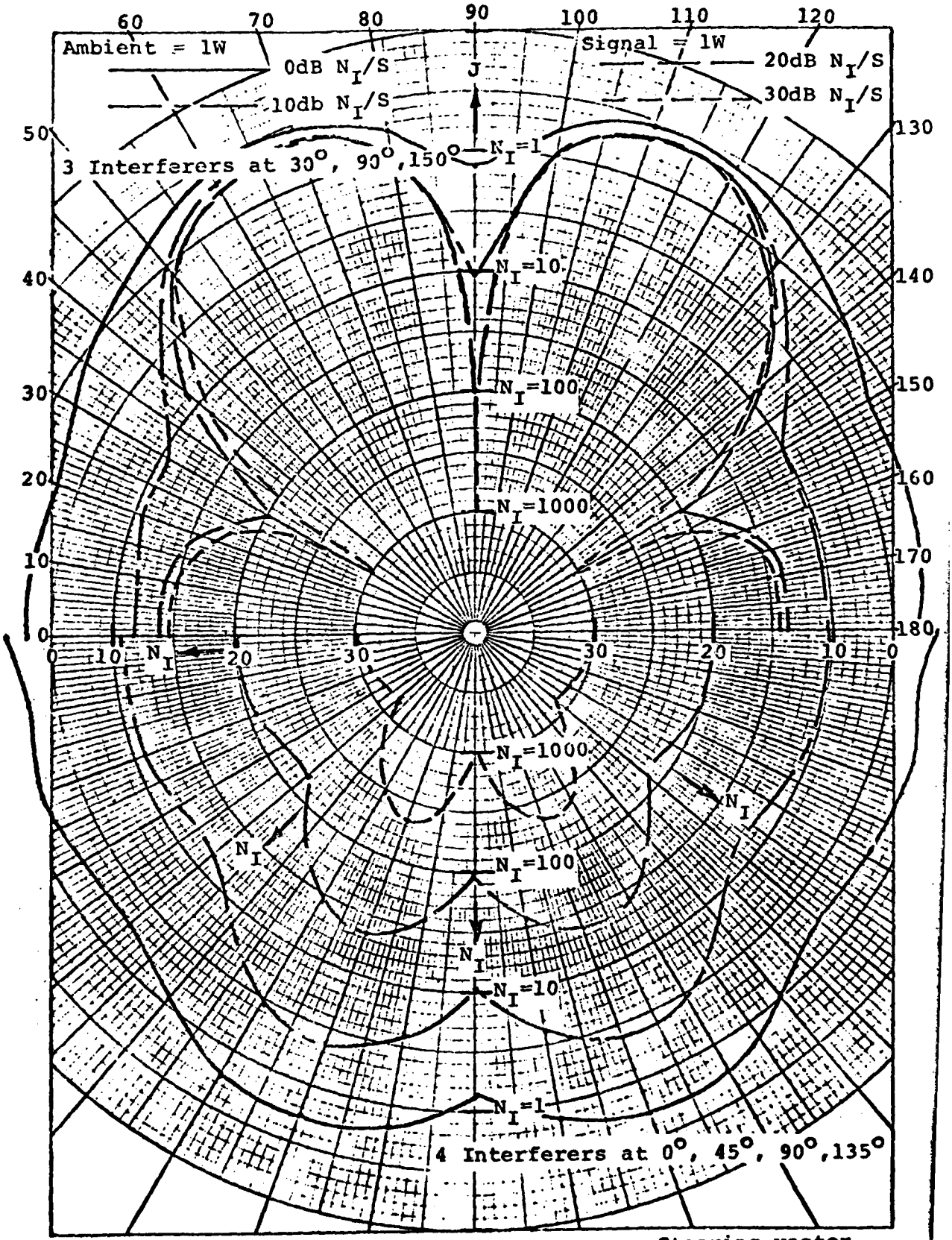

Fig. 12. SNR_o versus angle for 4-element array. Steering vector equals signal angle (top) 3 interferers, with the N_I varied from 1, 10, 100, to 1000W; N_a = 1W; S = 1W; (bottom) 4 Interferers, with other conditions same as for top.

In the top of the figure we have 3 interferers with equal powers, one at 30°, one at 90° and one at 150°. As the interferers powers are all increased from 20 db $N_{I/S}$ to 50 db $N_{I/S}$, minima in the received SNR form in the jammer directions and increase in depth with increased interferer power. However, two lobes in the direction of broadside $\pm$ 35° remain, where received SNR is close to ambient, i.e., regions of good interferer suppression.

In the bottom half of the figure we have 4 interferers roughly equally spread in angle over 180°. Now as the power of all interferers is increased, the available SNR for all received directions is decreased. For the geometry shown the decrease in available SNR is approximately equal to the interferer power.

Such a decrease in performance is of course expected when the number of interferers exceeds the "number of nulls which can be formed." The resulting performance often is not reported. A real system will, however, encounter many sources. In particular, an interferer may try to generate a wide band signal such that more than one "available null" is used up in suppressing a single jammer location. The performance under these conditions therefore is important system design information.

Fig. 13 to 18 explore the effect of a 4th interferer in more detail. In all these cases, 3 of the interferers are 1 KW, 30 db $\tilde{N}_{I/S}$ jammers. For Fig. 13 to Fig. 17, these are located at 45°, 90° and 135°. A fourth interferer initially at 0° is increased from -10 db $N_{I/S}$ to 30 db $N_{I/S}$ as we go from Fig. 13 to Fig. 17. The shape of the pattern does not

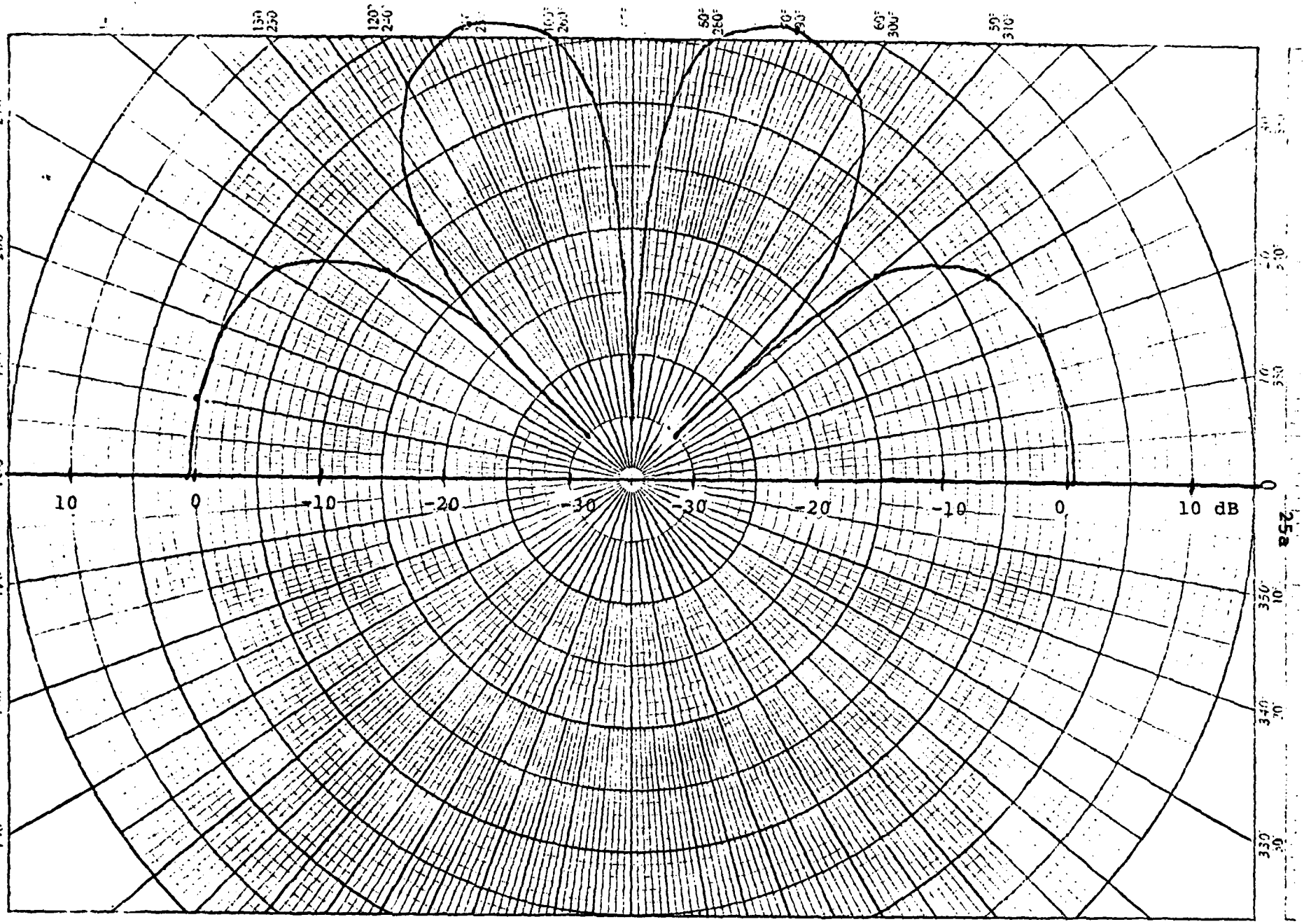

Fig. 13. SNR_o versus angle when steering vector equals signal angle, and 4 Interferers, 3 of which have $N_I = 10^3$ W at angles 45°, 90°, and 135°; 4th Interferer at 0° has .1W.

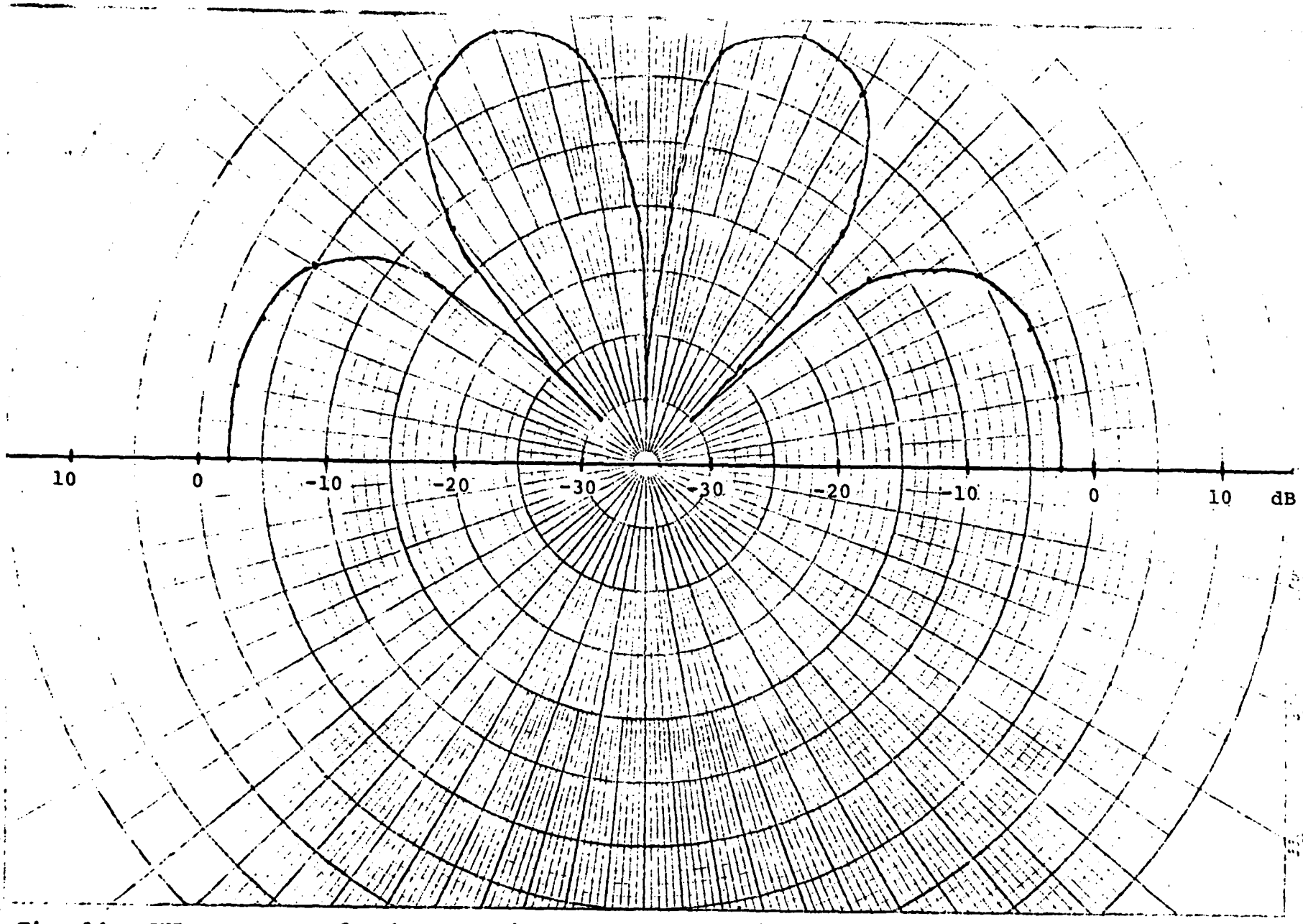

Fig. 14. SNR_o versus angle when steering vector equals signal angle, and 4 Interferers, 3 of which have $N_I = 10^3$W at angles 45^o, 90^o, and 135^o; 4^{th} Interferer at 0^o has 1W.

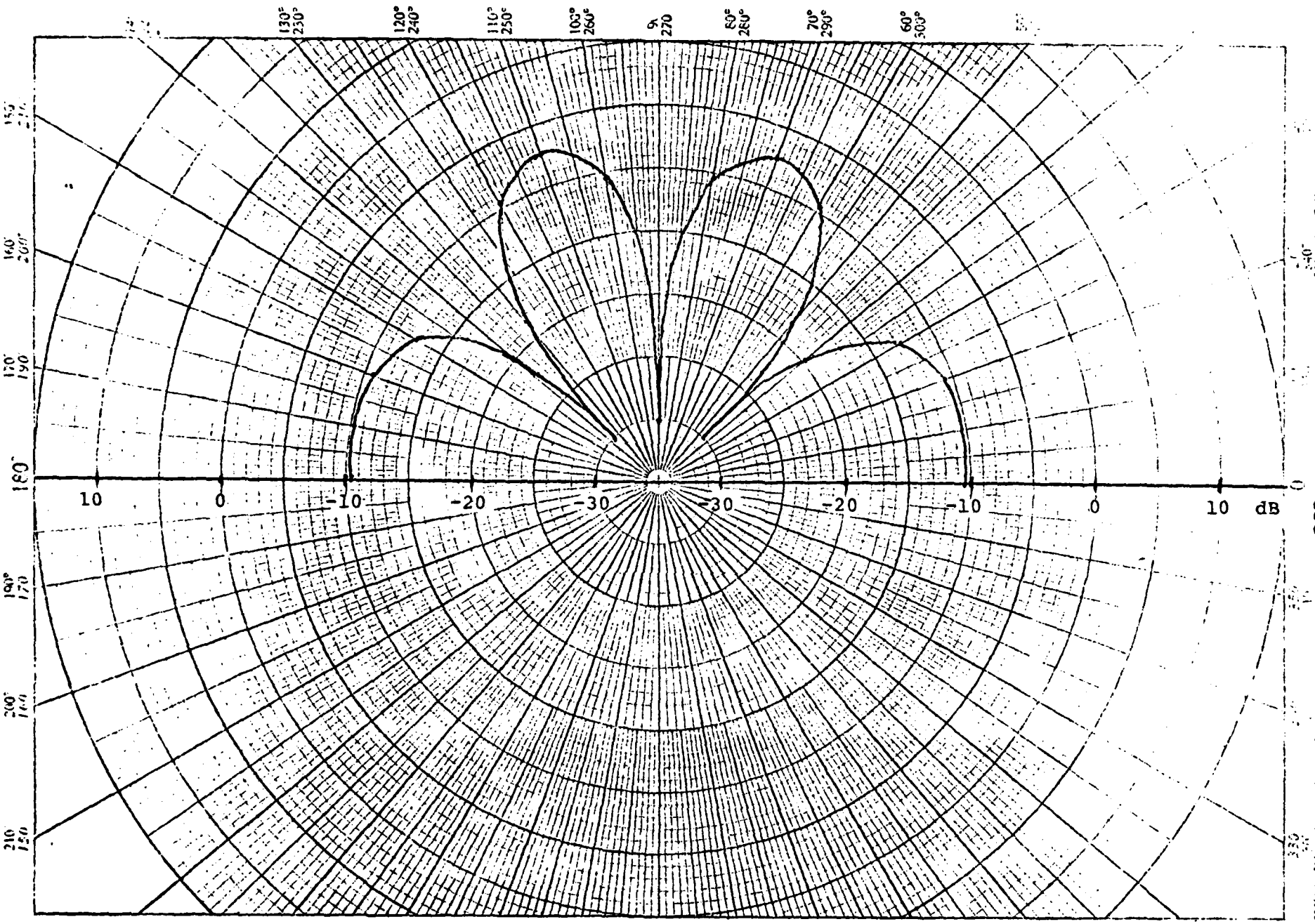

Fig. 15. SNR_o versus angle when steering vector equals signal angle, and 4 Interferers, 3 of which have $N_I = 10^3 W$ at angles 45^o, 90^o, and 135^o; 4^{th} Interferer at 0^o has 10W.

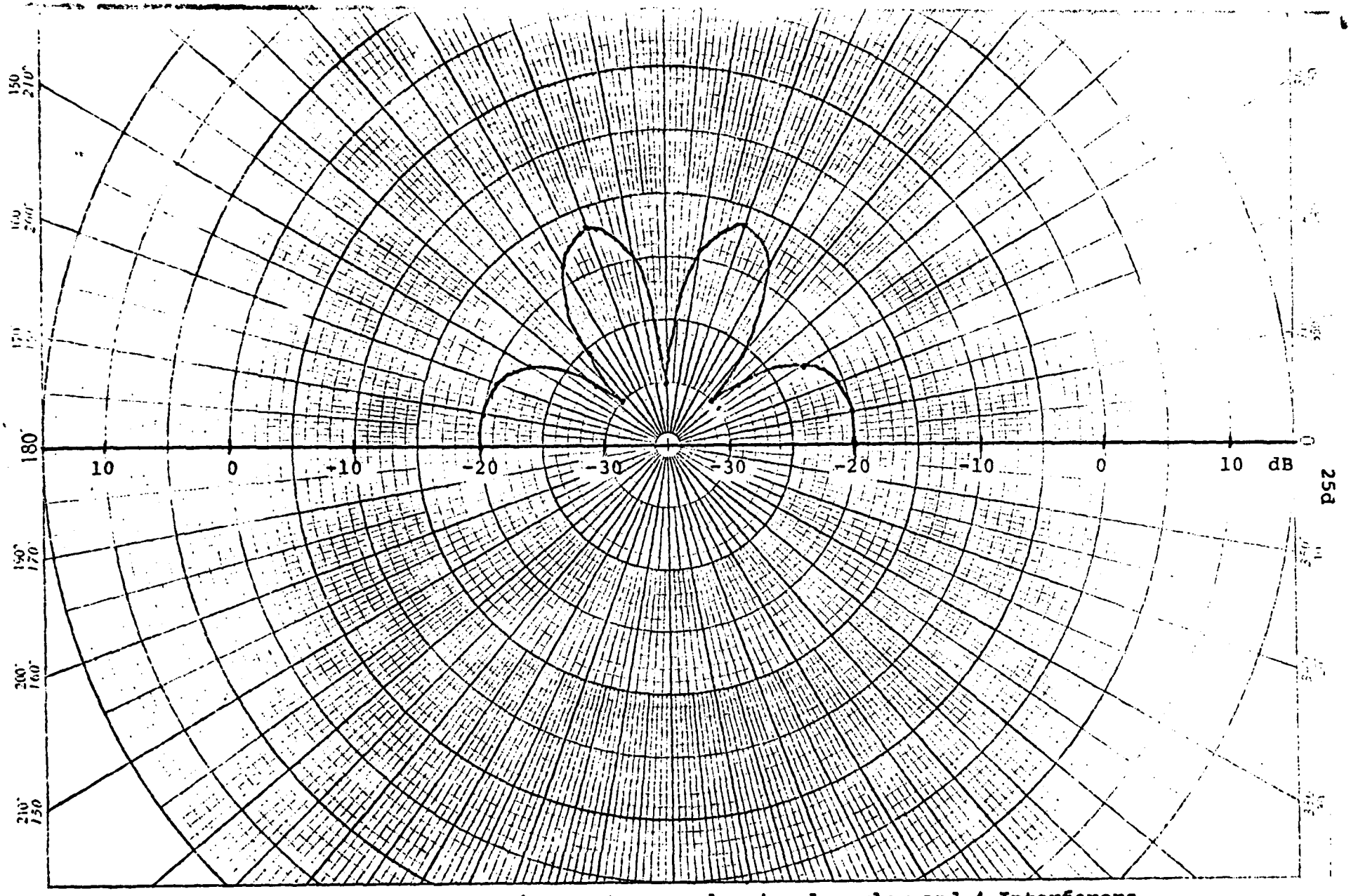

Fig. 16. SNR_o versus angle when steering vector equals signal angle, and 4 Interferers, 3 of which have $N_I = 10^3$W at angles 45^o, 90^o, and 135^o; 4^{th} Interferer at 0^o has 100W.

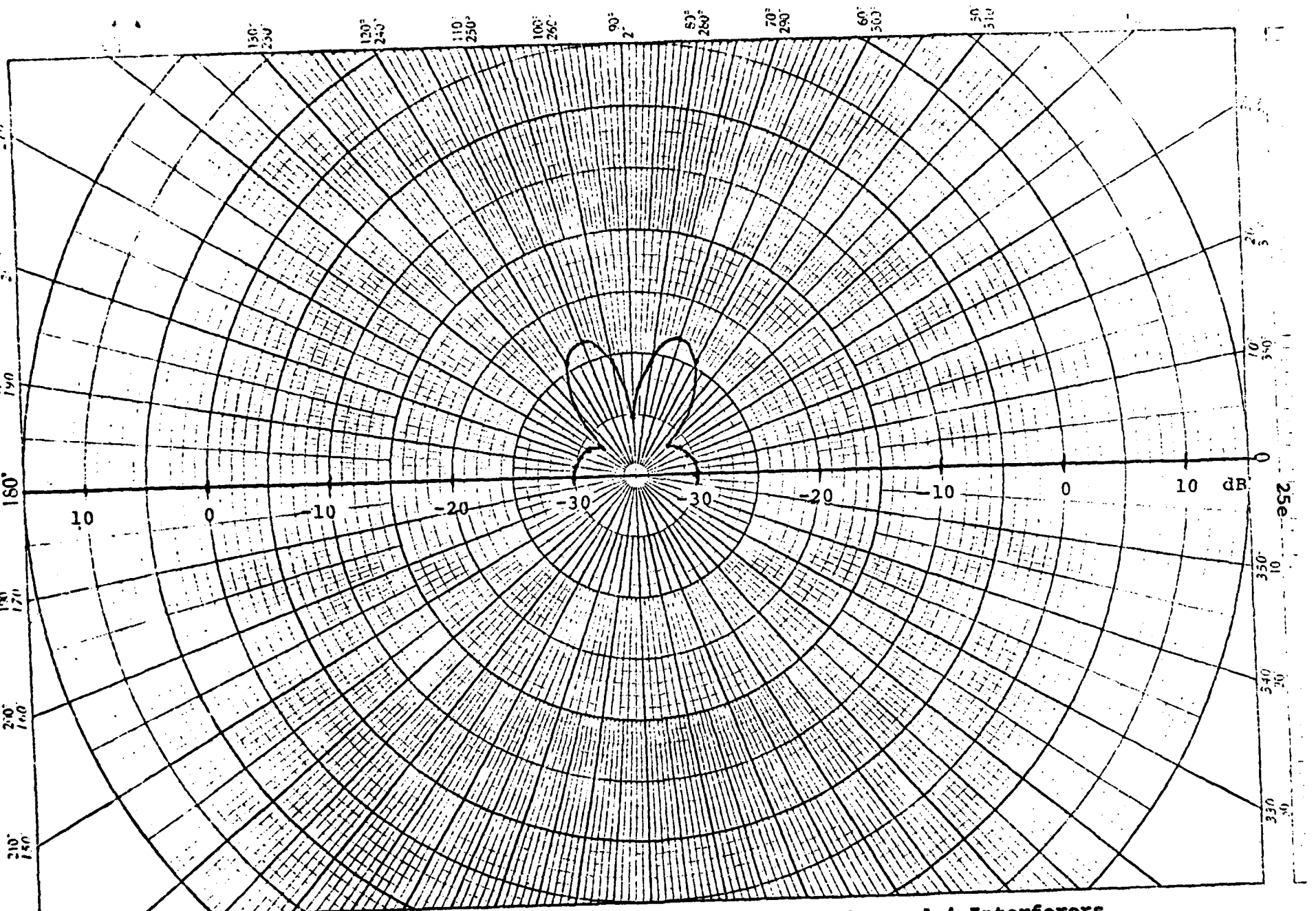

Fig. 17. SNR_o versus angle when steering vector equals signal angle, and 4 Interferers, each of which have $N_I = 10^3 W$ at angles 0°, 45°, 90°, and 135°.

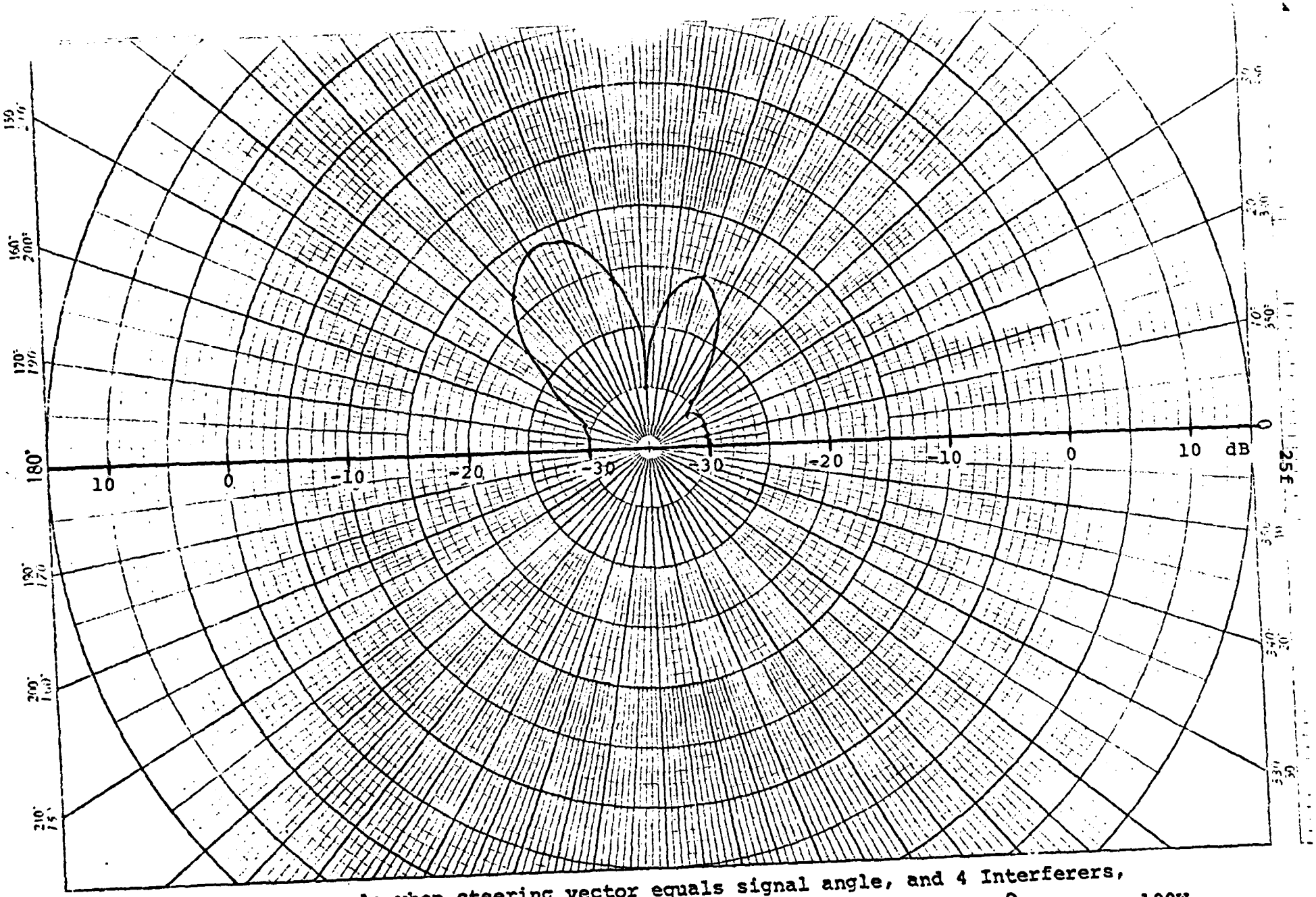

Fig. 18. SNR_o versus angle when steering vector equals signal angle, and 4 Interferers, 3 of which have $N_I = 10^3$W at 0°, 45°, and 90°; 4th Interferer at 135° has N_I = 100W.

change until the last step, but it is clear that even a rather weak 4th interferer can effectively reduce spatial processing gain for all angles.

In Fig. 18 a weaker (100 W) jammer is placed at 135°, instead of at 0° as in Fig. 17. The available remaining pattern is quite different for the two cases.

These figures illustrate some of the factors which must be considered in any adaptive array design. In particular, it is important to consider that theoretically there are wide range of angles where 3 or less interferers can be effectively suppressed so as to have little effect, independent of interferer strength. More interferer power just results in more effective suppression. This communication advantage is lost completely if one or more additional real or simulated interferers are introduced into the covariance matrix noise samples. The system must be designed so that it is difficult for the jammer to produce or simulate these extra interferers. The calculation in these sections are again optimal array performance, with assumed complete coherence between the 4 antenna elements for all signals.

We must emphasize that performance associated with the above curves implied a large number of apriori steering vectors or beams (one for each angle evaluated). While in concept one could envisage a large number of apriori beams (or steering vectors), in practice we are as usual only interested in the number sufficient to give the bulk of the achievable gain. We recall that, in the acquisition mode, both time of signal arrival and direction of arrival are unknown. We also recall

from Sec. 3 that in the case of the time function we used a sliding window which moved in increments of ¼ chip duration and detected the signal if it exceeded a threshold, at one or more sliding window positions. Similarly we can choose a finite number of assumed steering vectors for each time window and detect the signal when the combination of a time window and one or more steering vectors result in a signal output above a threshold level. To determine the number of different steering vectors which might be required to reliably detect the signal even when it does not match the assumed steering vectors exactly, we must know the beam width for different steering vectors and different numbers of interferers.

Again, we do not have an equation for the antenna pattern when an arbitrary number of interferers are present, but we do have computer programs for calculating the antenna pattern for the 4 element linear array and any assumed interferers pattern. The examples given below were obtained by the CMAT 5 program listed in Appendix B. The antenna array weights are normalized so that the noise output is unity. The decibel value plotted therefore match the performance SNR when the signal coincides with the steering direction.

Starting in Fig. 19 we first show a number of ambient noise antenna patterns which are generated by the array when no directional interferers are present. In Fig. 19 the steering vector is broadside at $+90^{\circ}$. The 4 element pattern has 3 lobes with nulls as shown. We consider the steering vector nulls to be perfect nulls (zero gain), where the phase of the received signal changes phase by 180°. This is in contrast to the minima of finite depth in the direction of a interferer which may be

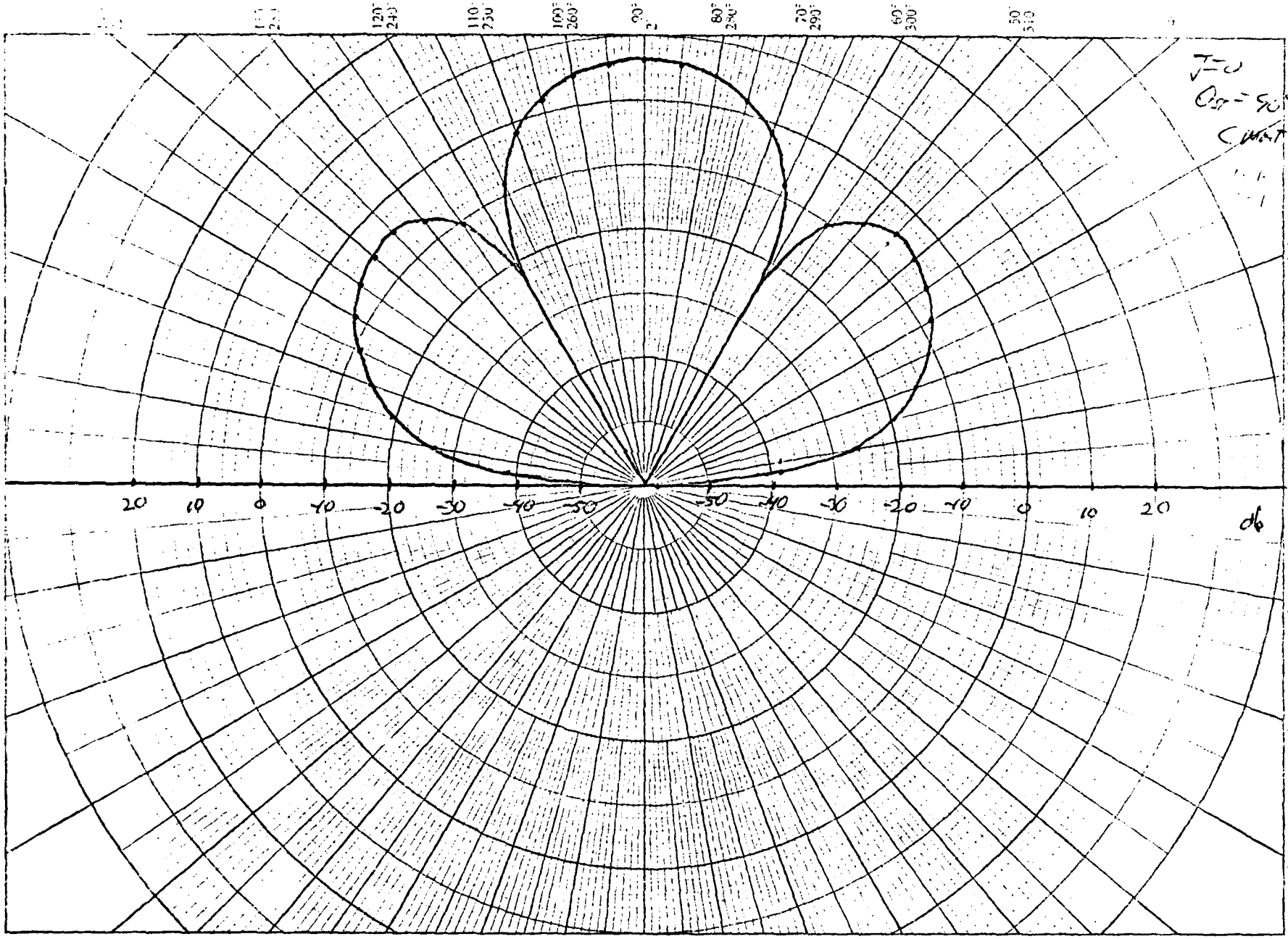

Fig. 19. SNR_o versus angle for a broadside (90°) steering vector with no Interferers present, and $N_a = S = 1W$.

produced by the adaptive algorithm. For our antenna array model such perfect steering vector nulls exist. A real antenna array may have defects such that the in-phase and quadrature signals do not go through zero at the same angle. It is important to distinguish between these nulls of the steering vector pattern, and "nulls" formed by the adaptive algorithm. The patterns in the lower half plane are mirror images of the patterns shown.[1.]

Figs. 20 and 21 show similar ambient beam patterns for steering angles of 45^{o} and 0^{o}, respectively. The 135^{o} beam pattern would be a mirror image of the 45^{o} pattern. Note that by using only 2 steering vectors, 45^{o} and 135^{o}, provides good coverage for signal reception is given for all directions except the nulls near broadside. Adding a third steering vector of 90^{o} covers these nulls. We could also add a 4th steering vector at 0^{o} for some redundant coverage. The conclusions are that about 4 steering vectors is enough to provide 360^{o} reception in ambient noise.

Fig. 22 shows the antenna power pattern[2.] when a N_I interferer at 90^{o} is added to the 45^{o} steering vector ambient pattern. A minimum or "null" more than 50 db deep forms in the interferer direction. The rest of the lobe structure also changes. However, the 45^{o} pattern plus the 135^{o} pattern still provide essentially complete 360^{o} coverage for signal array from the interferer at 90^{o} (and at -90^{o}).

Fig. 23 adds another 30 db $N_{I/S}$ interferer at 60^{o}, while

---

1. In most practical applications a linear array would be mounted on a ground plane which suppresses the lower half space.
2. The received noise is always normalized to one; therefore, the antenna gain pattern, which specifies the arriving signal power is equal to the output signal-to-noise ratio.

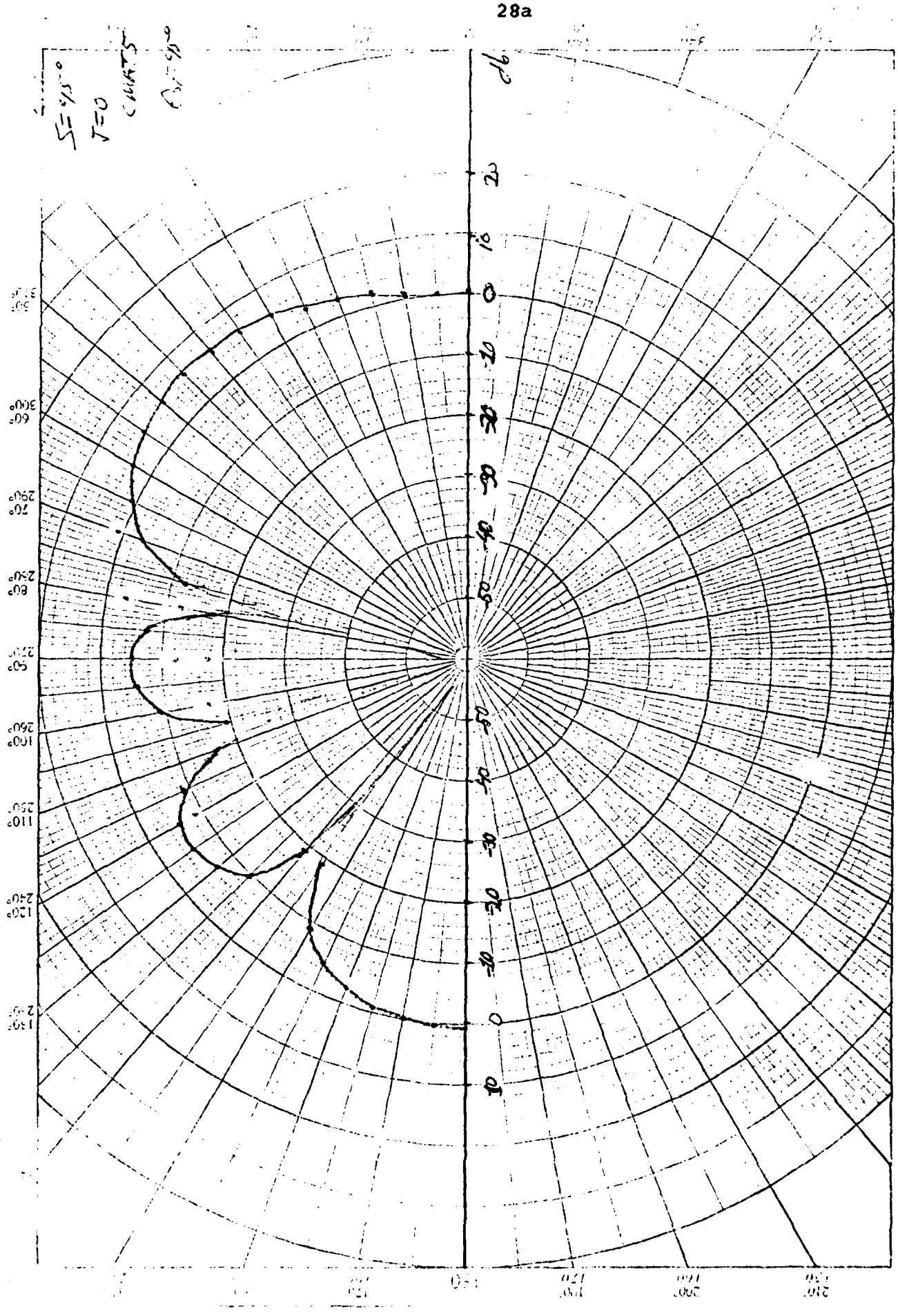

Fig. 20. SNR_o versus angle for a steering vector at 45^o with no Interferers present, and $N_a = S = 1W$.

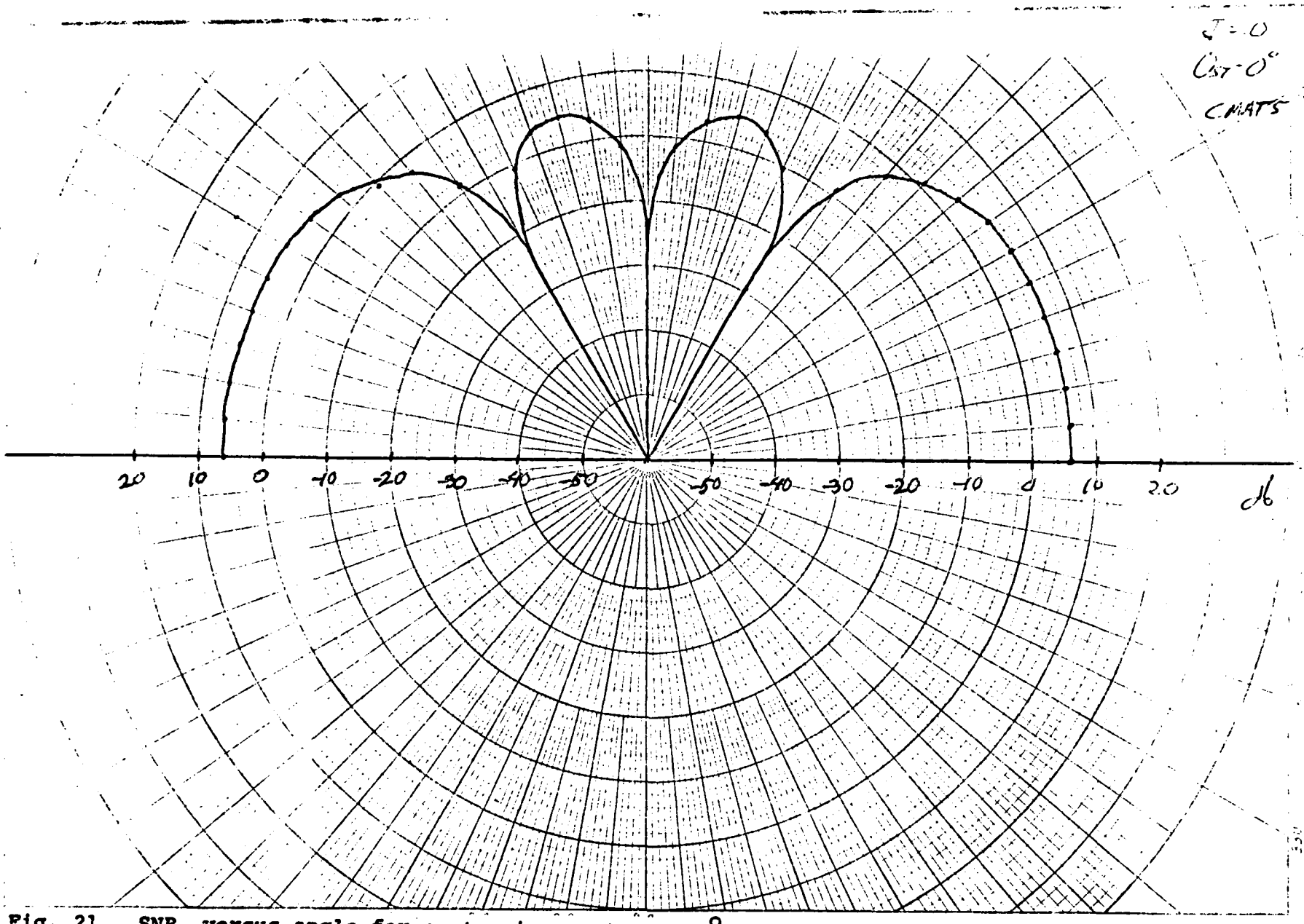

Fig. 21. SNR_o versus angle for a steering vector at 0^o (endfire) with no Interferers present, and N_a = S = 1W.

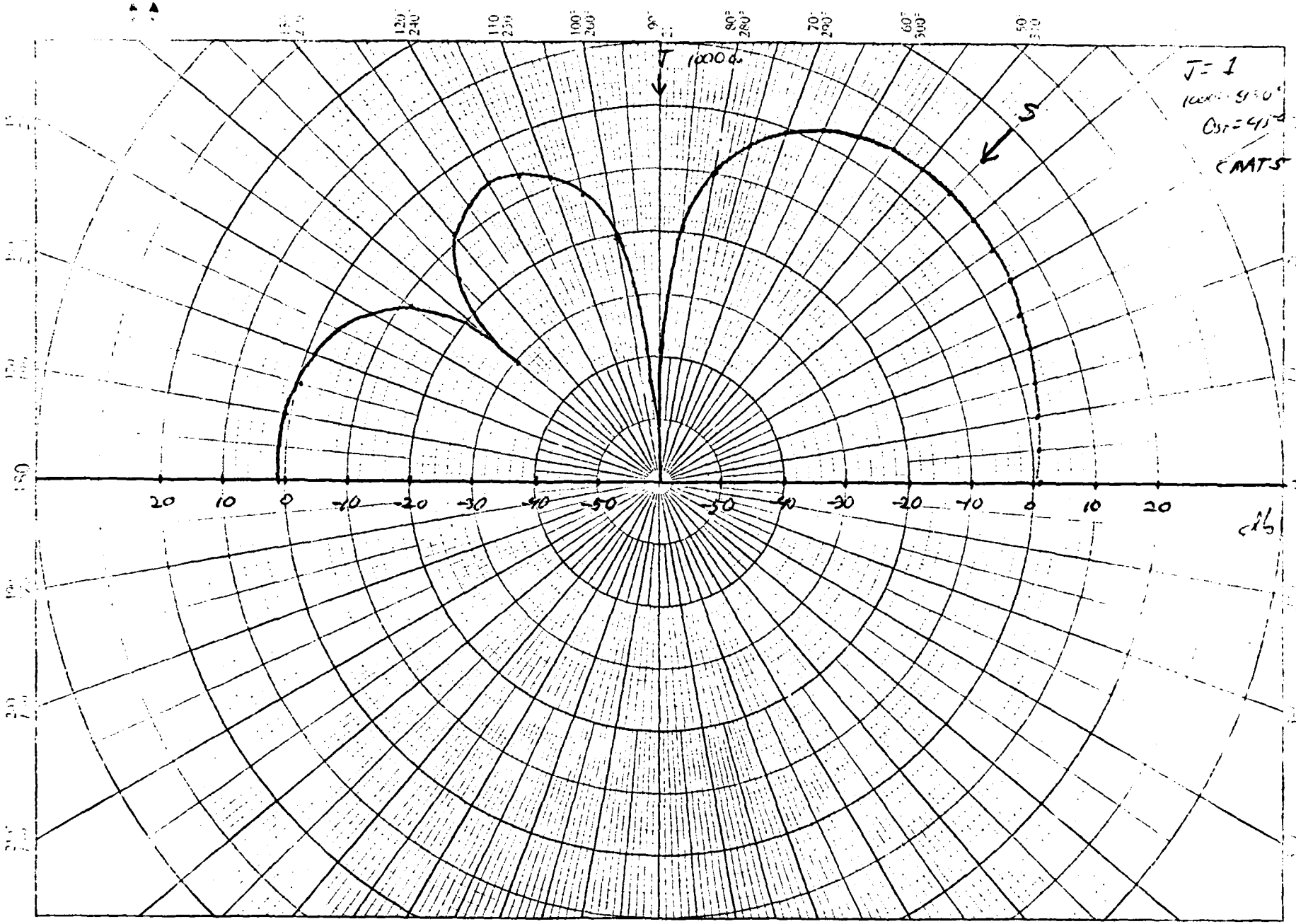

Fig. 22. SNR_o versus angle for a steering vector at 45^o with one Interferer of $N_I = 10^3 W$

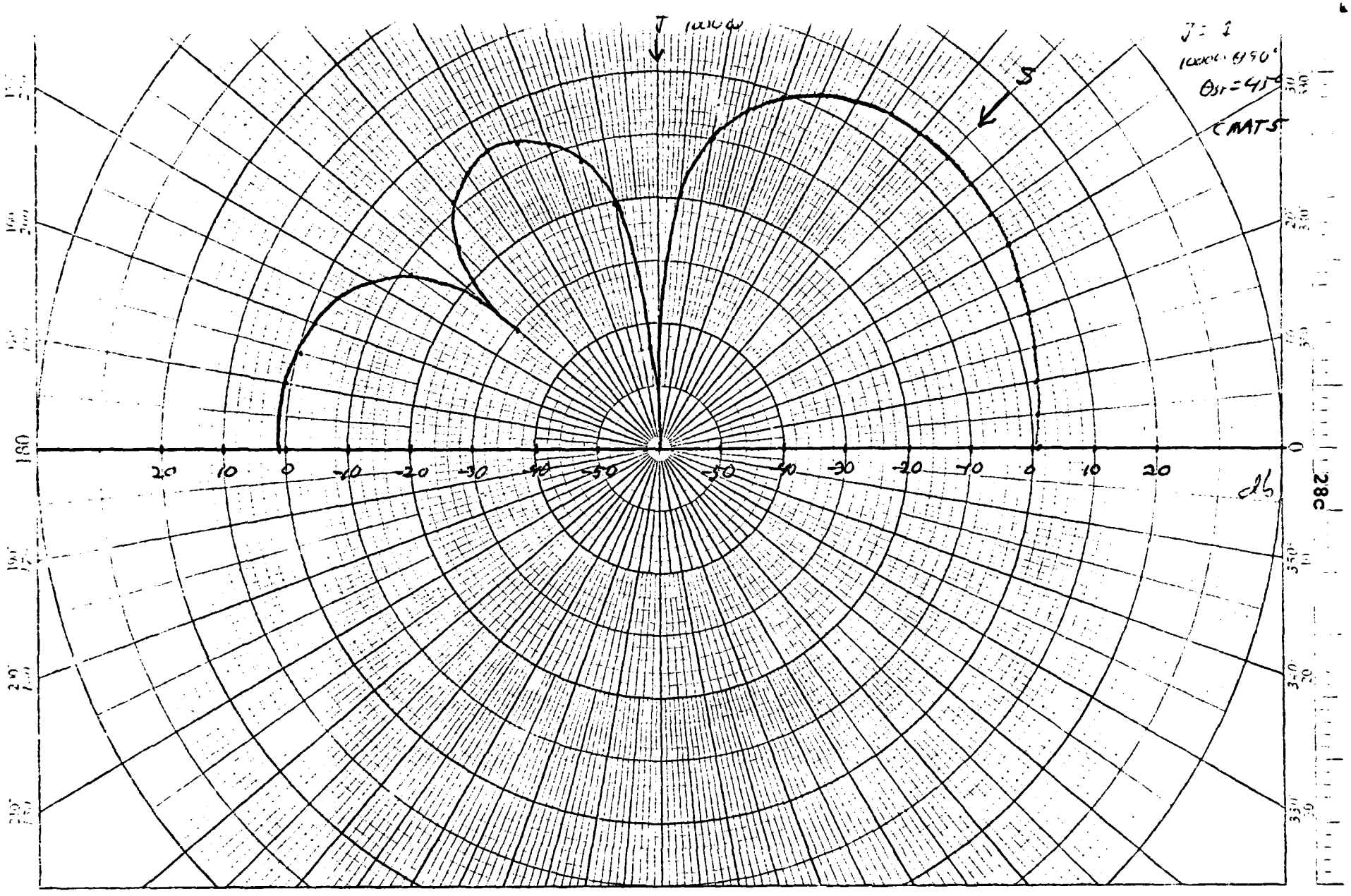

Fig. 22. SNR_o versus angle for a steering vector at 45^o with one Interferer of $N_I = 10^3W$ at 90^o, and $N_a = S = 1W$.

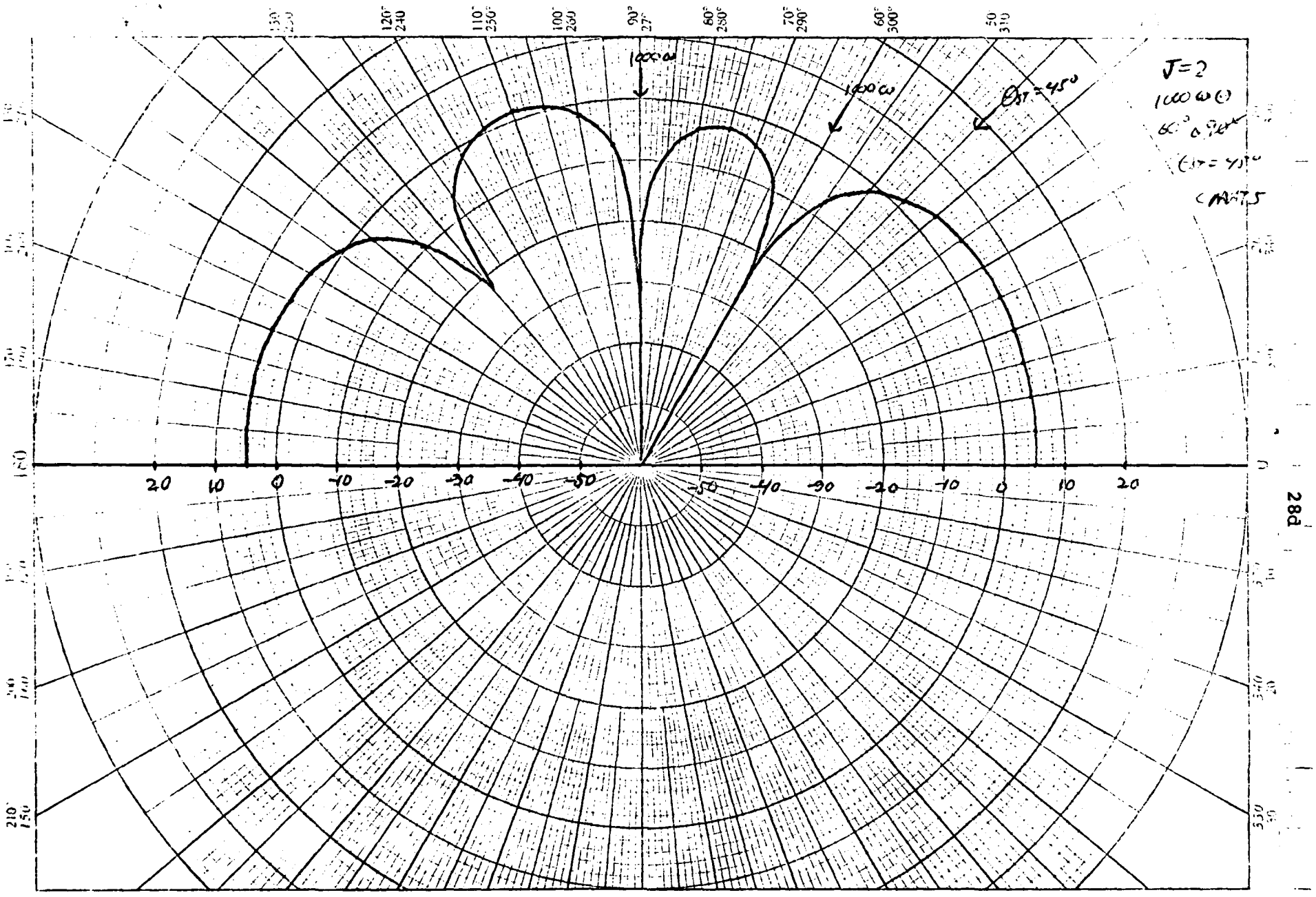

Fig. 23. SNR_o versus angle for a steering vector at 45°, with two Interferers of $N_I = 10^3 W$ each, at 60° and 90°, and $N_a = S = 1W$.

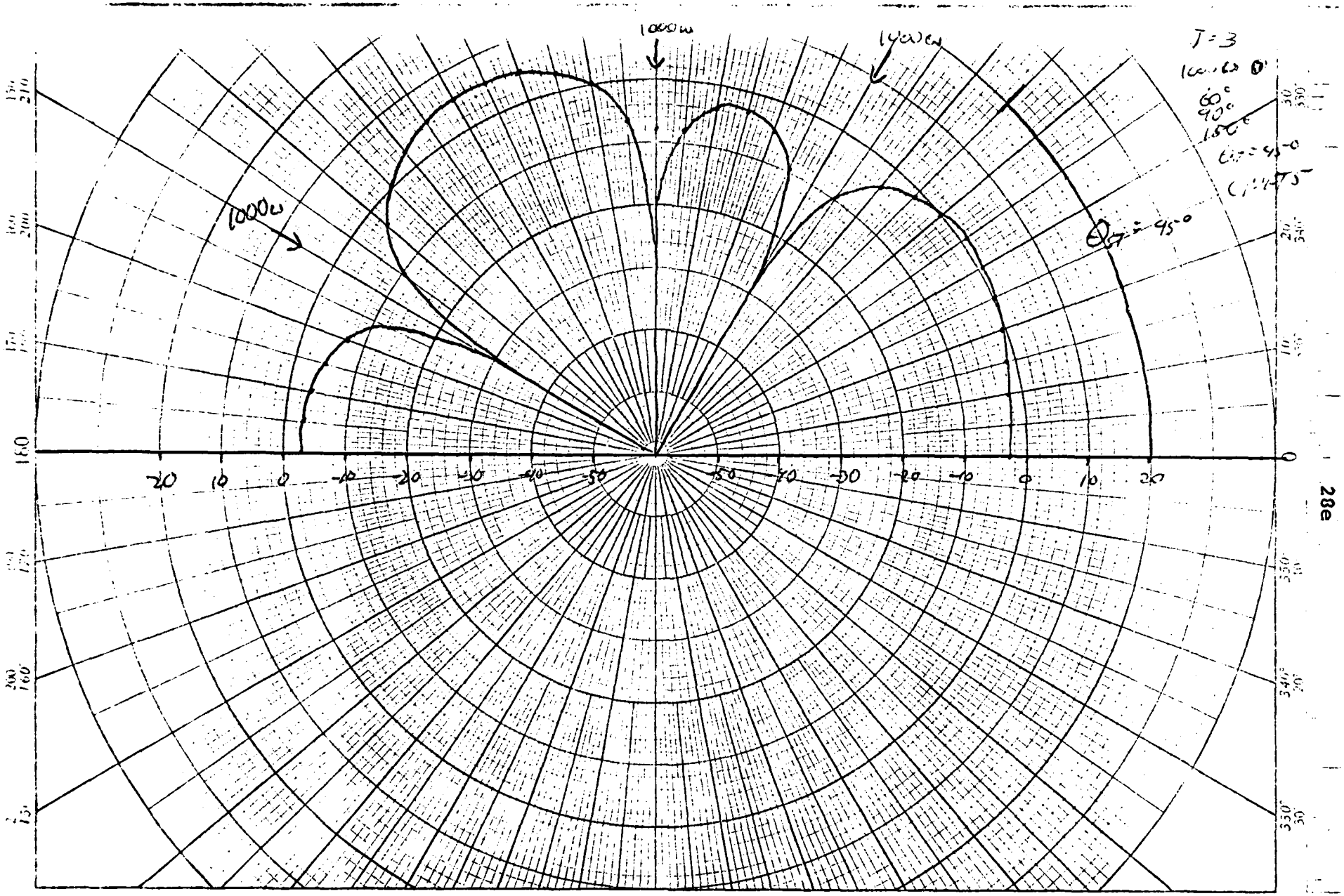

Fig. 24. SNR_o versus angle for a steering vector at 45°; with three Interferers of $N_I = 10^3$W each, at 60°, 90°, and 150°, and N_a = S = 1W.

Fig. 24 adds a third 30 db $N_{I/S}$ interferer at 150°. There are still large lobes which would give good signal reception for signals not near these interferers.

In Figs. 25 and 26 we have added two and three interferers to the 135° steering vector pattern. The combination of this with the corresponding 45° patterns gives at least one pattern with good coverage for all angles away from the jammers.

Figs. 27, 28 and 29 show something different. The steering vector here is 0°. Adding the two 30 db $N_{I/S}$ interferers at 90° and 60° in this case appears to have no effect at all on the 0° steering angle ambient pattern. The ambient pattern for this steering vector already had infinite nulls at 90° and 60°.

Adding the 3rd jammer does introduce a new minimum. In spite of the fact that these jammers are in "nulls" of the beam pattern, the covariance matrix does include the terms to form adaptive nulls in these directions. If a 4th interferer is introduced[1], the response degrades just as badly as if no beam nulls had occurred in any of the jammer directions. The algorithm does not appear to be exploiting the steering vector nulls efficiently in this particular case.

Figs. 30, 31 and 32 show this, plus another effect. Here we happen to have chosen a steering vector of 90° which coincides with the direction of the 90° interferer. The 90° jammer in this case can not produce a null, instead it reduces the antenna gain in all directions. If patterns for other steering vectors are available, this may not be serious. Otherwise communication for all directions is denied by the

---

1. No Figure is included to portray this 4-interferer case.

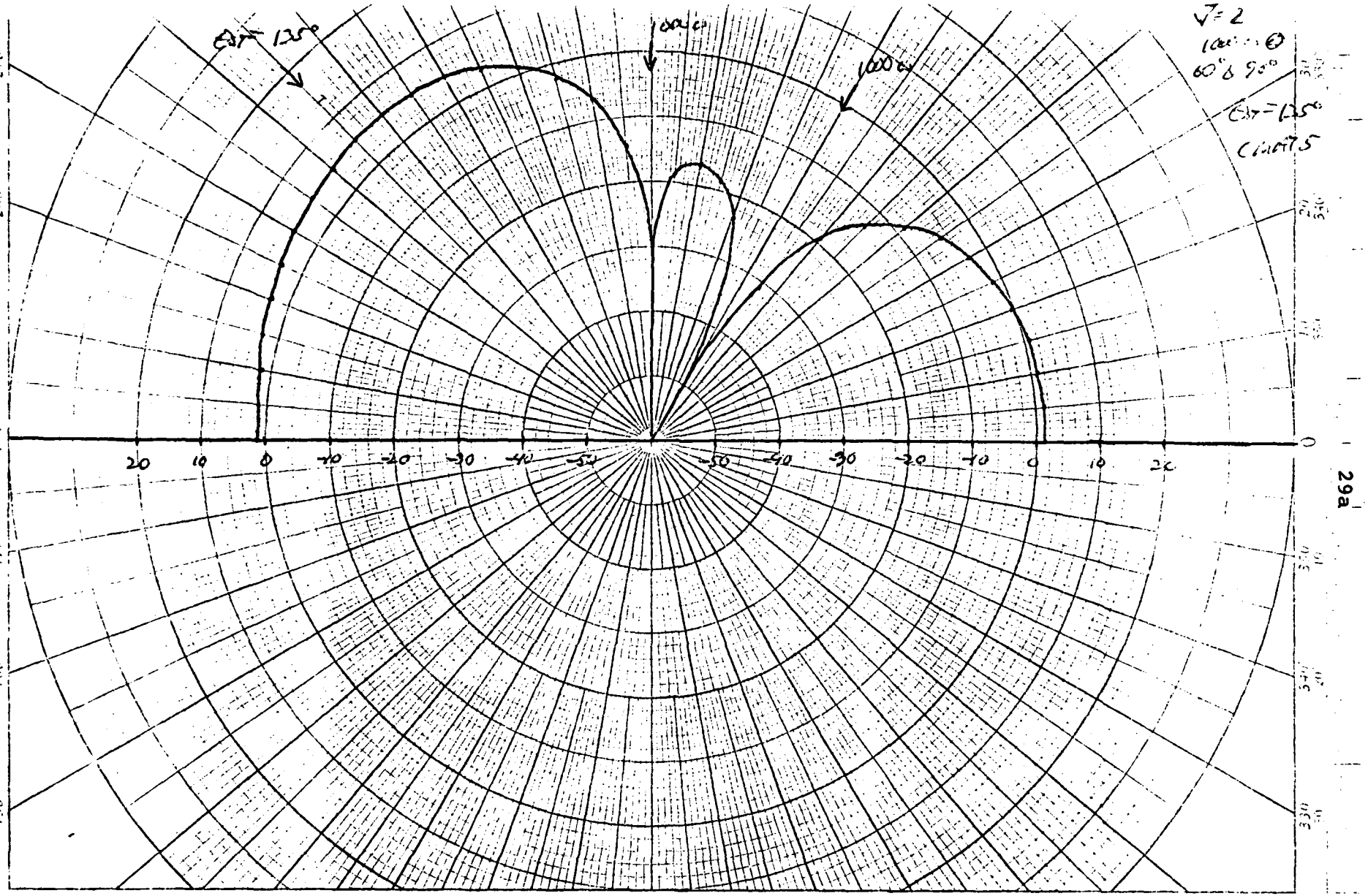

Fig. 25. SNR_o versus angle for a steering vector at 135°, with two Interferers of $N_I = 10^3$W each, at 60° and 90°, and N_a = S = 1W.

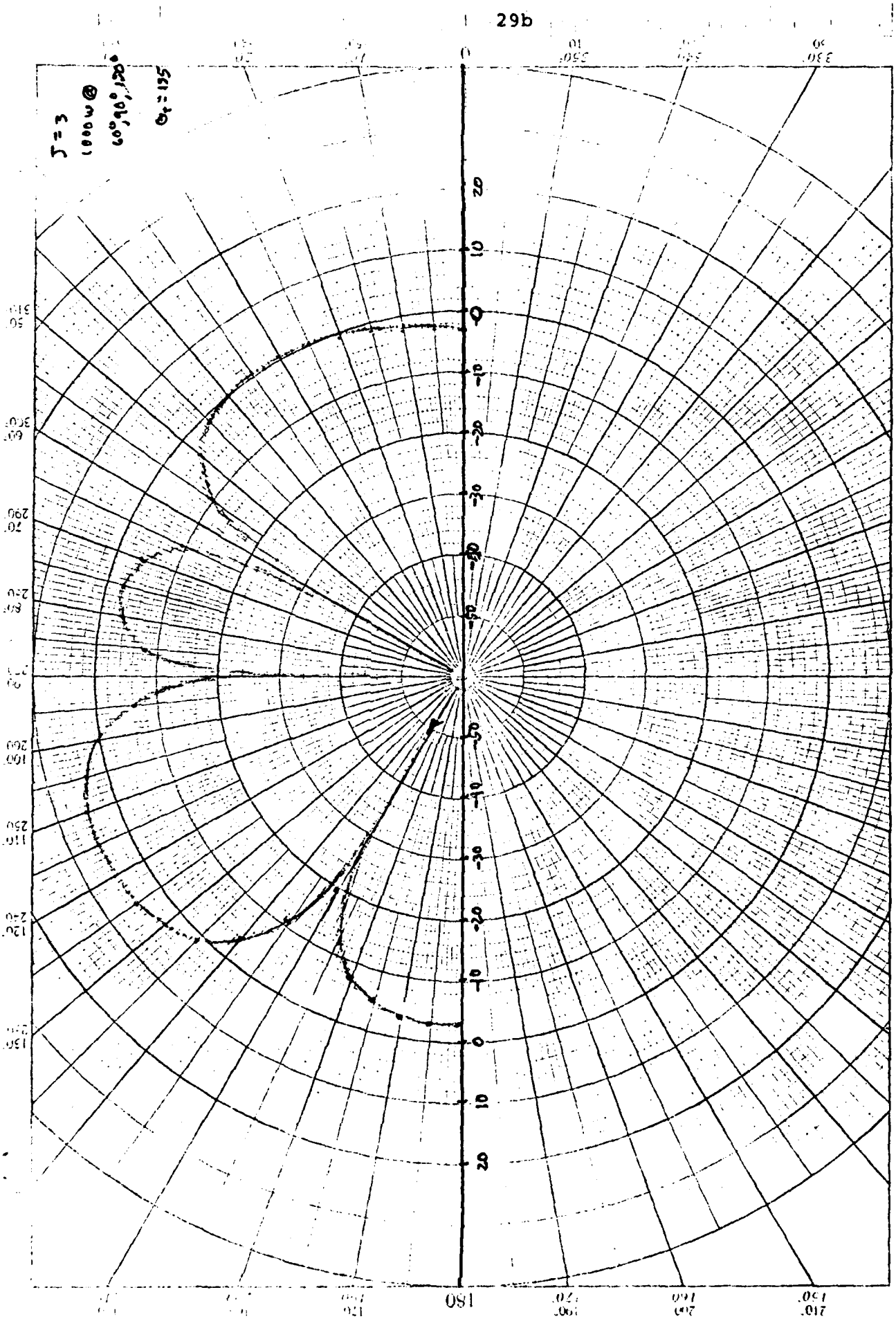

Fig. 26. SNR_o versus angle for a steering vector at 135°, with three Interferers of $N_I = 10^3$W each, at 60°, 90°, and 150°, and $N_a = S = 1W$.

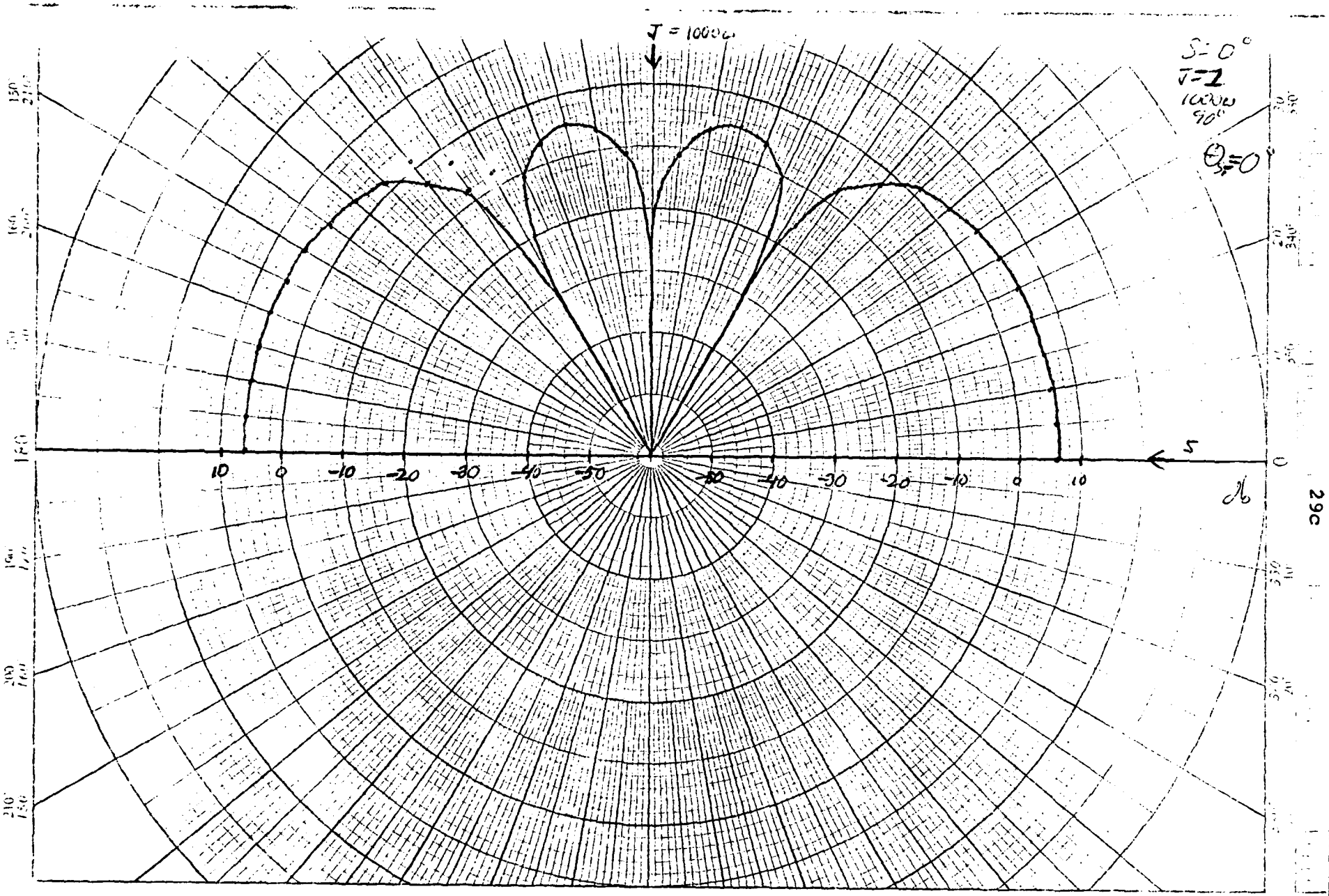

Fig. 27. SNR_o versus angle for a steering vector at 0^o, with one Interferer of $N_I = 10^3 W$ at 90^o and $N_a = S = 1W$.

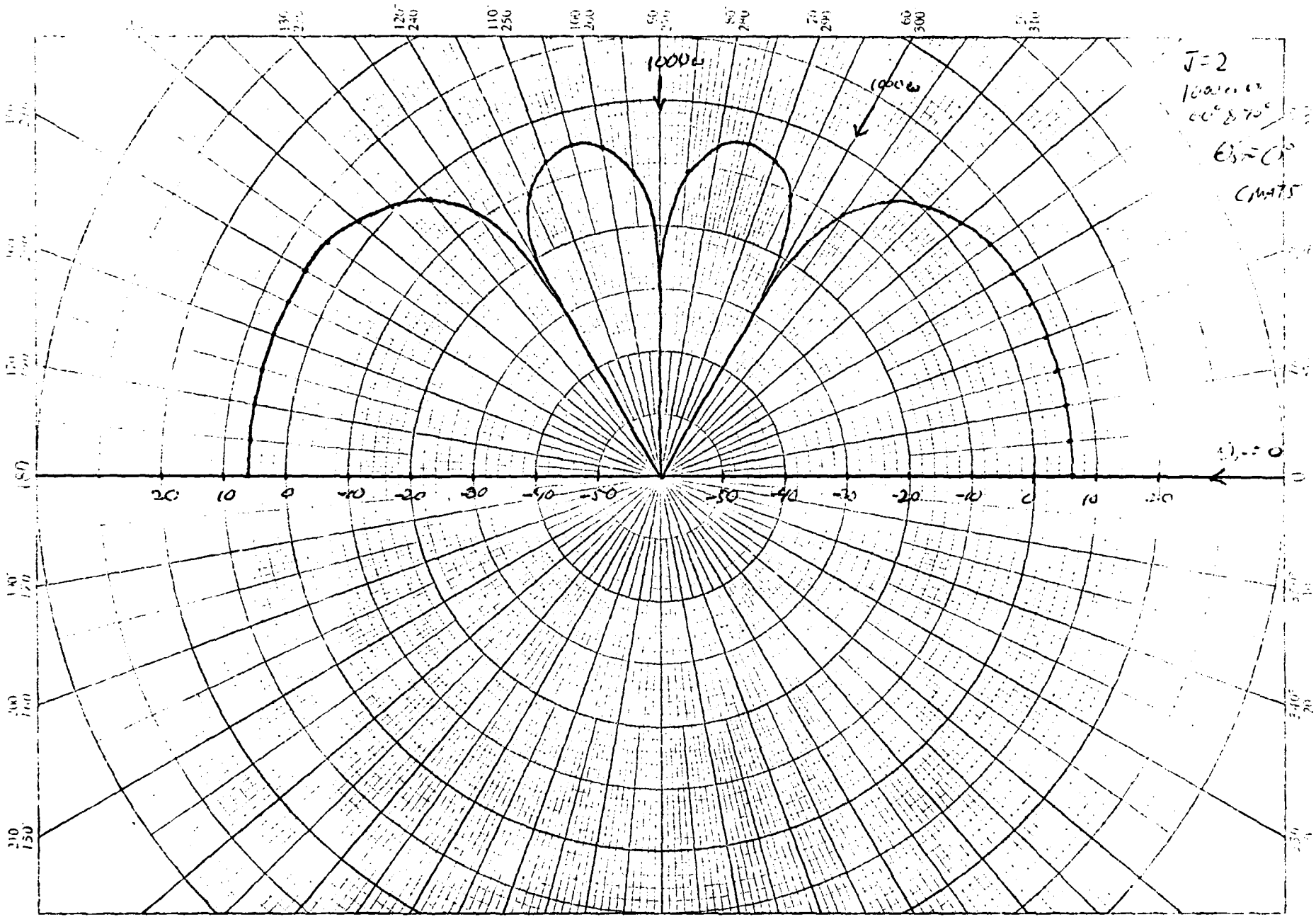

Fig. 28. SNR_o versus angle for a steering vector at 0^o, with two Interferers each with 10^3 at 60^o and 90^o, and N_o = S = 1W.

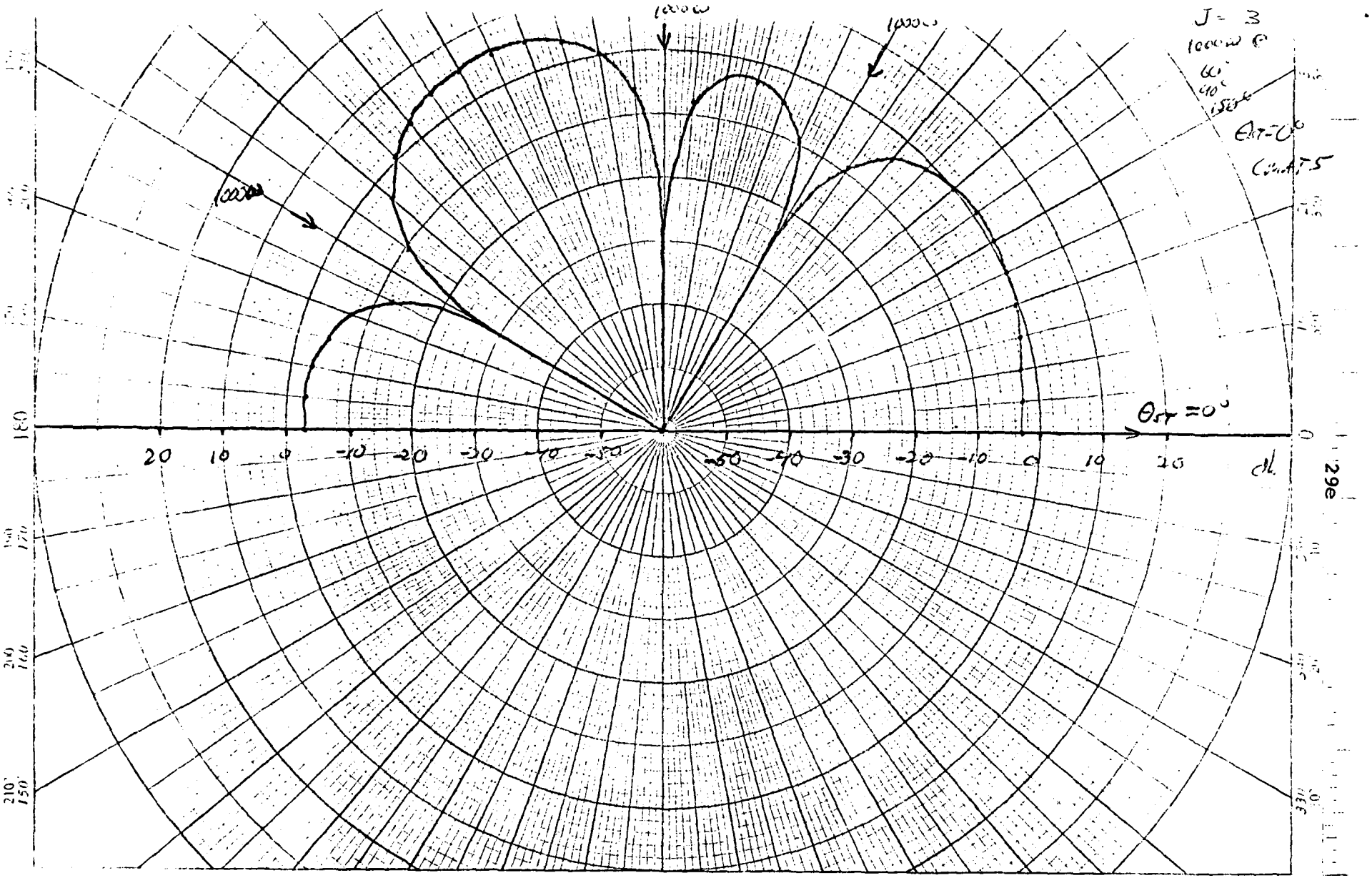

Fig. 29. SNR_o versus angle for a steering vector at 0°, with three Interferers each with $N_I = 10^3$W at 60°, 90°, and 150°, and N_a = S = 1W.

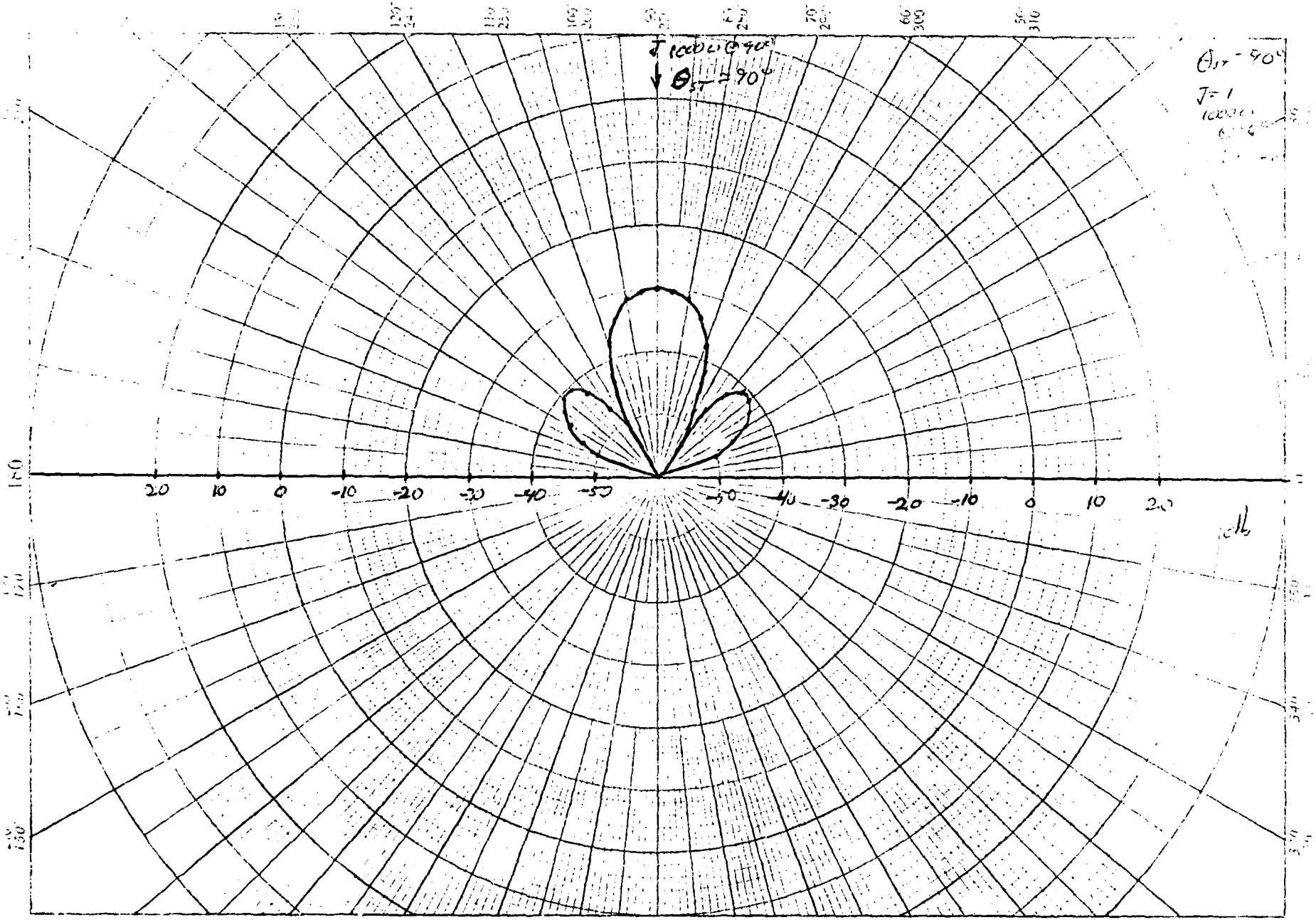

Fig. 30. SNR_o versus angle for a steering vector at 90°, with one Interferer of $N_I = 10^3 W$ at 90°, and $N_a = S = 1W$.

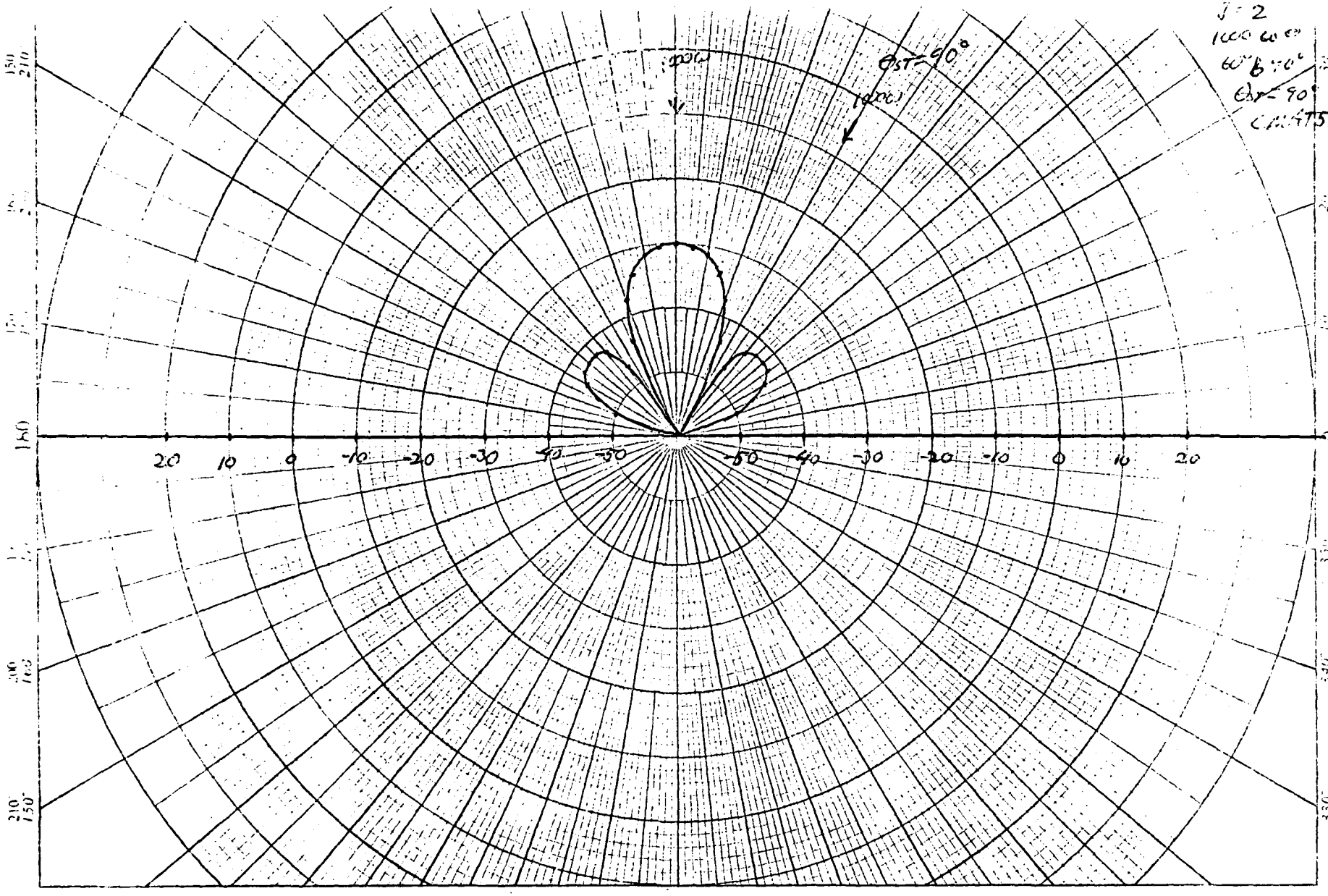

Fig. 31. SNR_c versus angle for a steering vector at 90°, with two Interferers each with $N_I = 10^3$W at 60° and 90°, and $N_a = S = 1$W.

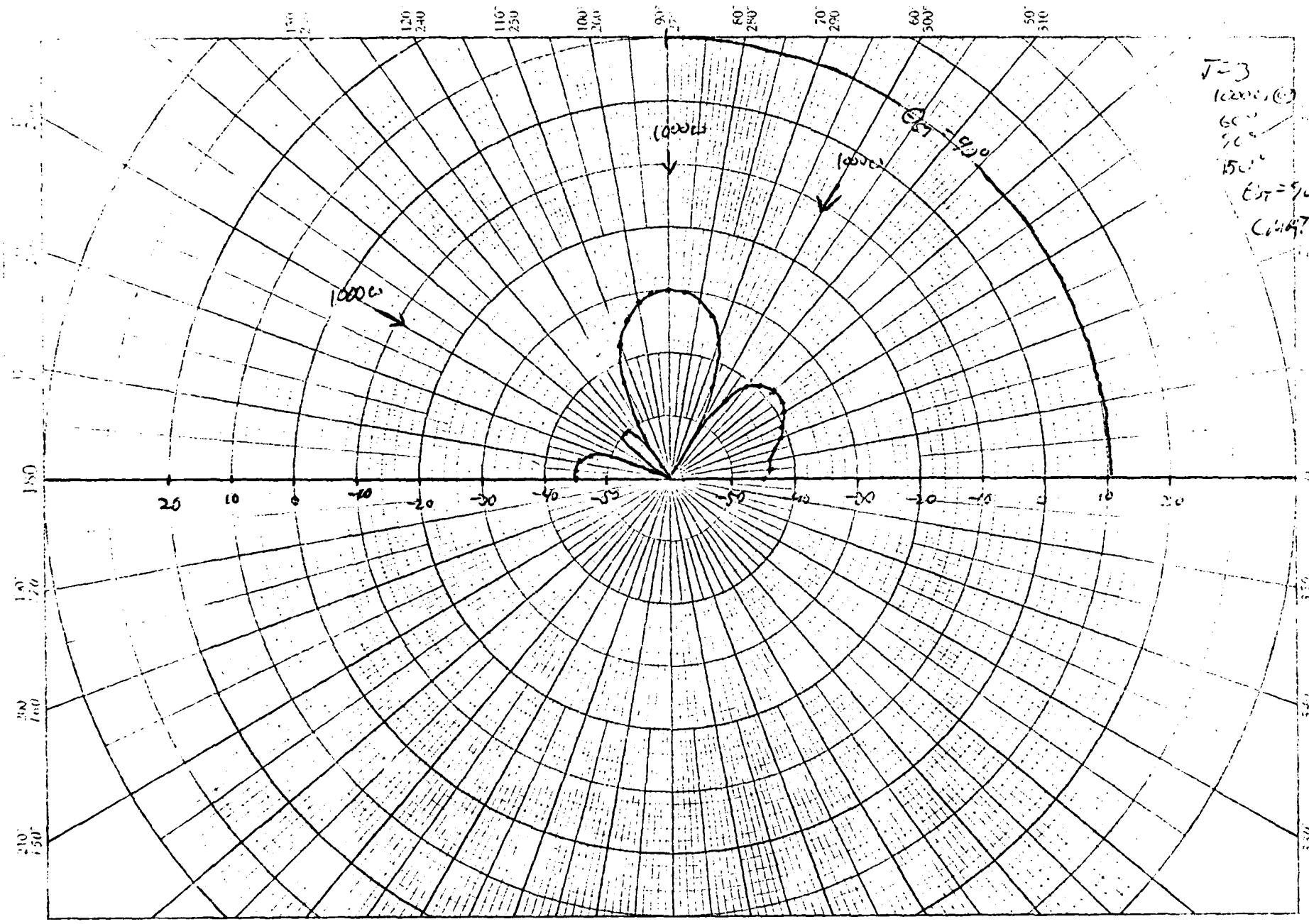

Fig. 32. SNR_o versus angle for a steering vector at 90^o, with three Interferers each with $N_I = 10^3$W at 60^o, 90^o, and 150^o, and $N_a = S = 1$W.

interferer which happened to be located in the chosen (assumed) steering vector direction, even though the signal may not be in the interference direction.

In Fig. 31 the 60° jammer is added. This happens to fall in a steering vector null and does not further degrade the pattern. The 150° jammer, when added, (Fig. 32) does change the pattern.

We see from the last example, that in choosing a minimum set of steering vectors one should have some redundancy. When one of the steering vectors is essential for coverage of certain signal arrival directions, an interferer which becomes too near that steering vector can reduce the coverage from that steering vector and leave a gap where no signal can be received. This gap is in addition to the gap which always forms near the jammer direction.

Figs. 33, 34, 35 and 36 show that the algorithm, in general, does not reduce the antenna power gain to zero in the direction of the interferer, but only reduces the gain by some rather large amount in the jammer direction. The reduction in gain is chosen so as to maximize the output SNR. When the interferer is much larger than either the signal or the ambient noise, then the optimum process requires a deep null at the jammer. If the interferer is weak, other factors become more important for maximizing output SNR. Note again in Fig. 35 that if by accident an interferer happens to line up with an assumed steering vector, the gain for that steering vector is suppressed in all directions.

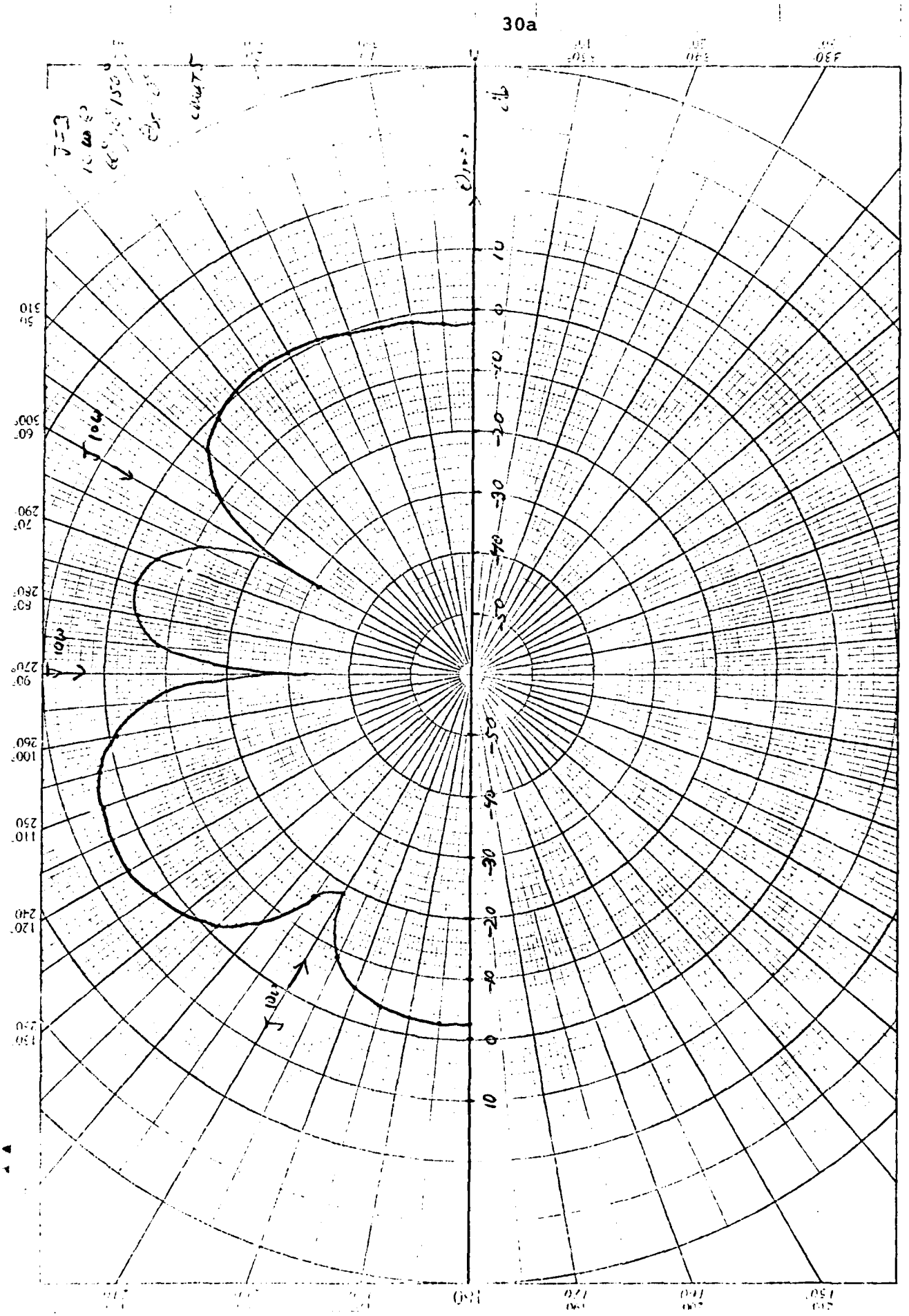

Fig. 33. SNR_o versus angle for a steering vector at 0^o, with three Interferers of N_I = 10W

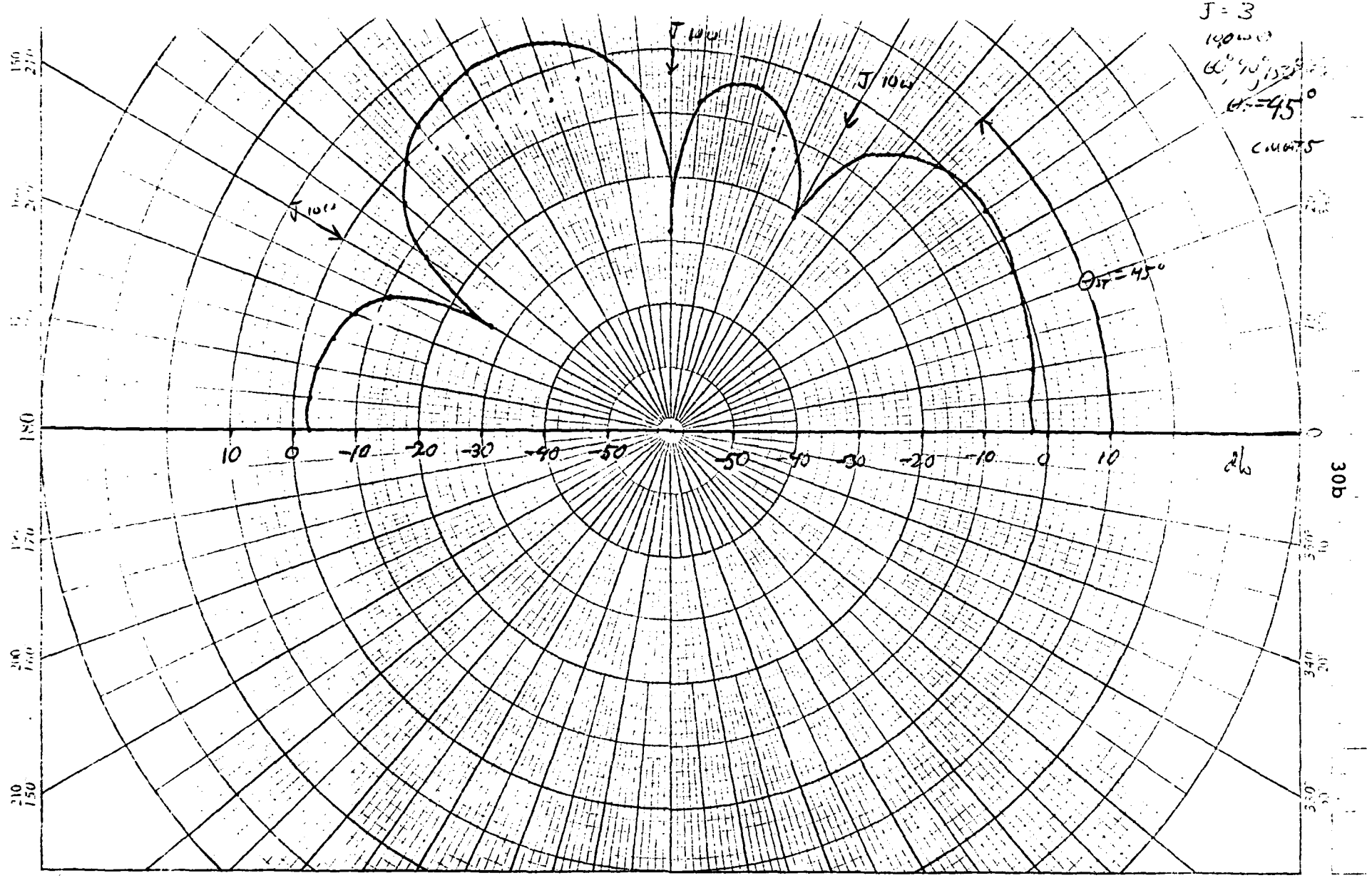

Fig. 34. SNR_o versus angle for a steering vector at 45°, with three Interferers of N_I = 10W each at 60°, 90°, and 150°, and N_a = S = 1W.

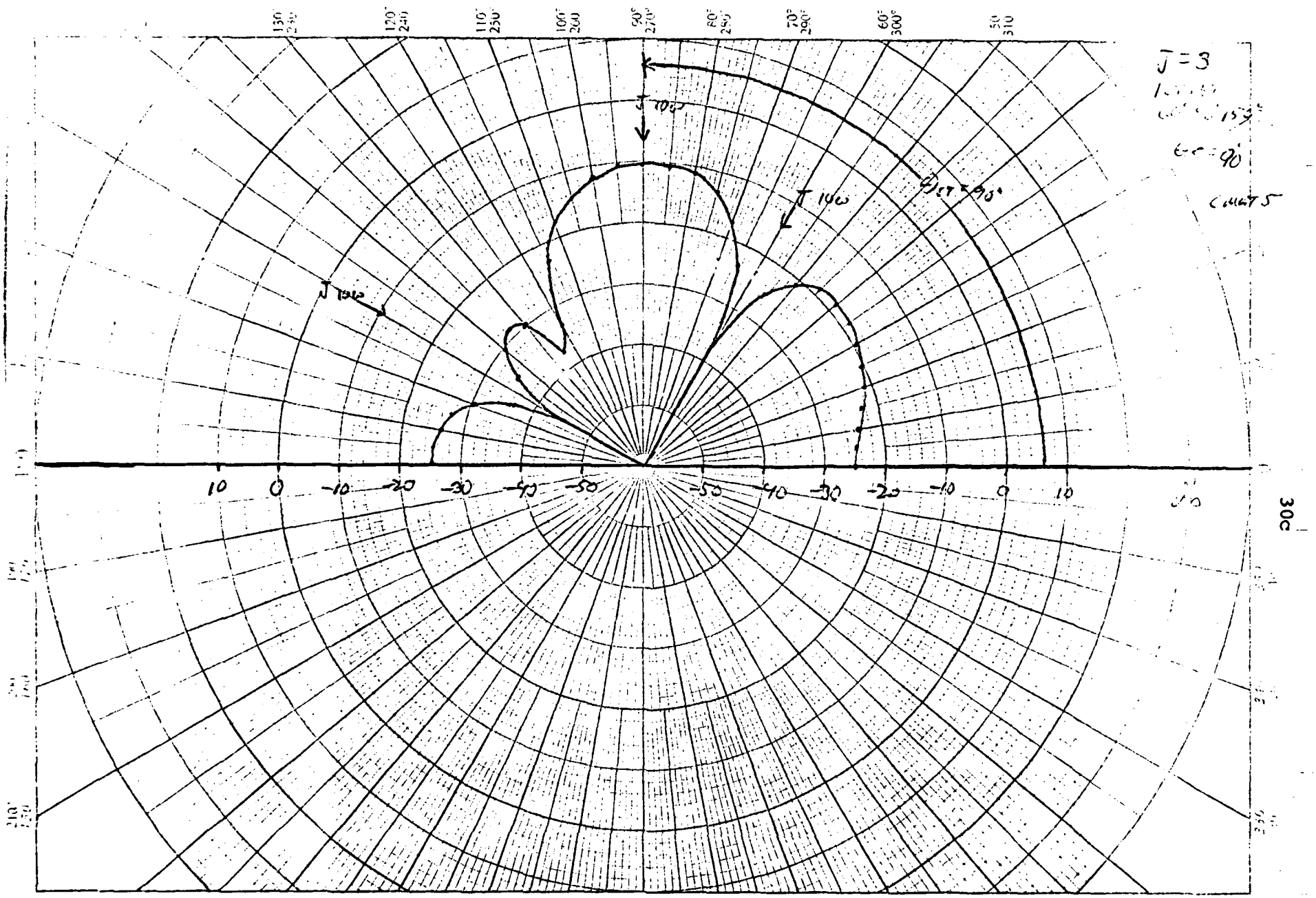

Fig. 35. SNR_o versus angle for a steering vector at 90^o with three Interferers of N_I = 10W
at 60^o, 90^o, and 150^o, and $N_s = S = 1W$.

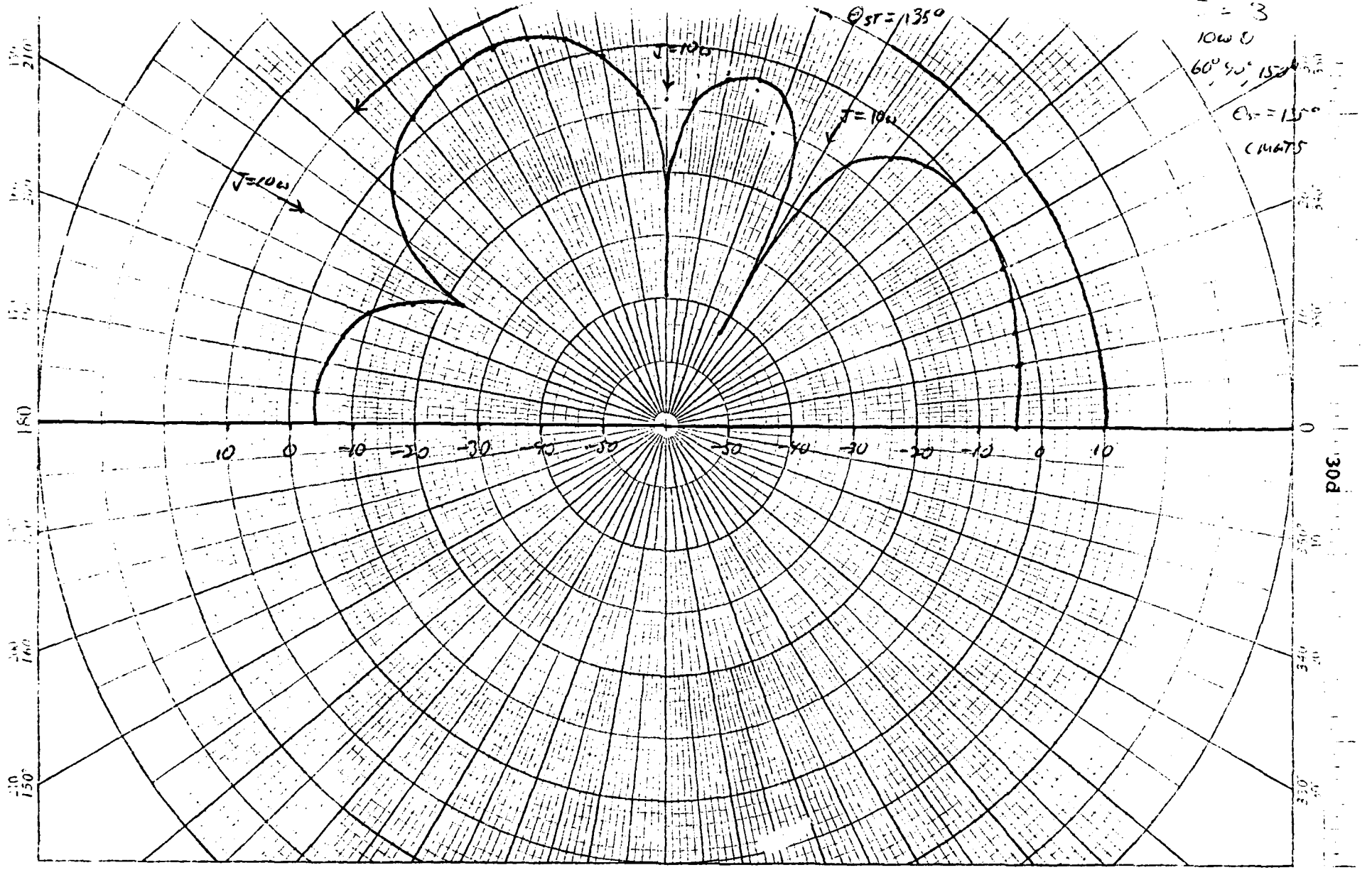

Fig. 36. SNR_o versus angle for a steering vector at 135° and three Interferers of 10W each at 60°, 90 °, and 150°, and N_a = S = 1W.

Figs. 37, 38, 39 and 40 were generated to determine how close to the steering angle a jammer must be in order for the interferer to completely suppress the antenna pattern in all directions. It appears that for suppression in all directions the interferer must be within a degree or so of the chosen steering angle for our 4 element array. Otherwise only a section of the ambient pattern is suppressed. Given 4 fixed steering angles, it is unlikely that more than one of 3 jammers would fall on any of the steering angles. However, there often are many other low level sources in the antenna field. All of these potentially can reduce the adaptive array gain, but only in proportion to their strengths.

Further examples demonstrate that 5 steering vectors, leads to acceptable losses at least during acquisition from the ideal performance which would be possible if the steering vector were directed at the actual signal source.

Fig. 41 assumes that the weights have been calculated for 4 steering directions, 0, 45, 90, and 135°. The signal has been processed for each of the weights. If the signal to noise output exceeds a preset threshold on any of the processed outputs, a signal is considered to be detected. The signal is then demodulated to see if a useful message is present. In Fig. 41, the solid line shows the improvement in SNR due to the array as a function of signal angle when no interferers are present. (The larger gains of the 4 steering directions (dotted lines) is always chosen). Close to the expected 6 db gain of the array is available over most angles. There is loss of ≈ 2db over omnidirectional coverage near 20° + 110°. This would be reduced by changing the 45° + 135° steering angles to angles closer to broadside. The ideal curve for steering angles always matched

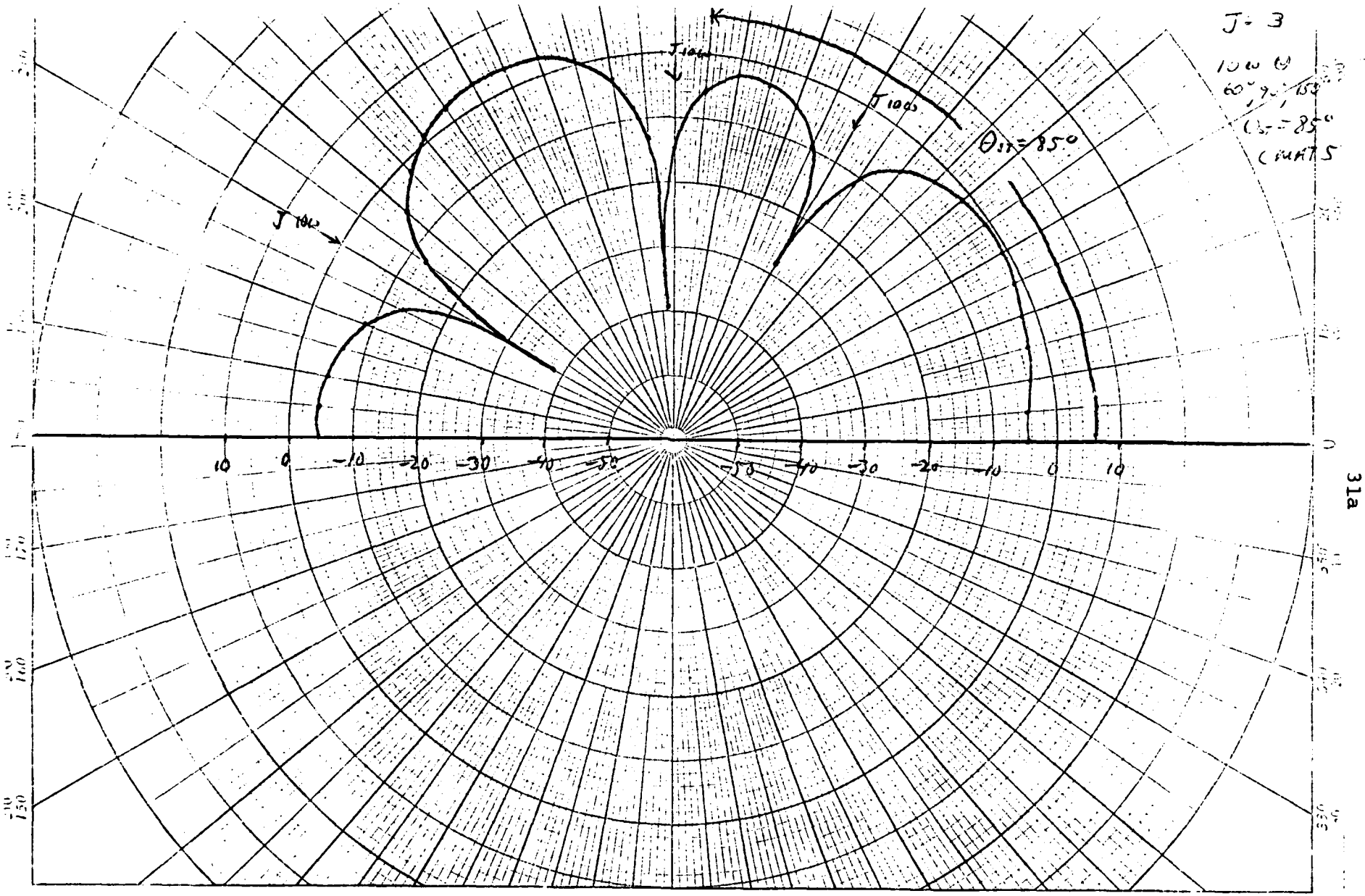

Fig. 37. SNR_o versus angle for a steering vector of 85°, with three Interferers of N_I = 10W each at 60°, 90°, and 150°, and N_a = S = 1W.

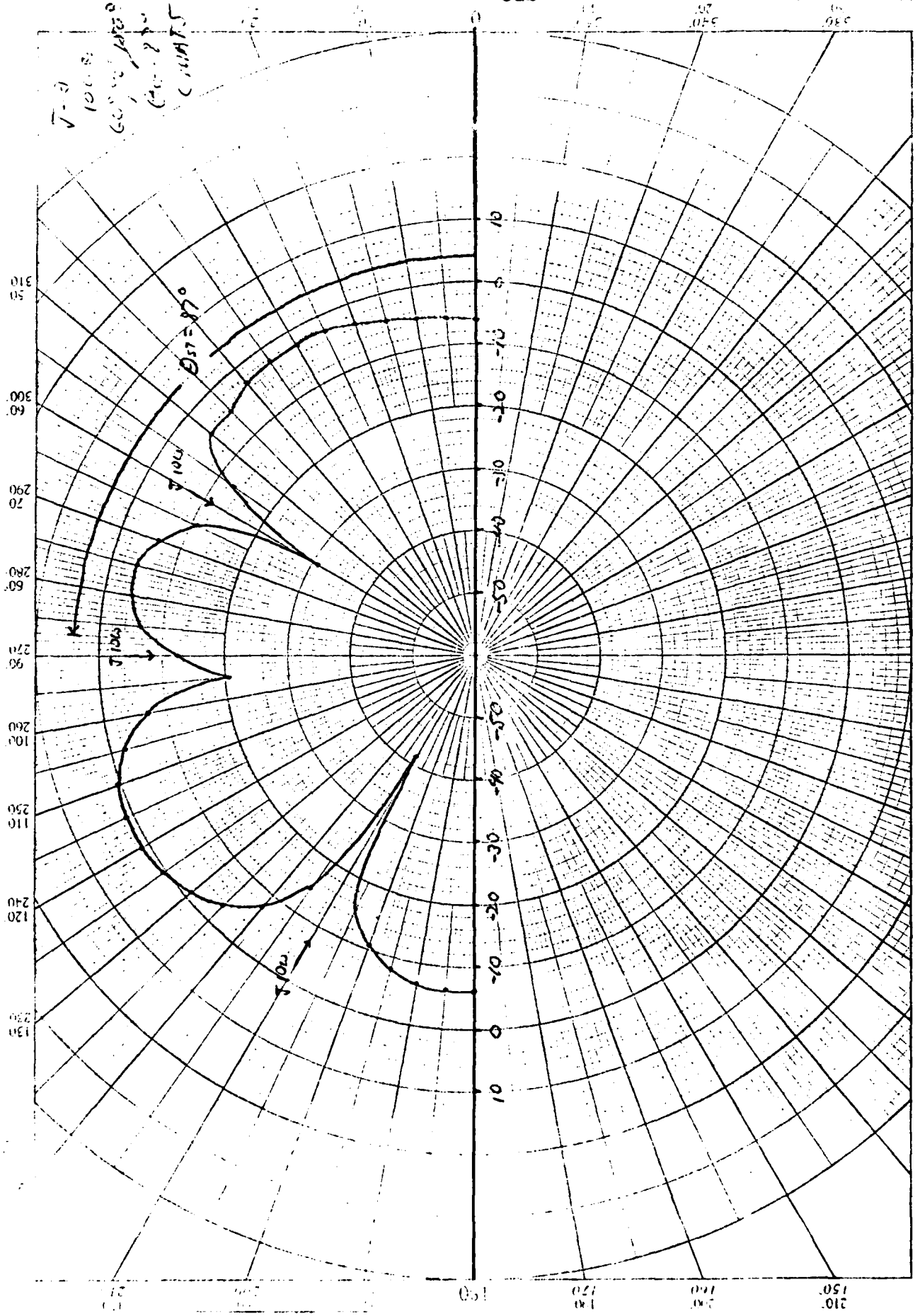

Fig. 38. SNR_o versus angle for a steering vector at 87°, with three Interferers at 60°, 90°, and 150°, and $N_a = S = 1W$.

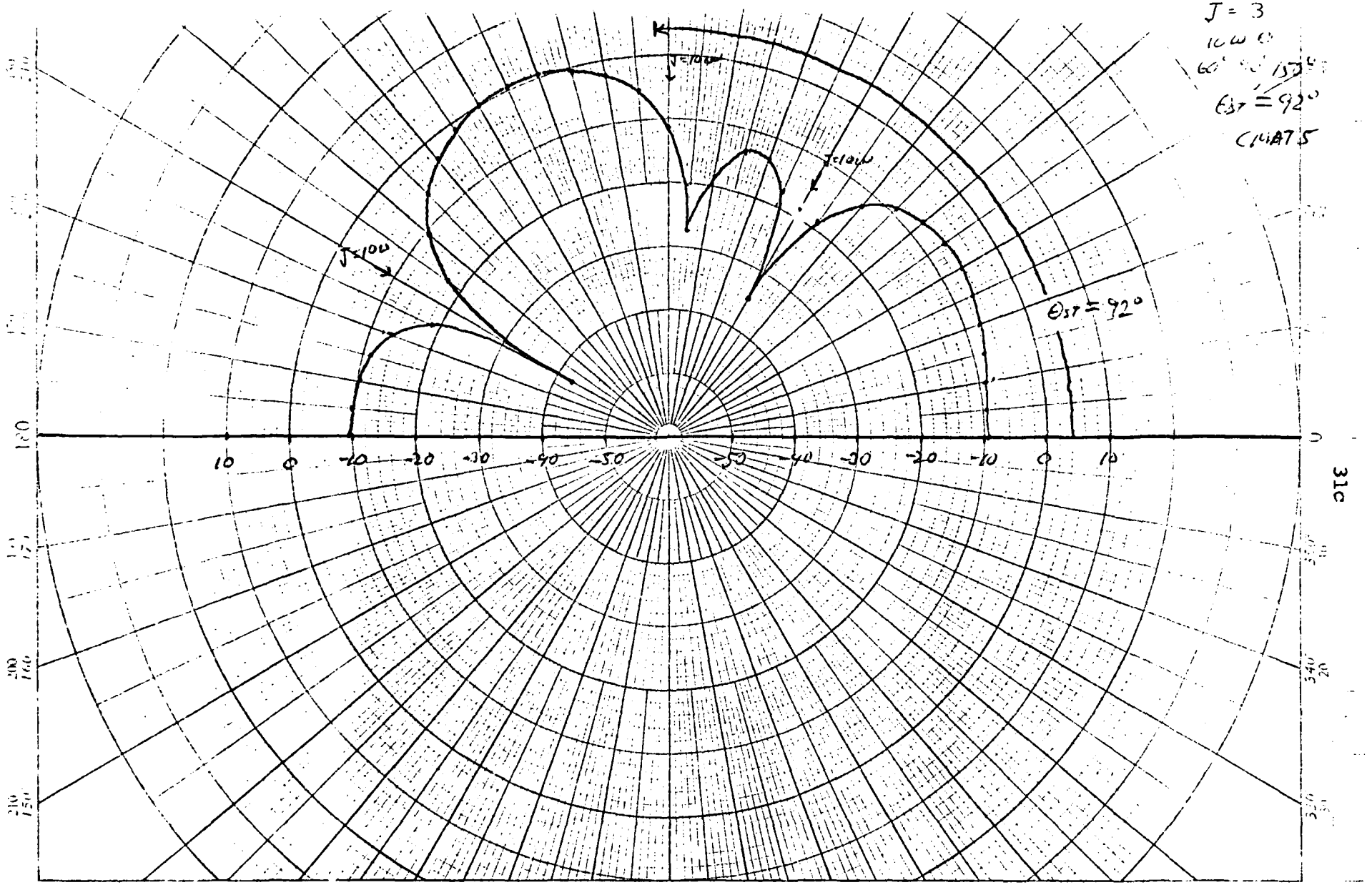

Fig. 39. SNR_o versus angle for a steering vector at 92°, with three Interferers of N_I = 10W each at 60°, 90°, and 150°, and N_a = S = 1W.

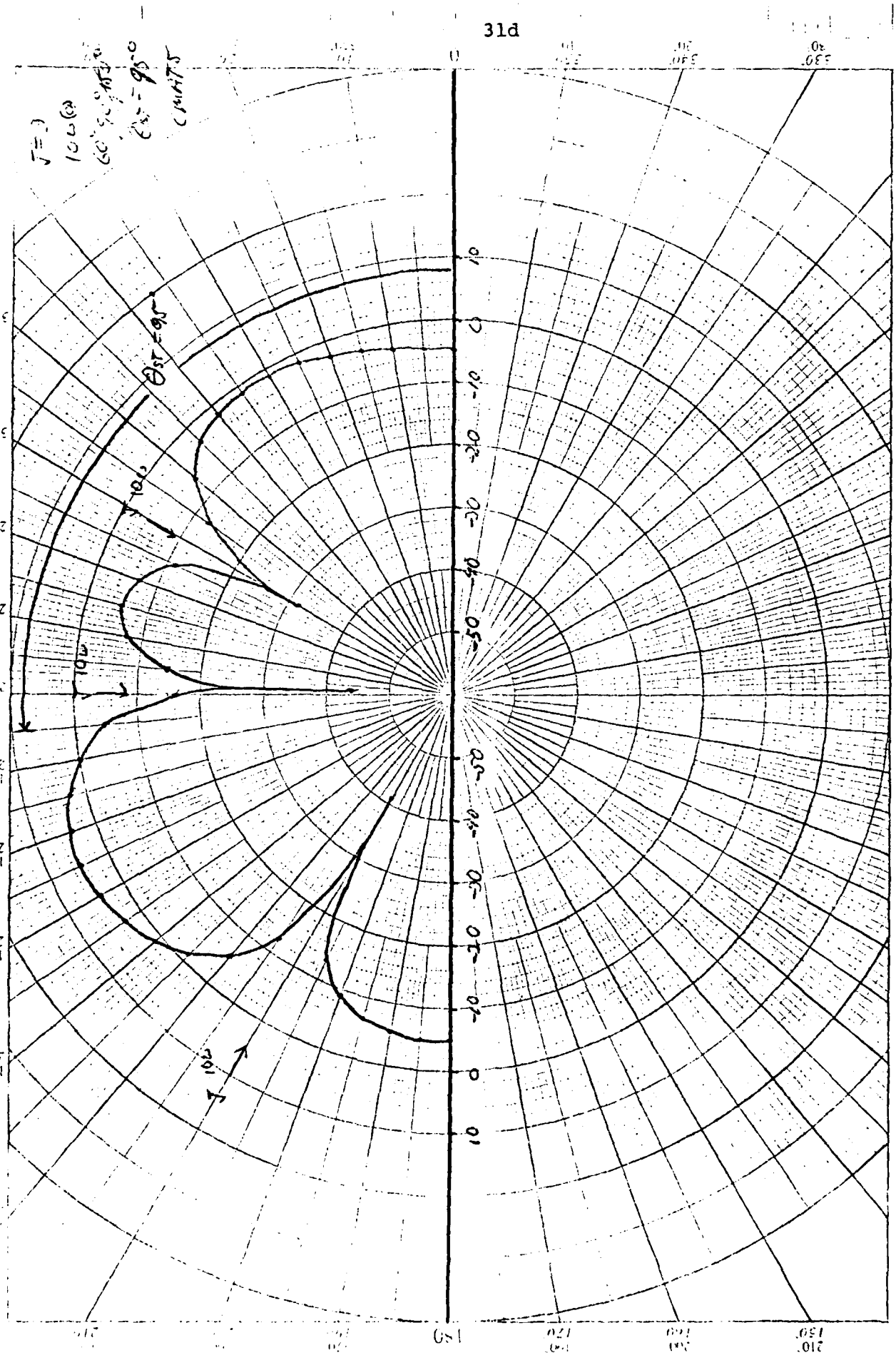

Fig. 40. SNR_o versus angle for a steering vector of 95^o, with three Interferers of N_I = 10W each at 60^o, 90^o, and 150^o, and N_a = S = 1W.

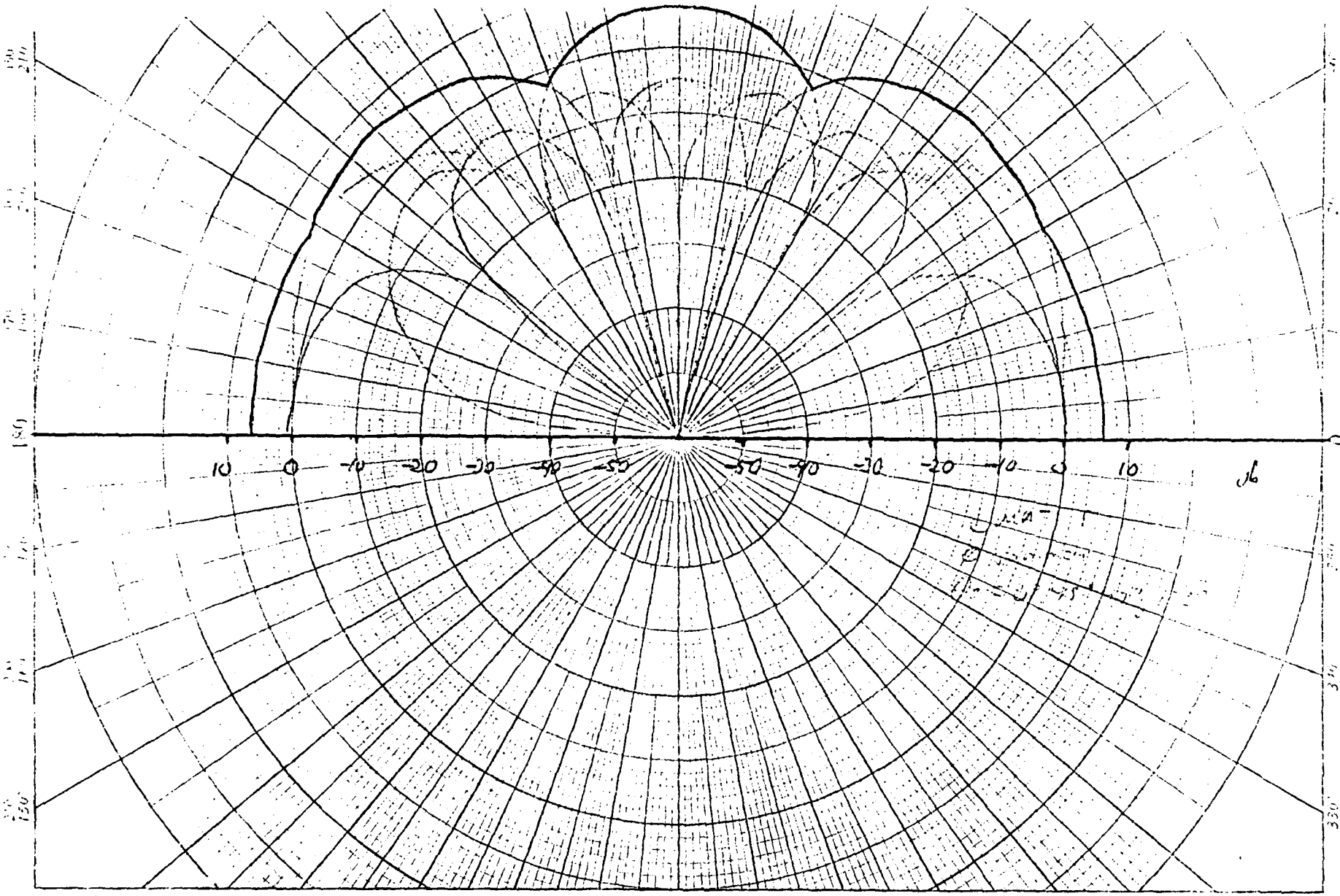

Fig. 41. SNR_o versus angle when the largest of 4 steering directions, at 0^o, 45^o, 90^o, and 135^o, is chosen, with no Interferers, and N_a = S = 1W.

to signal direction would be a 6 db circle.

When three interferers are present, the SNR available with these 4 steering vectors is shown in Fig. 42. Note that in this case one of the interferers happened to coincide in direction with the 90^{o} steering vector. This resulted in a large reduction in the antenna gain available for this steering vector (shown in dashed lines). If the 90^{o} interferer had been as much as 2^{o} or 5^{o} away from the 90^{o} steering vector, the antenna gain for the 90^{o} steering vector would have been much higher for all signals except those coming from the interferer direction. Fig. 43 shows the performance, for the same interferer conditions as Fig. 42, except that the correct steering vector is used for every angle.

We see that the worst performance with 4 preset steering factors occurs when an interferer happens to be exactly aligned with one of the preset steering angles. If the signal also happens to arrive from an angle near the interferer, its SNR is, of course, reduced both in the ideal case and when using only 4 steering vectors. However, with only 4 steering vectors, the SNR for some signals not near the interferer are also reduced somewhat from the ideal curve. This occurs only if the interferer is within $\pm 2^{o}$ to $\pm 5^{o}$ of one of the steering angles, which occurs with low probability. To avoid this potential (minor) problem, we suggest using 5 preset steering angles. If an interferer falls close to one of these, there will still be 4 other patterns which, combined, give close to theoretical optimum performance.

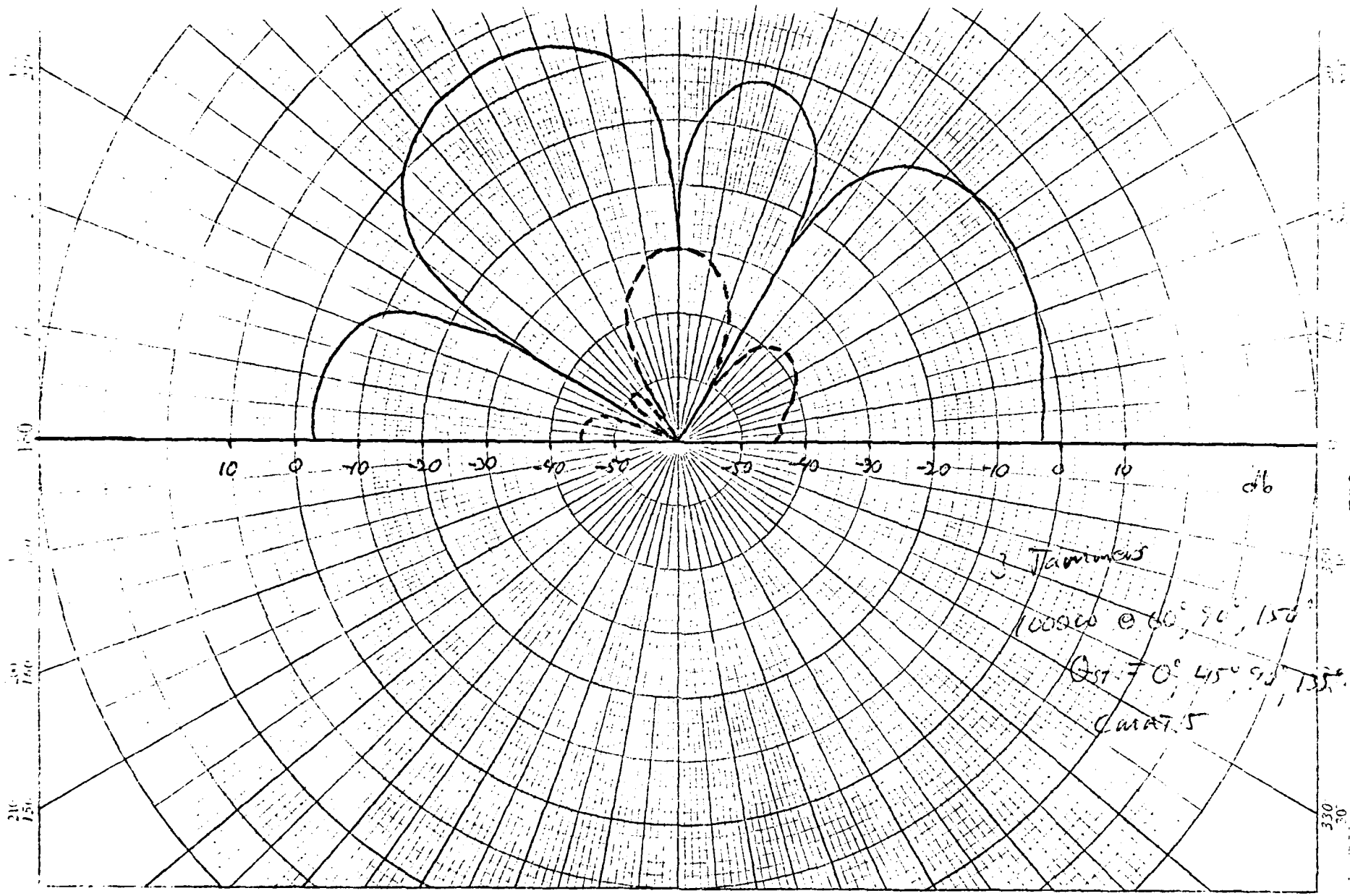

Fig. 42. SNR_o versus angle when the best of 4 steering vectors, at 0°, 45°, 90°, and 135° are used, with three 10^3W Interferers at 60°, 90°, and 150°, and $N_a = S = 1$W.

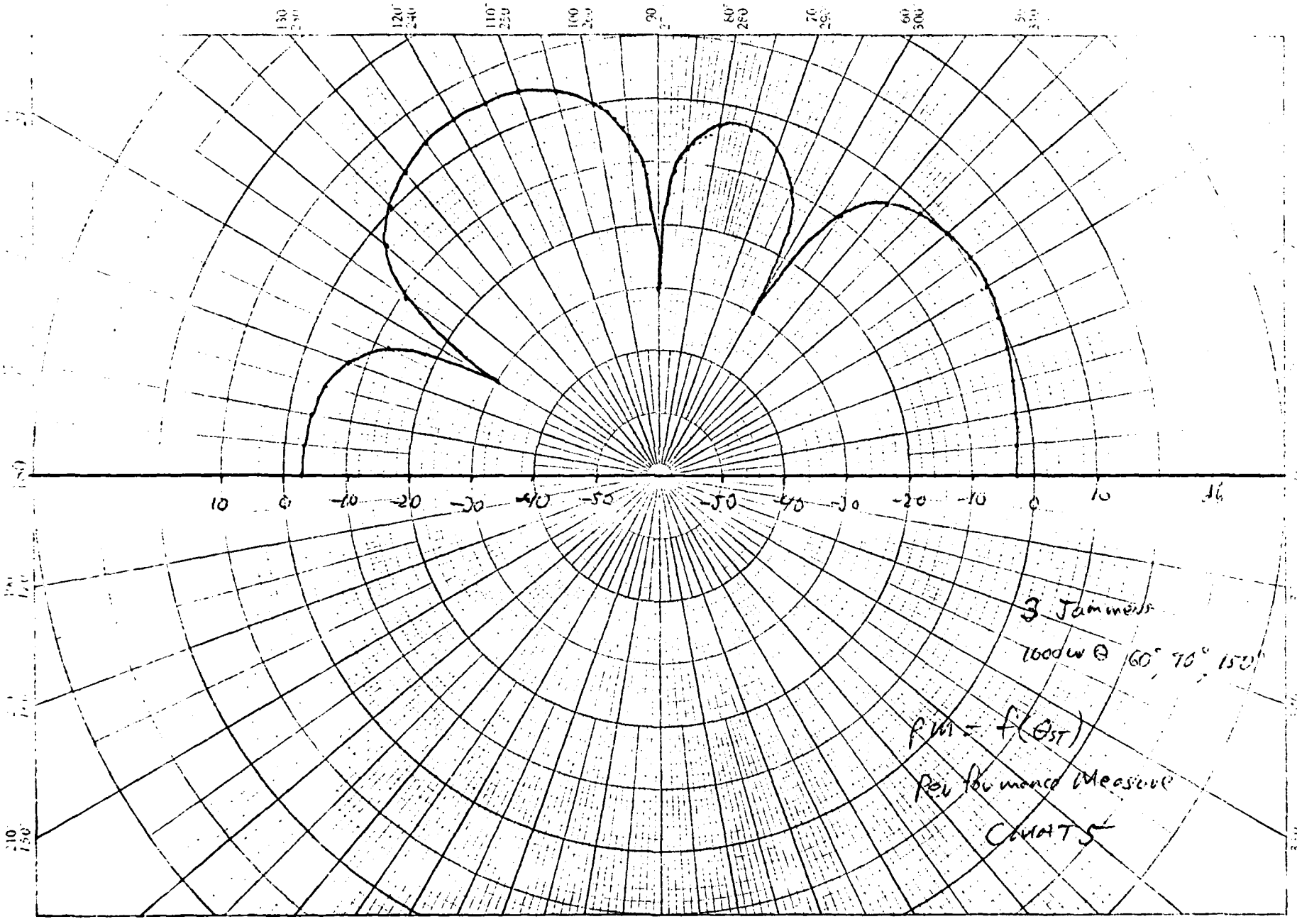

Fig. 43. SNR_o versus angle for the same Interferer conditions as in Fig. 42, where the correct steering vector is now used for each angle.

The conclusions are:

(1) The algorithm produces antenna patterns (equivalent to SNR patterns) which in the absence of interferers give quite broad receiving sectors. Three or four steering vectors cover 360^{o} adequately.

(2) The presence of interferers introduces narrow minima, not nulls, in the ambient patterns in the direction of the interferers. The depth of the minimum is automatically adjusted to maximize the received SNR when the signal comes from the direction of the steering vector.

(3) The received SNR is good over wide angles, both near the steering angle and in a"sidelobe area."

(4) Predicting what will happen in the real world is complicated because (a) interferers can appear in nulls of patterns formed by other interferers; (b) interferers can appear at the prechosen steering angles. In the first case the new interferer has no effect in pattern on SNR, but does use up a potential null produced by the covariance matrix. In the second case, the pattern in all directions is suppressed for that steering vector.

4.3 Effect of Number of Samples Used In Estimating Matrix

The results in Section 4.1 and Section 4.2 are theoretical and limiting in the sense that it is assumed the correct covariance matrix is known; i.e., the spatial angles and interferer and signal powers were inserted as analysis input. In the operational case, the covariance matrix must

be estimated from EM signals arriving at the elements. A basic item of interest is how many independent sets of samples of array output are needed to adequately estimate the covariance matrix. We first consider the ideal case where the steering vector is aligned with the desired signal direction.

The analysis and conclusions in Ref. 9 directly address this issue. The array processing envisaged in Ref. 9 consisted of both time and space sampling for SMI directly at the antenna elements. However, with intervening matched filters, as in our case, the filter-output samples retain their spatial integrity, even though the individual samples themselves are transferred by the matched-filter transfer-function. Therefore one should expect that the results concerning number of samples needed to estimate the covariance matrix reached in Ref. 9, should apply to our case.

We will briefly restate the results here. Ref. 9 uses a highly theoretical development to show that the normalized signal-to-noise ratio (rates of output SNR with ideal covariance matrix to output SNR with estimated matrix behaves as:

$$\text{Normalized SNR (db)} = 10 \log_{10} \frac{(K+2-n)}{K+1} \qquad (18)$$

where: n = number of independent samples used in estimating covariance matrix.

K = number of elements in the array

If one examines the 3 db loss point, one finds $n = 2K-3$. Hence, $n \simeq 2K$ if $K > 10$, for 3 db loss.

We should note that Equation (18) implies that only one sample is taken per element per sampling epoch; in the

general case, without matched filters ahead of the SMI processing, one will wish to take (say) ℓ samples per element, each separated by a small delay compared to the independent sample time, in order to prevent decorrelation of samples from wideband interferers. In that case, the n would be $n = 2k\ell-3 \approx 2k\ell$. In our case, with matched filters ahead of the SMI processing, there is much less advantage in taking more than one sample per element because, at current-(matched) sample time, the bandwidth is collapsed to that of the information bandwidth (see Section 5.2).

The result in Equation (18) was derived by finding the probability distribution of the normalized SNR (using a complex Wishart distribution), and verifying the result using simulation where 30 scatterers (as in radius clutter) provide the interference. In reviewing these results, our interest centered in the small element (K = 4) and small number of interferer ($n_j \leq 3$) case.

First we should note that the relatively small number of required samples from Equation (18) is surprising in the sense that, with these sample-sizes, the actual $\hat{M}$ is <u>not</u> close to M because of the cross-products resulting from the ambient and the large interferer terms. Upon analyzing this situation, we could show (see Ref. 13) that the important requirement is that the $\hat{M}$ eigenvalues line up with M eigenvalues. Therefore, only a relatively small number of samples may be required.

Fig. 44 shows degradation in normalized SNR as a function of number of samples n, and number of antenna elements K.

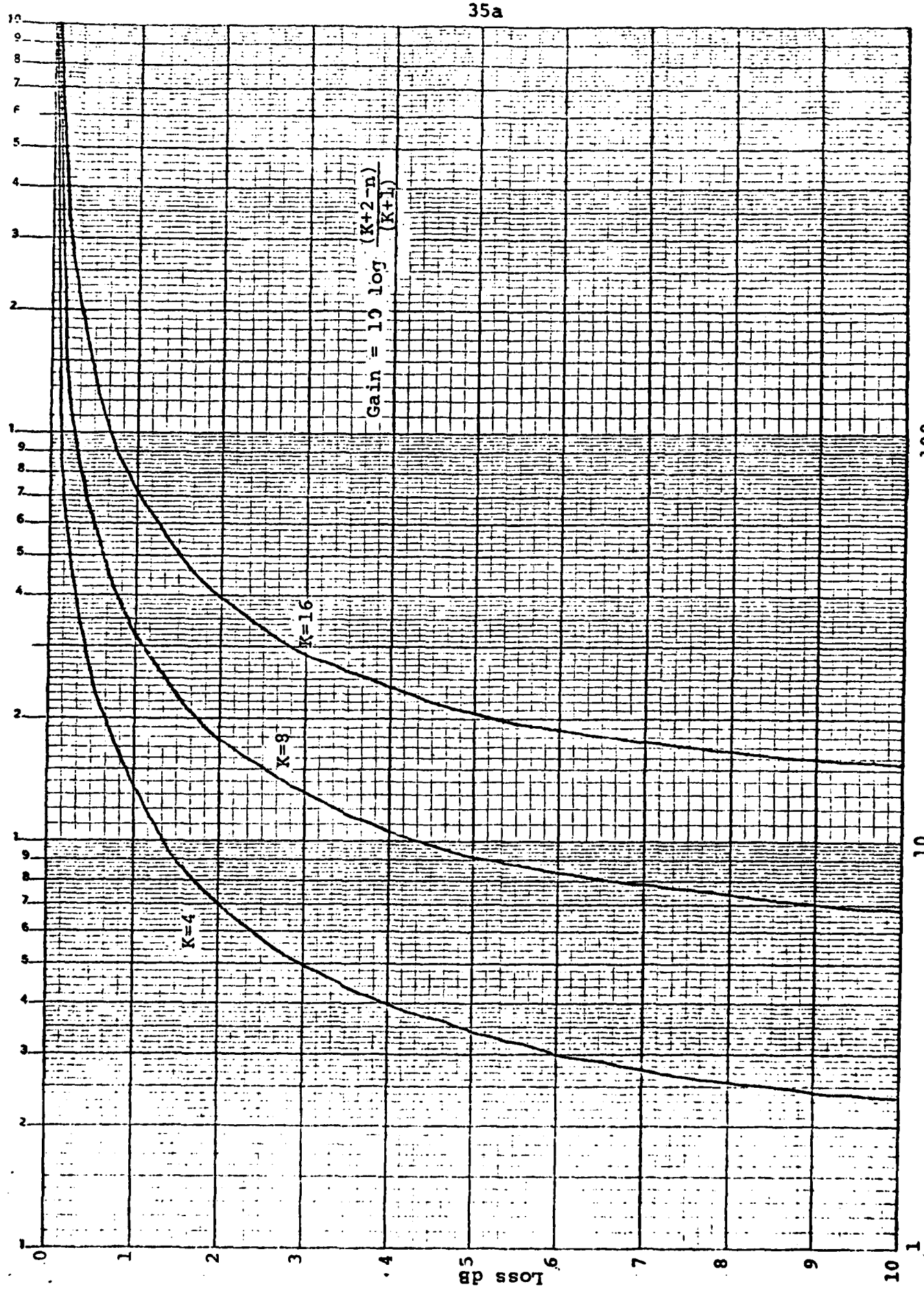

Fig. 44. Loss in normalized SNR_o as afunction of number of samples used in

It is based on Equation (18). For 4 element and 8 samples, the expected loss is 1.6 db. The number of samples required increases rapidly if better performances are required, or larger numbers of elements are used.. In Section 6, we report the results of a computer program which does both the matched filter time processing and the SMI array processing. The examples which have been computed appear consistent with the above theory. More examples would be needed for a statistical proof.

When the steering vector is not aligned with the received signal, the analysis is more complicated (Ref. 11). In general, more samples are needed for a given level of performance. The number of samples required depends on the degradation introduced by using the approximate steering vector. Since the degradation is small in our examples, we do not expect a significant increase in the number of samples required. However, we have no data to confirm this.

5. Comparative Advantage of PN Matched Filter Plus SMI

We will compare the performance here (using Fig. 6) with the general performance of the LMS closed-loop method depicted in Fig. 3 and the straight-forward method of using a power inverting adaptive array followed by a matched filter. These three appear to be the clear logical choices for combining PN with adaptive array.

In a communications application involving spread spectrum and adaptive arrays, the system must first acquire synchronization in both time (for the temporal processing) and direction (for the spatial processing) before the expected resistance to interference occurs. Therefore, it is the behavior in the acquisition mode that is the driving limitation in any system that combines spread spectrum with adaptive processing. First we recall that the asymptotic steady-state response of an LMS algorithm with known reference uses weights which are proportional to the same inverted noise covariance matrix that is estimated and used directly in any SMI processing. This leads us to conclude that the LMS loop of Fig. 3 and our procedure of Fig. 6 should give the same nominal steady-state results if: 1) the PN modem in the reference loop is synchronized; and 2) only narrowband or CW interference is encountered. We will argue that the PN matched filter arrange-

ment using multiple steering vectors is superior in the acquisition mode (matched time and direction unknown) and when matched-spectrum interference is contemplated.

First consider the case where an adaptive array (as in Fig. 2) is followed by a PN matched filter. In this case the adaptive array cannot separate signal samples from noise samples (for a continuous signal), and the array will treat the intended signal as another interferer: a signal will be nulled in accordance with its strength. Such "power inversion" algorithms (Ref. 10) can succeed if the ensueing temporal processing, via the matched filter, can restore a nulled signal to an adequate minimum output SNR. Even if this occurs, nulling the signal has two significant disadvantages over either the Fig. 3 closed-loop method or our method (Fig. 6): 1) degrees of freedom are consumed by the nearby (intended) signal transmitters, and 2) the field-of-view of the receiver has a segment or slice removed, that may deny access to another signal that is in or near the null.

Therefore, we believe it is basic to attempt to prevent nulling the signal when combining PH spread spectrum with adaptive arrays. Since the methods of Fig. 3 and Fig. 6 both have this property, we will emphasize their comparative properties.

It is necessary to emphasize that the significant difference between the two systems does not focus during steady-state, but occurs in the manner and success with which

they acquire in the acquisition mode, under worst case conditions. We will compare the two approaches in two aspects: acquisition and bandwidth effects.

5.1 Acquisition Comparison

Consider first the spatial uncertainty in the acquisition mode. Using a matched filter followed by SMI affords a natural way to handle spatial uncertainty: use parallel processing consisting of multiple apriori steering vectors corresponding to hypothesized signal directions, utilizing digital processing. In the above section we demonstrated by a series of experiments that one needs only 4 or 5 such apriori beams if the number of elements is 4.

In effect, closed-loop algorithms, such as in Fig. 3, tend to naturally be "serial" and analog, while open-loop ones extend naturally to parallelism and open-ended digital processing.

The next pertinent issue is transient response of the adaptive processing. As is well-known, the time-constant of closed-loop schemes depends on both the loop gain and the level of the received interfering power. The response time is limited by filter bandwidths and loop stability requirements. As a result, the performance of a scheme as in Fig. 3 is dependent on the actual signal, ambient, and interference levels encountered. With our use of the SMI method, convergence is independent of the interference environment.

Whereas conventional SMI will require use of 2K-3 consecutive independent (waveform) samples, note that with matched filters one can compute the necessary samples used for estimating the covariance matrix for the weights at each current sample, using the current contents of the transversal filter, by using a rapid digital processor. This is only slightly different from using the (say) eight previous filter-output samples to evaluate the weights for the current sample.

In any event, the transient response for either approach is essentially instantaneous, and independent of the received levels. This should be especially important in practice, especially for interferers that would attempt special methods such as blinking.

We now consider temporal synchronizing. To be truly interference-resistant, the PN modem in Fig. 3 must utilize a "long-code", so that time-sync must be searched over some apriori-established time-uncertainty. As noted in Ref. 2, the traditional way to accomplish time-sync is to use code slewing, where the local PN-code generator is run faster (or slower) than the incoming signal code. Hence, relative to the onset of intended signal transmission, there is added delay incurred between signal-onset and code-alignment. This causes what is sometimes called the "great race" problem: if the array time constant is faster than the modem acquire time-constant, the array will null the signal before it can be acquired by the modem.

This delay does not occur with our arrangements, because the matched-filter approach implies that a certain PN segment is anticipated, and is set-up in the filter. The matched-filter must anticipate maximum range-uncertainty plus clock drift. Currently emerging CCD and SAW programmable matched filters permit examing different range bins at an internal processing speed that is higher than the spread-spectrum bandwidth. In any event, so long as some method is found to provide two[1.] full-segments of a PN sequence, there will be no additional delay due to time sync, after onset of signal. One can avoid interference-exploitation of the two-period transmission by making it impractical to predict the PN segment that will be used.

5.2 Performance With Wideband Interference

A key issue that must be emphasized, when combining adaptive arrays with spread spectrum, concerns the degraded array performance with the conventional single-tap approach (as in Fig. 3) when the interferer uses a spectrum-matched interference signal. As one increases the intended signal bandwidth via spread-spectrum to increase temporal processing gain, one of course must anticipate possible use of an interference signal of equal bandwidth.

When array processing precedes temporal processing, as in Fig. 2, a de-correlation of interference signals occurs due to the finite-length of the array, at all incidence angles except broadside, if one uses only one tap per antenna element.

---

1. It is possible to avoid requiring two identical segments, but this is beyond the scope of the effort here.

This will cause the array processing gain to decrease linearly with increase in (PN) signal bandwidth. Adding multiple taps to each element as described in Ref. 3 and Ref. 5 can essentially remove the de-correlation effect.

One can demonstrate the result of de-correlation, in the steady-state, by assuming an interference spectral shape, finding its autocorrelation, and then computing the expected value of array cancellation as a function of interference bandwidth and maximum array time-delay (for end-fire, if a linear array) , as was done in Ref. 5. In Appendix E we calculated the de-correlation effect if only a single tap is used by first assuming an autocorrelation function for the interference and a single interferer. Then, using the (presumed known) corresponding covariance matrix of the interferer, the smallest eigenvalue (which is the steady-state solution) is found, as a function of bandwidth. In general, it was found that, with the single tap, the array processing gain decreases linearly with increase in interference (and PN signal) bandwidth (see Appendix E). As noted, the chief consequence of this issue is that the system of Fig. 3 must be altered to include multiple taps per antenna element.

To see how our approach (see Fig. 6) or a "code-stripping" approach, as in Fig. 4, would fare in this de-correlation aspect, we assumed one interferer (see Appendix E) and a broadside signal with unity power. The process output, $z(t)$ was then formed, in terms of the output interference power. Similar to the procedure used in Ref. 5, we assumed an autocorrelation formation for the filter output samples due to interference.

We then assumed the interference bandwidth matches that of the signal, and evaluated the minimum eigenvalues, as before. We found that, using the assumed exponential autocorrelation, that the interference output power is significantly lower than was the case for the previous (single tap) conventional arrangement (Fig. 3.). Although this was done for a single interferer, we believe similar results will hold for multiple interferers, up to the permissible degrees of freedom. Furthermore, the advantage for temporal processing ahead of spatial processing shown in Ref. 14 is dependent on the nature of the RF filter that could precede the temporal processing.

We conclude, then, that if the closed-loop arrangement used only a single tap per element, as in Fig. 3, that our arrangement (as in Fig. 6) would outperform it by an amount dependent on filter assumptions. However, if the closed-loop arrangement included multiple taps, it is likely that the steady-state performance of the two arrangements would be essentially equal.

AD-A112 114 MICHIGAN UNIV ANN ARBOR COOLEY ELECTRONICS LAB F/G 9/3
PN MATCHED FILTERS IN ADAPTIVE ARRAYS.(U)
SEP 81 M P RISTENBATT, T G BIRDSALL DAAG29-79-C-0220
UNCLASSIFIED 017818-F ARO-17104.1-A-EL NL

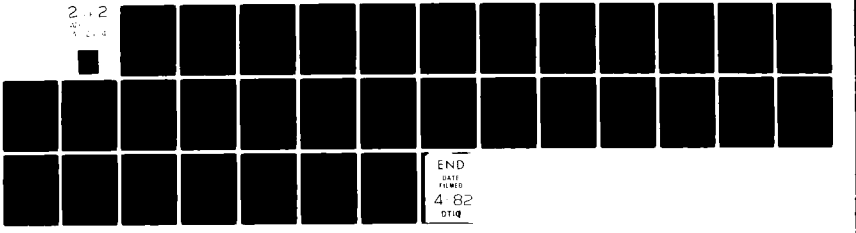

END
DATE FILMED
4 82
DTIC

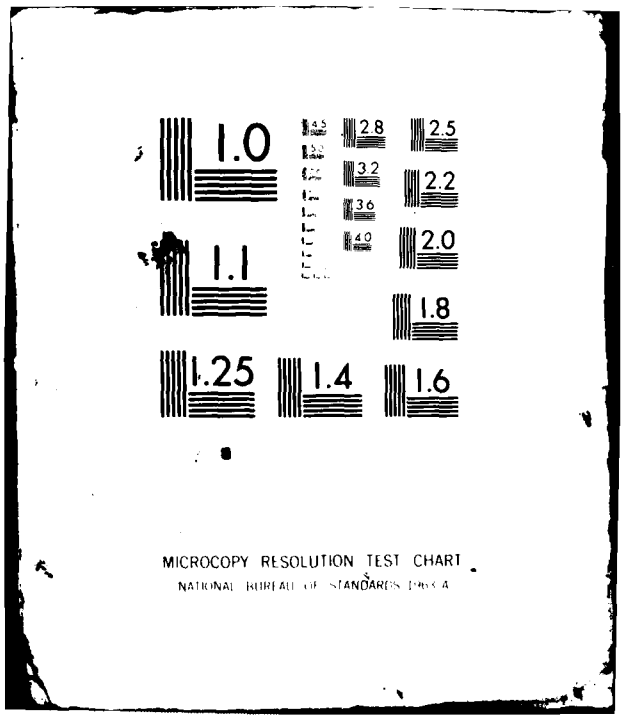
1.0
1.1
1.25
1.4
1.6
1.8
2.0
2.2
2.5
2.8
3.2
3.6
4.0
4.5
5.0
MICROCOPY RESOLUTION TEST CHART
NATIONAL BUREAU OF STANDARDS 1963 A

6. Simulation Demonstration

We constructed a computer-based demonstration of the arrangement shown in Fig. 6 both to provide evidence that the process works, and to serve as a learning aid. Now we estimate the covariance matrix from simulated noise samples, rather than assume it is known (as in Sec. 4.2). A PN matched-filter of length 255 was used for the temporal processing, and a 4-element linear array spaced at $\frac{\lambda}{2}$ was used. Six apriori steering vectors were used, placed at angles of $\pm$ 15° $\pm$ 45° and $\pm$ 75° from broadside. The adaptive array output for each of these was computed on a sliding window basis. The outputs are compared, with a threshold, looking for signal peaks. An estimated output SNR (based on a limited number of noise samples) was also calculated for each steering vector.

The desired signal consisted of 2 or more periods of a 255 bit maximal sequence. This signal was assumed to phase modulate a UHF carrier. The source was assumed to be located at +15°, which corresponds to one of the apriori steering vectors. The phase of the received signal at each antenna element was calculated. The computer was used to generate the complex samples of the demodulated signal for each antenna at the rate of 4 complex samples per sequence bit. Similar complex samples for the interference and ambient noise were added to the signal samples.

The matched filter outputs for filters consisting of one period of the sequence were calculated for the in-phase and quadrature component at each antenna element on a sliding window

basis.[1.] The window moves in increments of a sequence bit to avoid missing a signal peak. The resulting set of complex numbers are the signal inputs to the adaptive array processing.

One or two interfering sources were simulated by random number generators. They were assumed to transmit carriers phase and amplitude modulated by Gaussian noise. For assumed interference, source powers and source positions, the received amplitudes and phases were calculated. Corresponding random in-phase and quadrature demodulated interference samples were generated in the computer and added to the corresponding received signal samples. For each antenna element, independent in-phase and quadrative samples of Gaussian noise, representing ambient noise, were also generated and added to the signal samples.

The signal-free complex noise samples for calculating each sample covariance matrix were obtained from the outputs of the matched filter with the window displaced from the correct matched signal output. From 1 to 200 samples of the covariance matrix were calculated and averaged to investigate the effect of the number of samples used in the estimate of the covariance matrix. The nearest noise sample was displaced 2 bits from the expected signal output and the additional samples as required were displaced further in increments of ½ bit; i.e. 8 signal-free noise samples were obtained by sampling between 2 bits and 6 bits from the expected signal position at 2 complex samples per bit. For

---

1. The autocorrelation function of a maximal sequence of length L has a peak of amplitude L but is not exactly zero between peaks. It can be made exactly zero by using a phase modulation slightly less than 180^{o}. It can also be made exactly zero by using a modified "matched filter": a "replica reference" consisting of only the $\frac{L-1}{2}$ "ones" in the sequence. This was done in the program described here.

each noise sample position, a sample covariance matrix was calculated between the samples from the different antenna elements.

The estimated covariance matrix was obtained by averaging the sample matrices. It was then inverted and multiplied by one of the apriari steering vectors to find one set of combining weights. The matched filter signal output was combined using these weights as one possible signal output. This process was repeated for each of the 6 assumed steering vectors. The complete process from finding a new covariance matrix to calculating 6 more possible signal outputs was repeated continuously on a sliding window basis.

While this general program is flexible and can be used for a number of exploratory purposes, we will here emphasize three basic aspects: 1) the behavior of the array-pattern as a function of the number of samples used in estimating the covariance matrix, for various assumed conditions and 2) the behavior of the output time-axis in the vicinity of the peak (for various conditions) to demonstrate typical behavior.

6.1 Behavior of Array-Patterns Versus N

Here we report how the simulation array patterns behave, as a function of the number of samples used in estimating the covariance matrix. The series of results portrayed in Fig. 45 through Fig. 49 describe the array pattern, which is again equivalent to an output SNR, for one interferer through 5 interferers, respectively. For each Figure, the results are shown for estimating the covariance matrix based on either n = 2,4,8,16,32,200. The array pattern, in each case, for n = 200 can be regarded as the best simulated operating pattern. As can be seen, the array pattern in all cases has essentially the final "best" form for $n \geq 8$.

All the results in Fig. 45 through Fig. 49 were obtained by using one steering vector in the direction of the assumed signal direction of 1^{o}.

6.2 Behavior of Output Time Axes and SNR_o for n = 8

Using 8 consequentive samples directly ahead of the "current-value", on a sliding window basis, the time-axis behavior in the vicinity of the "matched point", at which acquisition should occur, is shown in Fig. 50 and Fig. 51. In Fig. 50, the time-axis output in the vicinity of 8 consequetive peaks corresponding to signal epochs is portrayed for the six steering vectors, with one interferer of $N_I = 10^3$ at 67^{o}, a signal of S = 1W at 15^{o}, and N_a = o.1W. The ideal SNR_o, using the given data in Eq. 7a, was found to be $SNR_o \simeq 380$. The simulation run, in the steering direction of 15^{o}, produced an

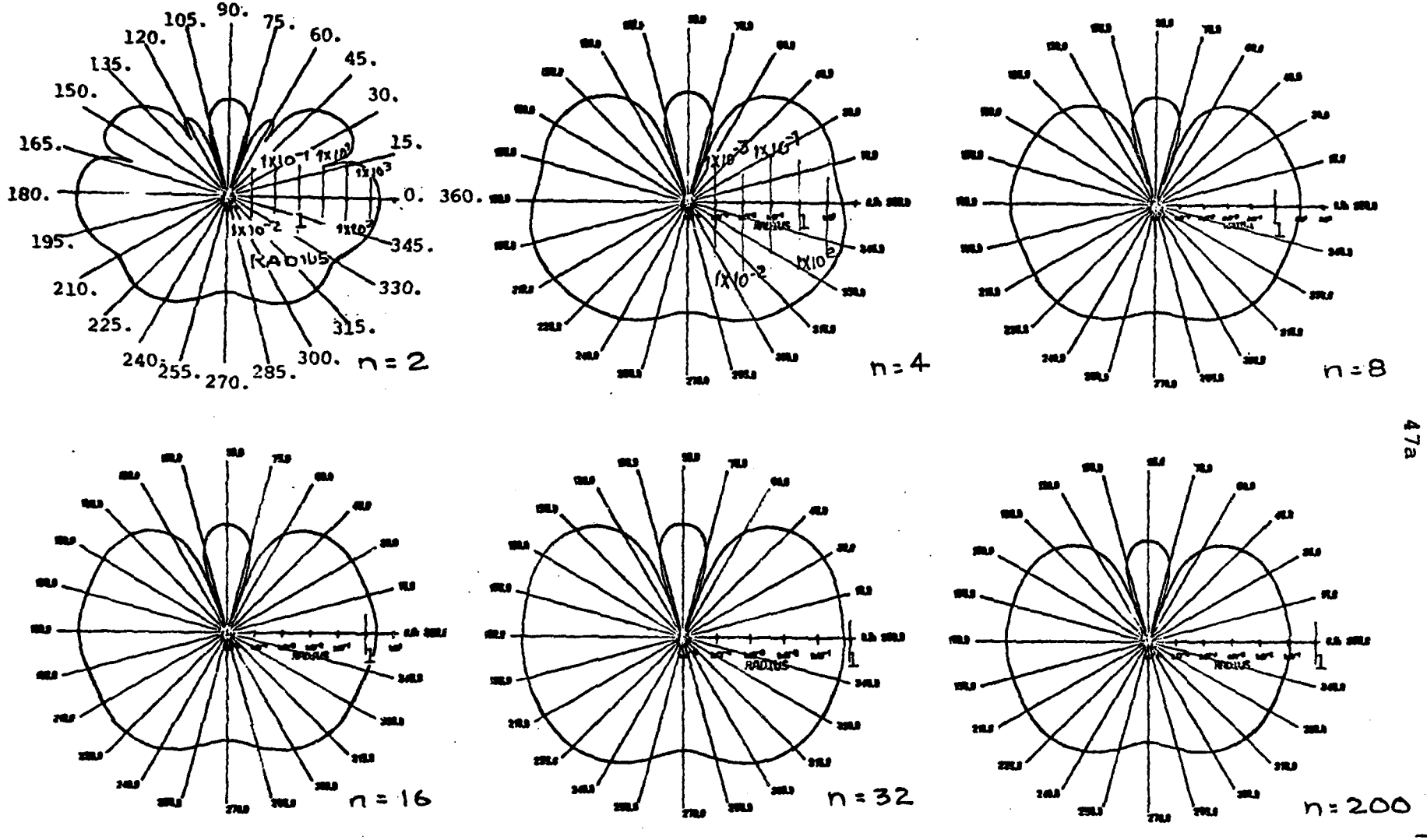

Fig. 45. SNR_o versus angle, when covariance matrix is estimated from arriving signals, with one Interferer of $N_I = 10^3$W at 70°; for averaging over 2,4,8,16,32, and 200 samples. (N_a = 0.1W, S = 1W at 1°)

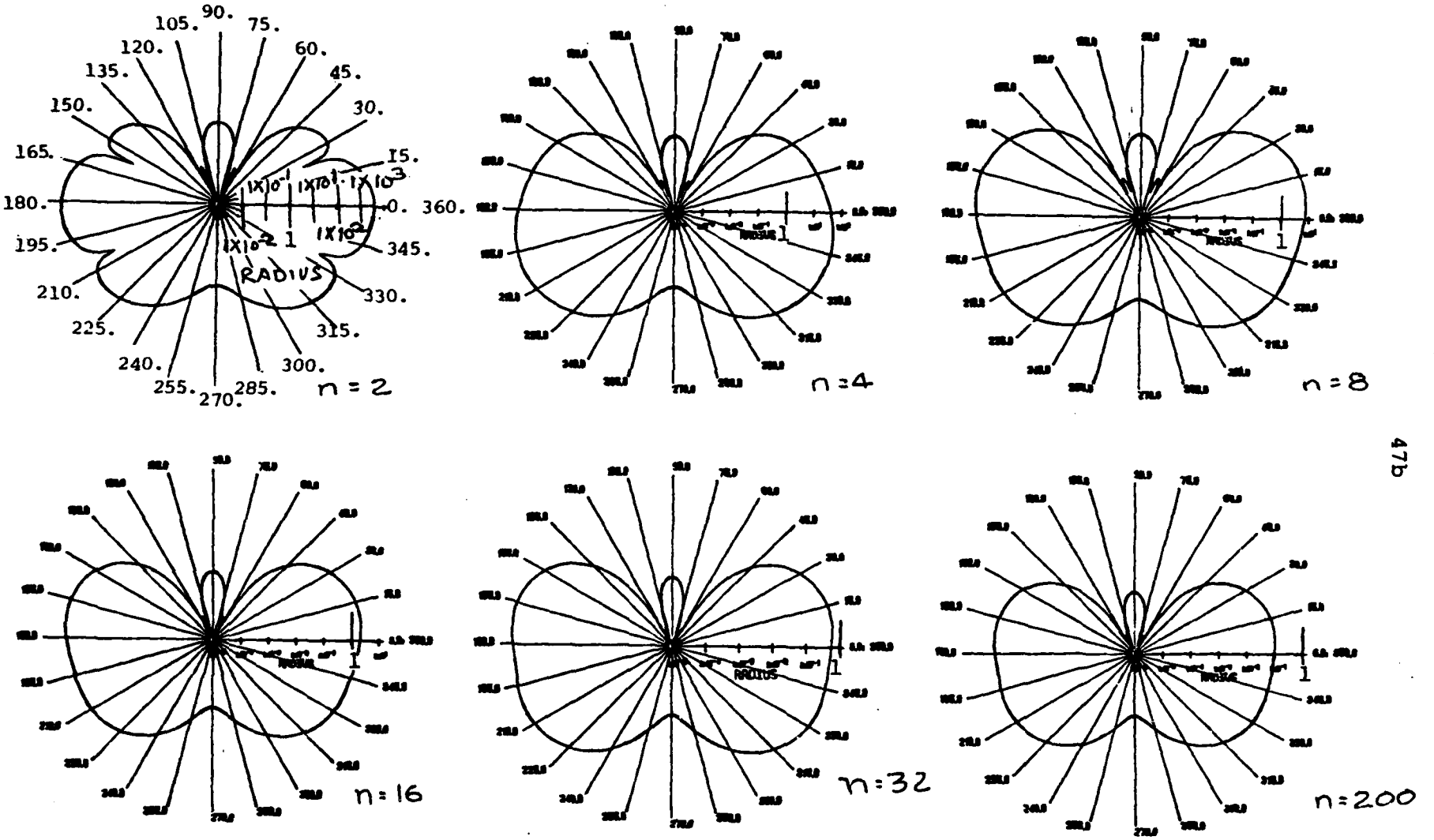

Fig. 46. SNR_o versus angle, when covariance matrix is estimated from arriving signals, with two Interferers of $N_I = 10^3$W at 70° and 120°, for averaging over 2,4,8,16,32, and 200 samples. (N_a = 0.1W, S = 1W at 1°)

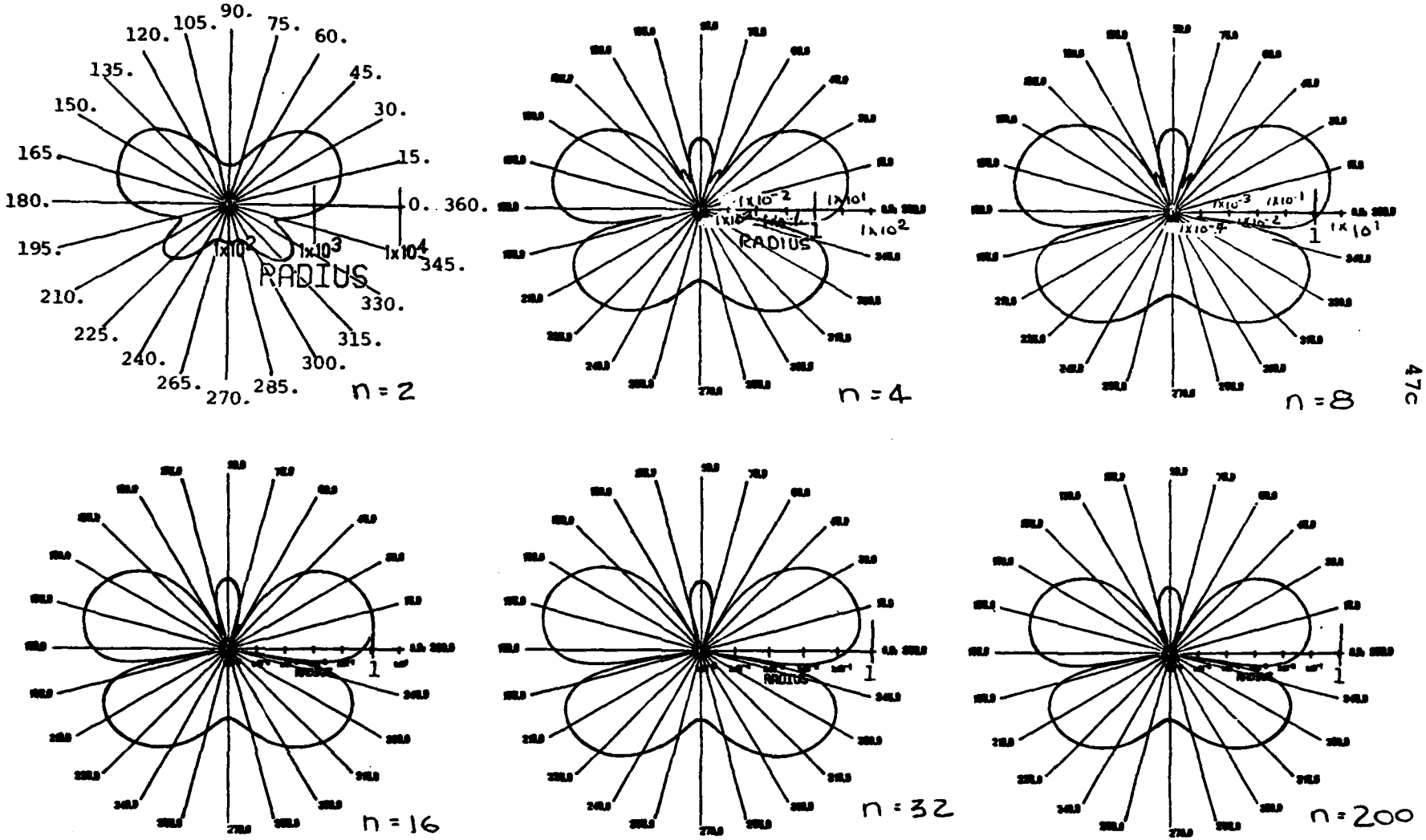

Fig. 47. SNR_o versus angle, when covariance matrix is estimated from arriving signals, with three Interferers of $N_I = 10^3$W at 70°, 120°, and 190° for averaging over 2,4,8,16,32 and 200 samples. (N_a = 0.1W, S = 1W at 1°)

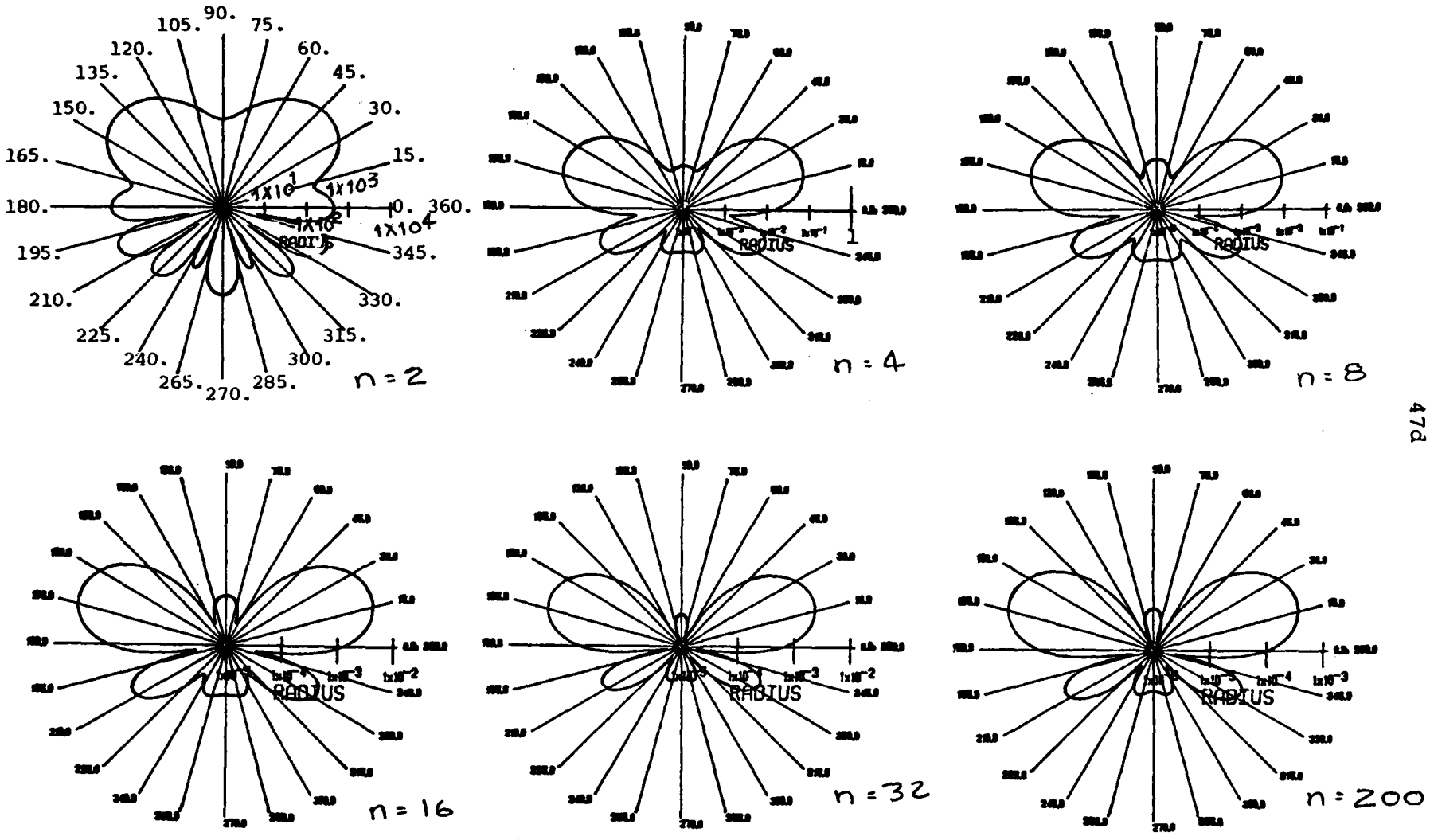

Fig. 48. SNR_o versus angle, when covariance matrix is estimated from arriving signals, with four Interferers of $N_I = 10^3$W at 70°, 120°, 190°, and 230°, for averaging over 2,4,8,16,32 and 200 samples. (N_a = 0.1W, S = 1W at 1°)

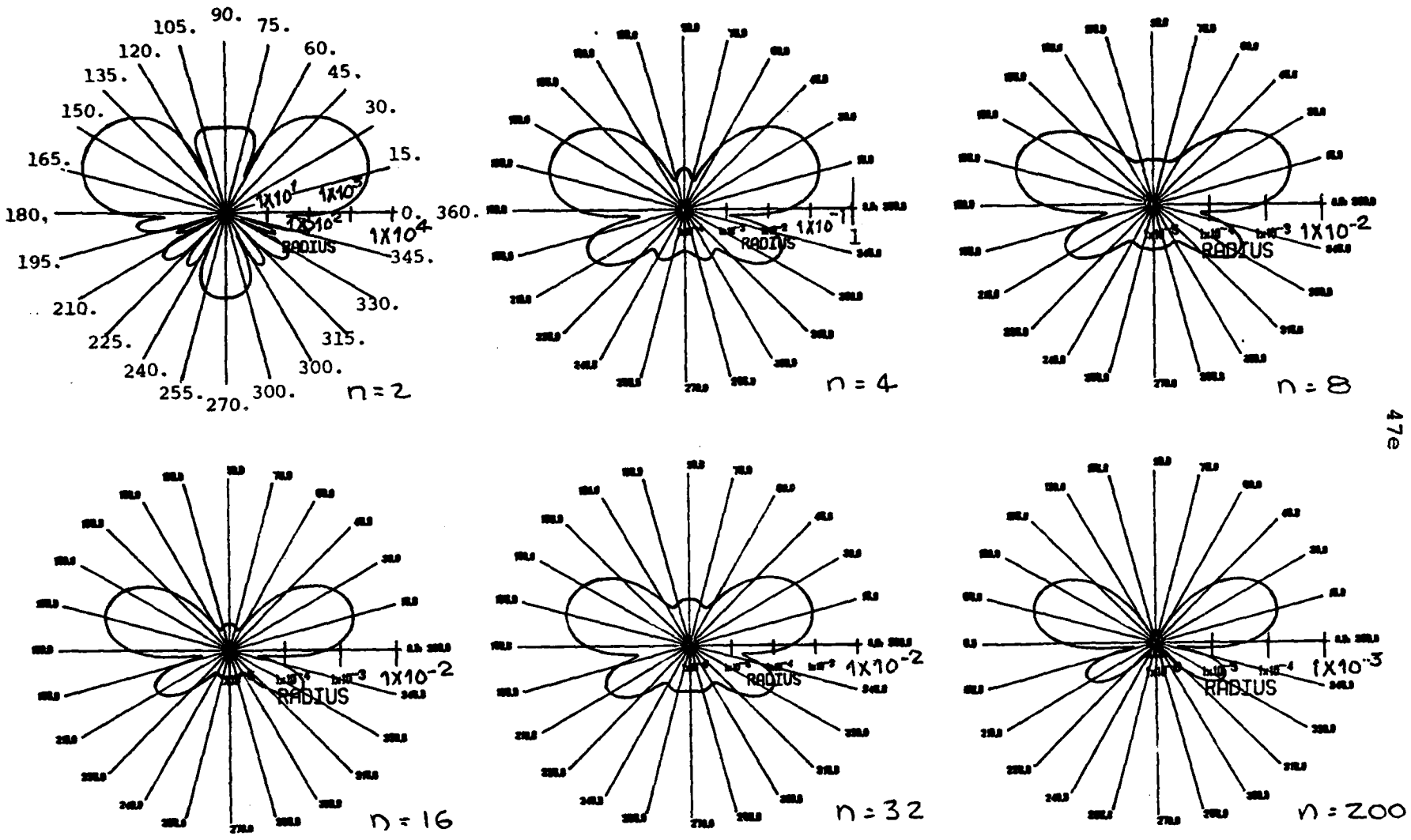

Fig. 49. SNR_o versus angle, when covariance matrix is estimated from arriving signals, with five Interferers of $N_I = 10^3$W at 70°, 120°, 190°, 230°, and 290°, for averaging over 2,4,8,16,32, and 200 samples. (N_a = 0.1W, S = 1W at 1°)

SNR_o of 208, calculated by dividing the peak value squared by the computed variance of the off-peak values. Thus, we were able to demonstrate operation within 2.6 dB of expected, in this particular (set of 8) trials. We see, then, that, for this particular simulation an adaptive processing gain of about (30-2.6) = 27.4 dB has been demonstrated; if the 24 dB associated with the 255-long PN processing is added, a total of about 51 dB gain has been demonstrated.

Fig. 51 shows the similar results if now two 500W interferers at 67^o and 30^o are present, with other conditions the same as Fig. 50. Essentially, this demonstrates operation with multiple interferers. The ideal SNR was found to be 163; this time, during the particular 8 trials, an $SNR_o \simeq 209$ was realized, which exceeds the predicted expected value. This, of course, can happen in any small-trial case when the SNR_o of concern is actually a random variable.

To emphasize, in viewing Fig. 50 and Fig. 51 it must be remembered that only the time axis in the vicinity of the matched points is included, to give a representative sample of non-peak behavior. The remaining portions were exised.

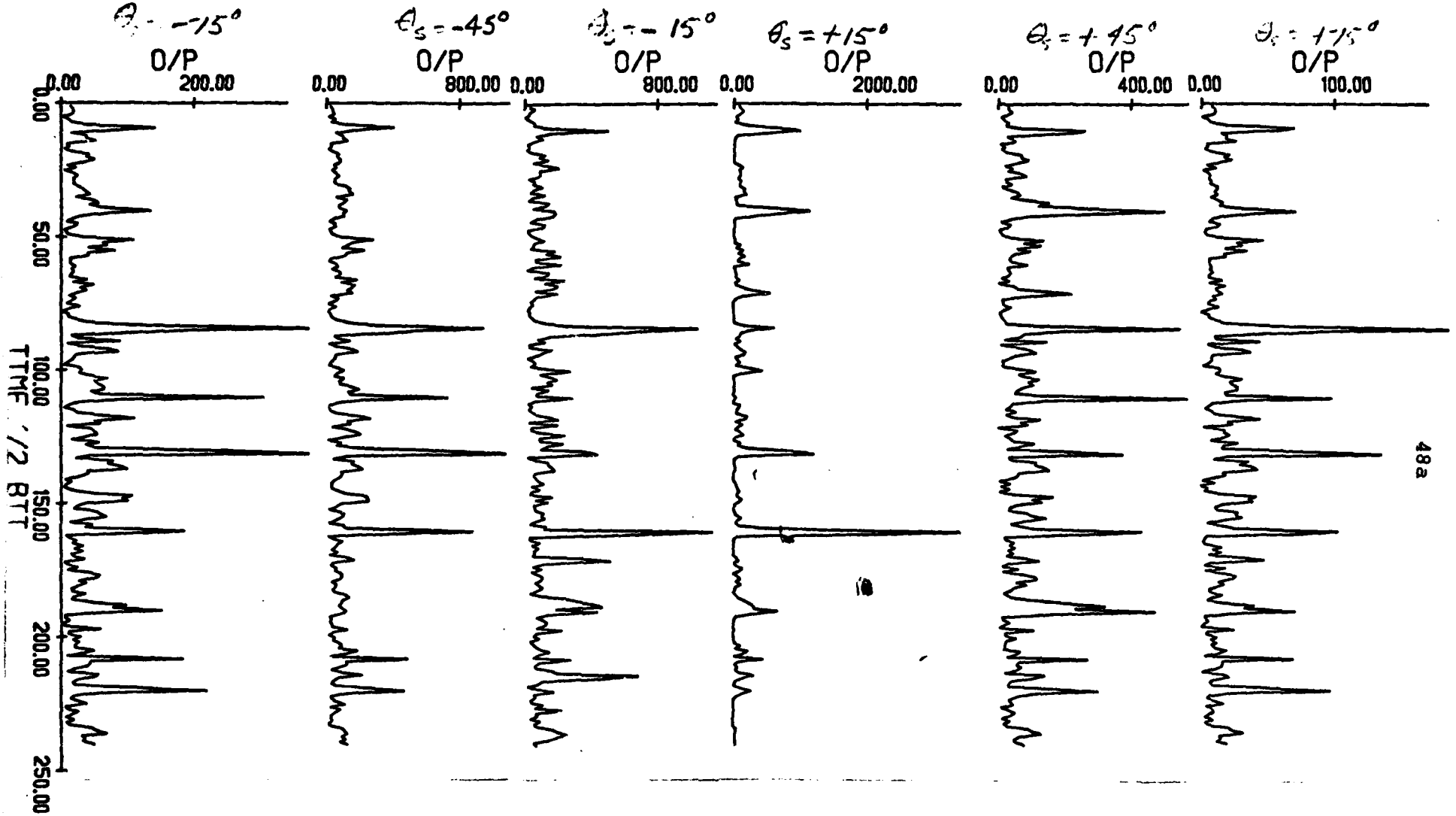

Fig. 50. Time axis output for 8 signal epochs from simulation with one Interferer of 10^3W at 67° and S = 1W at 15°; for 6 outputs corresponding to six steering vectors, showing behavior only in vicinity of peak.

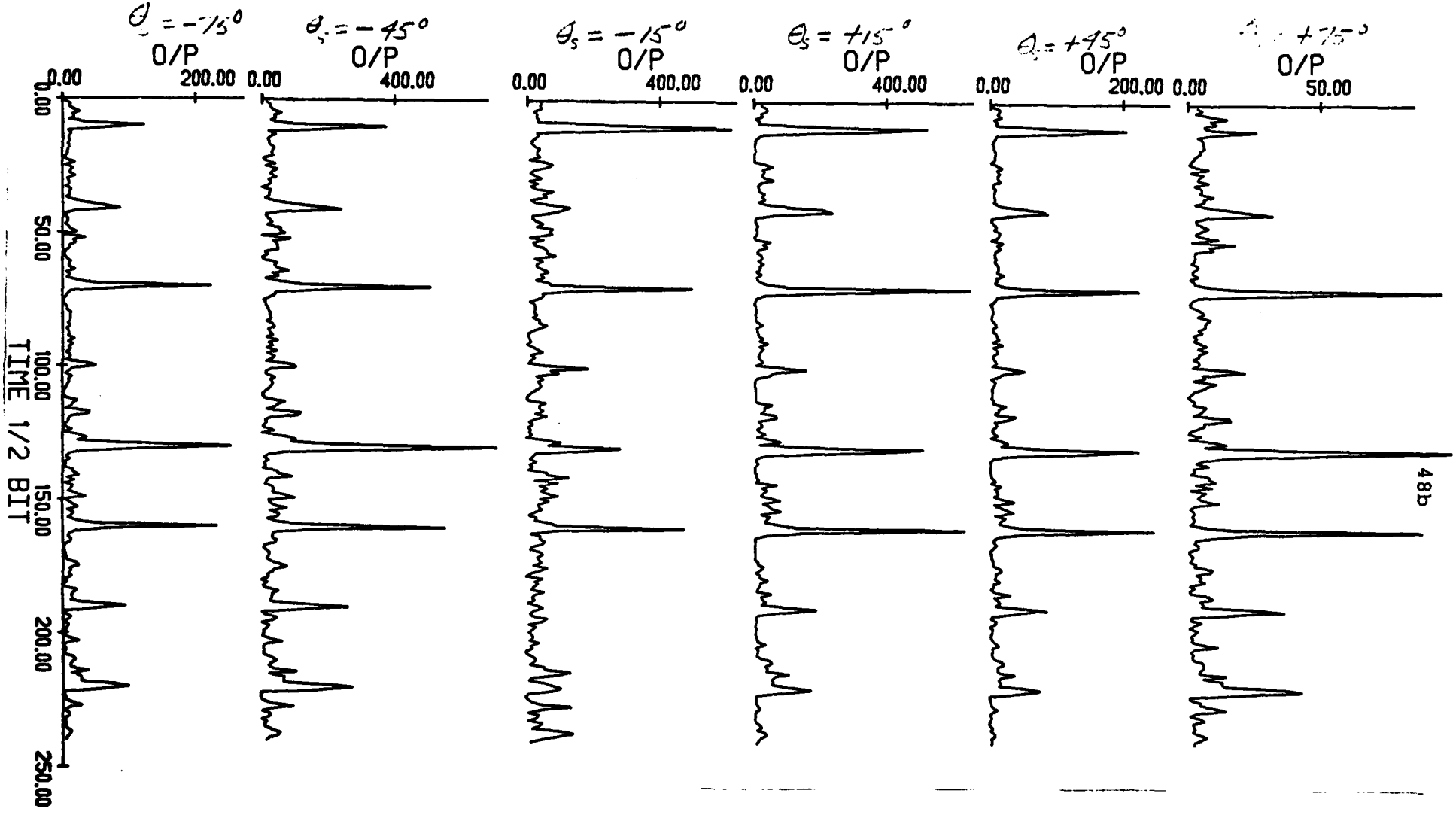

Fig. 51. Time axis output for 8 signal epochs from simulation, with two Interferers of 500W each at 17° and 30° and S = 1W at 15°, for 6 outputs corresponding to six steering vectors, showing behavior only in vicinity of peak.

7. Summary

This section complements the Abstract and Summary (p. i.) by reviewing the basic issues in light of the results described above.

A particular problem in space-time processing is the enhancement of the signal radiated from a "signal" point source at unknown distance and direction, and the suppression of one or more signals radiated from "interferer" point sources, together with the supppresssion of directionless "ambient" noise. The use of multi-element point receivers (an array) for directional selectivity, and the use of coded signals for source selectivity are two of the major design tools in creating systems that will have high space-time processing gain.

It is well known that, for mathmatical "optimization", one should treat both time and spatial processing as an integral nondifferentiated processing. However, the two proceses are separated here for ease of implementation.

The spatial processing operates to reduce the system gain to each and every point source, making no use of the time character of such sources; of course the time character is usually unknown. The time processing uses the time character of the "signal" source to distinguish it from the other souces. Something has to be done to prevent the space processing from reducing the gain to the "signal" source. Thus the traditional style system, with the spatial-processing first, is forced to violate the separation of time-and space-processing or be doomed to defeat. The time-processing-first system proposed

and discussed here attempts to overcome this problem by sorting out the "signal" source first (using a matched filter), and passing waveforms on to the space-processor in separated sets, one set containing nothing from the "signal" source, and a smaller set containing waveforms from the "signal" source, and a smaller set containing waveforms from all sources but with the signal source greatly enhanced. The idea is that the space processor "tunes up" on the waveform set that does not contain the signal source, and then applies that tuning to the set of waveforms containing the signal as well, thereby reducing the system gain to the non-signal sources, but retaining the gain to the signal source. However, the time-processing can only do the separation in an iterative hypothesis-testing fashion; i.e., it asks the subsequent space-processor "what would the output be if this set were signal free and this other set were to have the signal in it?" The actual operation achieves the gain of a joint time and space decision maker, and reflects the added complexity of joint time-space search.

The advantage of the time-processing-first configuration is that it is an open-loop. It is a well known folk theorem that open loop systems have a lower performance threshold than corresponding closed loop systems; that is, at low values of whatever limits their performance, usually some SNR or power ratio, the open loop system will continue to perform well while the closed loop system fails.

The effort here has demonstrated the expected perform-

ance of the PN matched filter followed by an SMI spatial processing. Steady-state performance has been emphasized. This initaial evaluation was limited to studying a 4-element linear array with $\lambda/2$ spacing, and consisted first of writing the classical matrix equations for the performance of the SMI algorithm with multiple apriori steering vectors. We defined the array performance measure in terms of the output signal-to-noise ratio, SNR_o, under the assumption that the steering vector is pointed in the direction of each angle considered. The input quantities for this array performance-measure calculation were the matched-filter-output signal and ambient noise powers, and the interferer powers and directions. These quantities were used to compute a deterministic noise covariance matrix, which was then inverted and multiplied by the particular steering vector needed for each angle.

This optimum SNR_o performance measure versus angle for the array processing was programmed using BASIC language, for use on our own internal minicomputer. A variety of interferer cases were run and studied to ascertain optimum performance.

An altered version of this program permitted studying the theoretical output SNR_o versus angle when only a small number of steering vectors are used. This permitted studying the relation between the nulls from the steering vector and those from the interferers. It was concluded that if 4 parallel steering vectors are used, along with a decision algorithm that responds to the highest SNR_o, one can provide SNR_o versus angle behavior that is nearly omni-directional except for the angles immediately on or

adjacent to the interferer angles.

Another large computer program was written, using FORTRAN language, and run on the large time-shared computer, that demonstrated the entire operation studied here, including the matched filter, covariance matrix estimation and inversion, and SMI processing. We used this program, for a few interferer cases, to demonstrate the entire operation under realistic conditions where the covariance matrix must be estimated from arriving matched-filter output samples.

In this simulation a PN matched-filter of length 255 was used for the temporal processing, and a 4-element linear array spaced at $\lambda/2$ was used. Six apriori steering vectors were used, placed at angles of $\pm 15^{\circ}$ $\pm 45^{\circ}$ and $\pm 75^{\circ}$ from broadside. The adaptive array output for each of these was computed on a sliding window basis. The outputs are compared, with a threshold, looking for signal peaks. An estimated output SNR (based on a limited number of noise samples) was also calculated for each steering vector.

The desired signal consisted of 2 or more periods of a 255 bit maximal sequence. This signal was assumed to phase modulate a UHF carrier. The source was assumed to be located at $\pm 15^{\circ}$, which corresponds to one of the apriori steering vectors. The phase of the received signal at each antenna element was calculated. The computer was used to generate the complex samples of the demodulated signal for each antenna at the rare of 4 complex samples per sequence bit. Similar complex samples for the interference and ambient noise were added to the signal samples.

The matched filter outputs for filters consisting of one period of the sequence were calculated for the in-phase and quadrature component at each antenna element on a sliding window basis. The window moves in increments of a sequence bit to avoid missing a signal peak. The resulting set of complex numbers are the signal inputs to the adaptive array processing.

One or two interfering sources were simulated by random number generators. They were assumed to transmit carriers phase and amplitude modulated by Gaussian moise. For assumed interference source powers and source positions, the received amplitudes and phases were calculated. Corresponding random in-phase and quadrature demodulated interference samples were generated in the computer and added to the corresponding received signal samples. For each antenna element, independent in-phase and quadrative samples of Gaussian noise, representing ambient noise, were also generated and added to the signal samples.

The signal-free complex noise samples for caluclating each sample covariance matrix were obtained from the outputs of the matched filter with the window displaced from the correct matched signal output. From 1 to 200 samples of the covariance matrix were calculated and averaged to investigate the effect of the number of samples used in the estimate of the covariance matrix.

The estimated covariance matrix was obtained by averaging the sample matrices. It was then inverted and multiplied by one of the apriori steering vectors to find one set of combining weights. The matched filter signal output was combined using these weights as one possible signal output. This process was repeated

for each of the 6 assumed steering vectors. The complete process from finding a new matrix to calculating 6 more possible signal outputs was repeated continously on a sliding window basis.

With this simulation we verified the fact that one needs only about $2K = 8$ consequetive samples to estimate the covariance matrix. The resulting output demonstrated processing that was within 3 dB of predicted. Since interferers of 10^3W and a signal of one watt was used, an array gain of 30 dB was expected. The simulation resulted in an array gain of 27 dB which, along with the 24 dB gain of the matched filter, results in a demonstrated 57 dB of anti-interference processing gain.

The general conclusion of the above predecessor effort is that using the method evolved here, including the 4 parallel steering vectors, may likely be the best way to combine PN waveform processing and adaptive array processing. The advantages are: 1) the combination does not initially (before sync) attempt to null the signal, but offers immediately the full combined processing gain; 2) the response to either signal turn-on or interferer variation is near instantaneous, and does not depend on loop time-constants; 3) there is no constraining relation between interferer size and time-response, as there is for a closed-loop system; 4) the de-correlation of wide-band interferers, at array input, is signifi-cantly reduced; 5) there is no "great race" problem between modem synchronization and array nulling, as there is when a PN reference is used in a closed-loop; and 6) the technique here should be more resistant to specific and determined interferer attacks (such as blinking).

It is recommended that the potential exhibited by these results be exploited by further study. In particular, it is recommended that the performance evaluation begun here be generalized and refined, and that the implementation aspects of this technique be determined.

APPENDIX A

Review of Linear Beamformer Notation and Theory Notation

by T. G. Birdsall

1) Let * denote conjugate and T represent vector or matrix transpose

2) Let y or y(t) be the column vector of instantaneous inputs, or the complex demodulation of the inputs.

$$y^T = (y_1, y_2, \ldots y_k) \tag{A.1}$$

3) In the absence of signal, i.e., when the input is ambient noise plus interferers, let M be the autocovariance matrix of the input. We assume M is positive definite

$$M = E(yy^{*T}) = \left[E(y_i y_j^{*T})\right] \tag{A.2}$$

M is hermetian, i.e.,

$$M^{*T} = M, \quad (M^{-1})^{*T} = M^{-1} \tag{A.3}$$

4) In the absence of interferers, i.e., just in ambient noise, we assume

$$M = aI \tag{A.4}$$

5) A linear beamformer uses weights to obtain a single number for each "steering direction"

$$W^T = (W_1, W_2, \ldots W_k) \tag{A.5}$$

For a given set of weights the beamformer output Z is

$$Z = W \cdot y = W^{*T} y \qquad (A.6)$$

Single-Look SKEA+KGN Theory

The theory of signal detectability provides a guide in the form of a solution if the signal were known exactly except for amplitude and if the noise were wide-sense-stationary gaussian noise with zero mean and known autocovariance M. It states that if V_θ is a unit vector proportional to the input if it were caused by a signal from direction θ, (in the absence of noise) then the weights to be used in the presence of noise should be proportional to

$$W_\theta = M^{-1} V_\theta \qquad (A.7)$$

Performance Evaluation:

A common array characterization is the beam pattern resulting from a fixed set of weights, plotted versus the direction of arrival of a unit signal. Let θ be the direction used in setting the weights, and ϕ be the actual signal direction.

$$\text{beam pattern} = W_\theta^{*T} V_\phi = V_\theta^{*T} M^{-1} V_\phi \qquad (A.8)$$

The beam pattern is conjugate symmetric in the two angles θ and ϕ, and gives the designer or evaluator a measure of beam width and sidelobe levels.

More direct characterizations of the beamformer performance when the signal direction is known (or hypothesized) would be the beam output due to signal, the beam output power due to noise, or the signal-to-noise ratio, each plotted versus the direction of arrival of the desired signal. All three of these plots are identical when the weights

$$W_\theta = M^{-1}V_\theta \qquad (A.7)$$

are used, and when the actual direction coincides with the steered direction. This all-purpose pattern is called the PEP, the performance evaluation pattern, P_θ.

$$P_\theta = V_\theta^{*T}M^{-1}V_\theta \qquad (A.9)$$

These properties will be quickly proved.

(a) P_θ = beam output magnitude for unit signal in steered direction

(proof: by (A.8) P_θ is the beam output. It is real and positive because M^{-1} is positive definite)

(b) P_θ = mean-square beam noise output.

(proof: $E(|z|^2 \text{ no signal}) = E(zz^{*T})$

$= E(W^{*T}yy^{*T}W) = W^{*T}MW$

$= V_\theta^{*T}M^{-1}MM^{-1}V_\theta = V_\theta^{*T}M^{-1}V_\theta$

(c) P_θ = beam output signal-to-noise power ratio

(proof: From (a), P_θ is the beam output magnitude due to the signal in the steered direction, so P_θ^2 is the beam output signal power; from (b), P_θ is the noise power; hence SNR = $P_\theta^2 / P_\theta = P_\theta$).

Spatial Whitening

Although theoreticians love the weights given by (A.7) because of the triple property of the P.E.P. P_θ, it is often more practical to adjust the weights so that the noise on the beam output is independent of the steered direction. This is known as spatial whitening

For spatial whitening

$$W_\theta = \frac{M^{-1}V_\theta}{\sqrt{P_\theta}} = \frac{M^{-1}V_\theta}{\sqrt{V_\theta^{*T} M^{-1} V_\theta}} \qquad \text{(A.10)}$$

These weights are just as optimum as those given by (A.7) since the theory only said the weights must be proportional to those of (A.7). If the weights of (A.10) are used the 3 performance statistics are

$$\left.\begin{array}{l} \text{Beam output magnitude for unit signal in steered direction} = \sqrt{P_\theta} \\ \text{Beam output mean-squared noise} = 1 \\ \text{Beam output SNR} = P_\theta \end{array}\right\} \text{(A.11)}$$

Example: Linear Uniform Array, Single Interferer plus Ambient, Narrowband

Consider a k-element array of uniformly spaced receivers, and a unit arrival from radians off endfire, $0 \leq \theta \leq \pi$

$$y_{n+1}(t) = y_1(t - \frac{nd\cos\theta}{c}) \qquad (A.12)$$

where d is the element spacing and c is the speed of propagation.

Model the narrowband signal as a complex phaser

$$y_1(t) = g(t)e^{j(2\pi fct+\phi(t))} \qquad (A.13)$$

$$y_{n+1}(t) = g(t-\frac{ndcos\theta}{c})\ e^{j(2\pi fct - \frac{2\pi fcndcos\theta}{c})}\ e^{j\phi(t-\frac{ndcos\theta}{c})} \qquad (A.14)$$

The usual "narrowband assumption" is that the array delays, ndcosx/c, can be neglected in the amplitude and phase modulation arguments, so

$$y_{n+1}(t) = g(t)e^{j(2\pi fct+\phi(t))}e^{-j2\pi fcnd\ cos\theta/c} \qquad (A.15)$$

For brevity we define the "electrical phase",

$$\bar{\theta} = 2\pi fcd\ cos\theta/c \qquad (A.16)$$

So

$$y_n(t) = y_1(t)e^{-j(n-1)\bar{\theta}} \qquad (A.17)$$

When $d \leq c/2fc$, (A.16) may be inverted to find the physical θ from the electrical $\bar{\theta}$.

All this was done so that V_θ, "a unit vector in (electrical) direction $\bar{\theta}$", could be made explicit

$$V_\theta = \frac{1}{\sqrt{k}} \begin{bmatrix} 1 \\ e^{-j\bar{\theta}} \\ e^{-j2\bar{\theta}} \\ \cdot \\ \cdot \\ \cdot \\ e^{-j(k-1)\bar{\theta}} \end{bmatrix} \qquad (A.18)$$

The entire arrival from physical direction θ and electrical direction $\bar{\theta}$ is the vector valued time function

$$y(t) = \sqrt{k}\, V_\theta\, y_1(t) \qquad (A.19)$$

where V_θ specifies the space effects and $y_1(t)$ the time-effects. The spatial autocovariance is

$$M = E(y(t)y^{*T}(t)) = V_\theta V_\theta^{*T} E\,|y_1(t)|^2\, k \qquad (A.20)$$

For convenience we denote the matrix $V_\theta V_\theta^{*T}$ as M_θ

$$M_\theta = V_\theta V_\theta^{*T} \qquad (A.21)$$

For ambiant noise of power a, plus a simple interference with power b from direction θ, the input autocovariance is

$$M = aI + bM_\theta \tag{A.22}$$

This is a very simple autocovariance. We point out that

$$|V_\theta|^2 = 1 \rightarrow M_\theta^2 = V_\theta V_\theta^{*T} V_\theta V_\theta^{*T} = V_\theta V_\theta^{*T} = M_\theta \tag{A.23}$$

M_θ does not have an inverse, but with the ambient noise, M does have an inverse

$$M^{-1} = a^{-1}\left[I - \frac{b}{a+b} M_\theta\right] \tag{A.24}$$

The weights for steering (signal) direction ϕ are

$$W_\phi = M^{-1}V_\phi = a^{-1}\left[V_\phi - \frac{b}{a+b} V_\phi V_\phi^{*T} V_\phi\right] \tag{A.25}$$

Now

$$V_\phi^{*T} V_\phi = \frac{1}{k} \sum_{n=0}^{k-1} e^{j(\bar{\theta}-\bar{\phi})} = e^{jk(\bar{\theta}-\bar{\phi})/2} \sin(\tfrac{k}{2}(\bar{\theta}-\bar{\phi}))/\sin(\tfrac{1}{2}(\bar{\theta}-\bar{\phi})) \tag{A.26}$$

This is the well-known beam pattern for the uniform line array Let us give it a symbol

$$\text{Def} \qquad B(x) = e^{jkx/2} \sin(\tfrac{kx}{2})/k \sin(\tfrac{x}{2}) \tag{A.27}$$

So

$$V_\theta^{*T} V_\phi = B(\bar{\theta}-\bar{\phi}) \tag{A.28}$$

and

$$W_\phi = a^{-1}\left[V_\phi - \frac{b}{a+b} B(\bar{\theta}-\bar{\phi}) V_\theta\right] \qquad (A.29)$$

This has the intuitive sense of pointing toward ϕ and away from θ.

The performance evaluation pattern is

$$P_\phi = V_\phi^{*T} W_\phi = a^{-1}\left[1 - \frac{b}{a+b} B(\bar{\theta}-\bar{\phi}) V_\phi^{*T} V_\theta\right] \qquad (A.30)$$

$$P_\phi = a^{-1}\left[1 - \frac{b}{a+b} B(\bar{\theta}-\bar{\phi}) B(\bar{\phi}-\bar{\theta})\right] \qquad (A.31)$$

$$P_\phi = a^{-1}\left[1 - \frac{b}{a+b} \mid B(\bar{\theta}-\bar{\phi}) \mid^2\right] \qquad (A.32)$$

Let us summarize the example, using a non-unit signal. Let the signal have power s, and come from direction ϕ; let the ambient have power a, and the single interference come from direction θ with power b. The output signal to noise ratio is

$$SNR = \left(\frac{s}{a}\right)\left[1 - \frac{b}{a+b} \mid B(\bar{\theta}-\bar{\phi}) \mid^2\right] \qquad (A.33)$$

and the steering weights are proportional to

$$W_\phi = V_\phi - \frac{b}{a+b} B(\bar{\theta}-\bar{\phi}) V_\theta \qquad (A.34)$$

APPENDIX B

Computer Program by T. G. Birdsall

```
'LIST SCMAT5
'edit  scmat5 p=J
'scomp scmat5+r2,p+end cmat5 p=y
'end    cmat5
DIM   X(15),Y(15),U(15),V(15)  'INPUT=X+JY, OUTPUT=U+JV, MATRICES
DIM   S6(4),T6(4),S7(4),T7(4) 'INPUT & STEERING VECTORS
      P1=3.PI/180 \ P2=2*3.PI
 50   PRINT\PRINT\PRINT\PRINT "CMAT5 (T0315APRIL81)"
      PRINT "4 ELEMENT UNIFORM LINE ARRAY, .5 WAVELENGTH SPACING"
      PRINT "CMAT5 COMPUTES BEAM PATTERNS WITH NOISE-NORMED STEERING"
      C0=.5
      FOR E=0 TO 15 \ X(E)=0 \ Y(E)=0 \ NEXT E
      PRINT "INTERFERENCE AUTOCORRELATION MATRIX, R, IS COMPLEX, ";
      PRINT "HERMETIAN, & TOPLITZ"
      PRINT "  THE SUM OF V V^*T FROM STRONG DIRECTIONAL SIGNALS, AND"
      PRINT "  A UNIT IDENTITY DUE TO NON-DIRECTIONAL AMBIENT NOISE."
      PRINT "THE STEERING VECTOR OF RECEPTION S (SIGNAL ONLY) IS"
      PRINT "  W =  R-INVERSE-CONJUGATE  S"
      PRINT "THE PERFORMANCE PATTERN IS  W DOT S  FOR ALL DIRECTIONS S"
      PRINT "THE NORMED STEERING IS  W / SQROOT(W DOT S)"
      PRINT\PRINT "AMBIENT LEVEL = 1 AT EACH SENSOR, I.I.D."
      FOR E=0 TO 15 STEP 5 \ X(E)=1 \ NEXT E
      PRINT "PLEASE DESCRIBE THE DIRECTIONAL INTERFERENCE"
 70   PRINT "NUMBER OF SOURCES =";\INPUT N7
      FOR I=1 TO N7
      PRINT "POWER, DIRECTION ANGLE : ";\INPUT J, A
      A1=P2*C0*COS(P1*A) \ A2=A1/P1
      FOR R=1 TO 4 \ FOR C=1 TO 4 \ E=4*R+C-5 \ A3=(C-R)*A1
      X(E)=X(E)+J*COS(A3) \ Y(E)=Y(E)+J*SIN(A3) \ NEXT C \ NEXT R
      NEXT I

100   FOR E=0 TO 15 \ U(E)=0 \ V(E)=0 \ NEXT E   'SET U+JV=IDENTITY
      FOR E=0 TO 15 STEP 5 \ U(E)=1 \ NEXT E

      'BIG STEP IS TO INVERT R, THEN CONJUGATE RESULT
      '1ST PHASE, FORM LOWER TRIANGLE ZEROS
200   FOR R=1 TO 4
      'NORMALIZE SO DIAG ELEMENT = 1
      E=5*R-5 \ N=R \ A=X(E) \ B=Y(E) \ GOSUB 600
      'CREATE ZEROS BELOW THAT 1
      M=R \ FOR N=R+1 TO 4 \ E=4*N+M-5 \A=X(E) \B=Y(E) \GOSUB 500 \ N. XT
      NEXT R
      '2ND PHASE, FORM UPPER TRIANGLE ZEROS
      FOR C=4 TO 2 STEP -1 \ FOR R=1 TO C-1 \ E=4*R+C-5
      N=R \ M=C \ A=X(E) \ B=Y(E) \ GOSUB 500
      NEXT R \ NEXT C
      'NOW CONJUGATE RESULT
      FOR E=0 TO 15 \ V(E)=-V(E) \ NEXT E

300   PRINT\PRINT "STEERING ANGLE START, STOP, STEP =";\INPUT Z1,Z2,Z.
      PRINT "CALC ANGLE START, STOP, STEP =";\INPUT N1,N2,N3\PRINT
      FOR A=Z1 TO Z2 STEP Z3
       PRINT "STEERING ANGLE ="%;A
       PRINT "UNNORMED WEIGHT VECTOR:"
       PRINT "REAL","IMAG","MAG","PHASE (DEG)"
       GOSUB 400 'S7+JT7 IS WEIGHTS, R8 AT A8 IS PERFORMANCE
       FOR I=1 TO 4 \ X9=S7(I) \ Y9=T7(I) \ GOSUB 3300 \ A9=360*A9
        PRINT %8.05;X9,Y9,R9, %6.02;A9 \ NEXT I
```

```
        PRINT "PERFORMANCE MEASURE = "%8.05;R8;"AT ";%6.02;A8;"DEG"\
        PRINT "NORMED WEIGHT VECTOR USED IN BEAM PATTERN IS"
        PRINT "REAL","IMAG","MAG","PHASE"
        R0=SQR(R0)
        FOR I=1 TO 4 \ S7(I)=S7(I)/R8 \ T7(I)=T7(I)/R8
         X9=S7(I) \ Y9=T7(I) \ GOSUB 3800 \ A9=360*A9
         PRINT %8.05;X9,Y9,R9, %6.02;A9 \ NEXT I
       PRINT "- - -(BEAM POWER PATTERN)- - -"
       PRINT "ANGLE","POWER GAIN"
       FOR B=A1 TO A2 STEP A3 \ B1=P2*C0*COS(P1*B)
        FOR I=1 TO 4 \ S6(I)=COS((I-1)*B1) \ T6(I)=SIN((I-1)*B1) \ NEXT I
        GOSUB 600 'CALC THE DOT PRODUCT
        PRINT %;B, %8.05;R8*R8
       NEXT B \ PRINT \ NEXT A
390    PRINT "1=>MORE ANGLES, 2=>CHANGE INTERFERENCE : ";\INPUT Q
       IF Q=1 THEN 380 \ IF Q=2 THEN 50 \ GOTO 390

'SUB400 FINDS THE WEIGHTS & ON-BEAM DOT PRODUCT, THE PERFORMANCE EVALUAT
400    A1=P2*C0*COS(P1*A) \ A2=A1/P1  'A1 IS RAD, A2 IS DEG, (ELEC PHA )
       FOR I=1 TO 4 \ S6(I)=COS((I-1)*A1) \ T6(I)=SIN((I-1)*A1) \ NEXT I
       GOSUB 700 \ GOSUB 500  'FIND STEERING VECTOR AND DOT PRODUCT
       RETURN

'SUB500   ROW N = ROW N  - (A+JB) * ROW M     N=/=M
500    FOR C5=1 TO 4 \ E1=4*N+C5-5 \ E2=4*M+C5-5
       X(E1)=X(E1)-A*X(E2)+B*Y(E2)
       Y(E1)=Y(E1)-A*Y(E2)-B*X(E2)
       U(E1)=U(E1)-A*U(E2)+B*V(E2)
       V(E1)=V(E1)-A*V(E2)-B*U(E2)
       NEXT C5 \ RETURN

'SUB600   DIVIDE ROW N  BY  A+JB
600    Z6=A*A+B+B \ A6=A/Z6 \ B6=-B/Z6  'A6+JB6 = 1/ A+JB
       FOR C6=1 TO 4 \ E=4*N+C6-5
       'OLD VALUE = S6+J T6, NEW VALUE = S7+J T7
       S6=X(E) \ T6=Y(E) \ GOSUB 660 \ X(E)=S7 \ Y(E)=T7
       S6=U(E) \ T6=V(E) \ GOSUB 660 \ U(E)=S7 \ V(E)=T7
       NEXT C6 \ RETURN
660    S7=A6*S6-B6*T6 \ T7=A6*T6+B6*S6 \ RETURN

'SUB700   MATRIX  U+J V  *  VECTOR  S6+J T6 = VECTOR  S7+J T7
'         VECTOR  S6+J T6   IS UNCHANGED
700    FOR R=1 TO 4 \ R1=4*R-5 \ S7(R)=0 \ T7(R)=0
       FOR C=1 TO 4 \ E=R1+C
         S7(R)=S7(R)+U(E)*S6(C)-V(E)*T6(C)
         T7(R)=T7(R)+V(E)*S6(C)+U(E)*T6(C)
       NEXT C \ NEXT R \ RETURN

'SUB800   X9+J Y9 =  VECTOR  (S6+J T6)  DOT  (S7+J T7)
'         RETURN   X9 + J Y9  AS  R9 AT A8 DEGREES
800    X9=0 \ Y9=0 \ FOR I=1 TO 4
       X9=X9+S6(I)*S7(I)+T6(I)*T7(I)
       Y9=Y9+S6(I)*T7(I)-T6(I)*S7(I) \ NEXT I
       GOSUB 3800 \ R8=R9 \ A8=360*A9 \ RETURN

'CONTINUE WITH MAIN PROG*END     SUB3800 IN MAP
```

REFERENCES

1. William F. Gabriel, "Adaptive Arrays - An Introduction," Proc. IEEE, Vol. 64, No. 2, February 1976.

2. Ralph T. Compton, Jr., "An Adaptive Array in a Spread-Spectrum Communication System," Proc. IEEE, Vol. 66, No. 3, March 1978.

3. G. H. Piesinger, "Active Reference Null Steering for Spread Spectrum Signals," IEEE International Conference on Communications, 1977.

4. L. J. Ricardi, A Summary of Methods for Producing Nulls in an Antenna Radiation Pattern, Technical Note 1976-38, Lincoln Laboratory, Massachusetts Institute of Technology, Lexington, Massachusetts, September 2, 1976.

5. M. E. Somin, et al., Wide Bandwidth Array Techniques, Final Report for period February 1979 - July 1980 Hazeltine Corporation, Greenlawn, New York, August 1980.

6. Larry L. Horowitz, et al., "Controlling Adaptive Antenna Arrays with the Sample Matrix Inversion Algorithm," IEEE Transactions on Aerospace and Electronic Systems, Vol. AES-15, No. 6, November 1979.

7. M. P. Ristenbatt and E. K. Holland-Moritz, "PN Matched Filters in Adaptive Arrays," NTC'78 Conference Record, Vol. 3, IEEE Catalog No. 78CH1354-0-CSCB, December 1978.

8. M. P. Ristenbatt, "Pseudo-Random Binary Coded Waveforms," Chapter 4, Modern Radar - Analysis, Evaluation, and System Design, ed. by Raymond S. Berkowitz, John Wiley & Sons, Inc., New York, New York, 1965.

9. I. S. Reed, et al., "Rapid Convergence Rate in Adaptive Arrays," IEEE Transactions on Aerospace and Electronic Systems, Vol. AES-10, No. 6, November 1974.

10. R. T. Compton, Jr., "The Power-Inversion Adaptive Array: Concept and Performance," IEEE Transactions on Aerospace and Electronic Systems, Vol. AES-15, No. 6, November 1979.

11. D. M. Boroson, "Sample Size Considerations for Adaptive Arrays," IEEE Transactions on Aerospace and Electronic Systems, Vol. AES-16, No. 4, July 1980.

REFERENCES (Cont.)

12. T. G. Birdsall, Internal Memo to ARO Project, April 10, 1981.

13. T. G. Birdsall, Internal Memo to ARO Project, June 24, 1981.

14. T. G. Birdsall, Internal Memo to ARO Project, July 27, 1981.

Unclassified

SECURITY CLASSIFICATION OF THIS PAGE (When Data Entered)

REPORT DOCUMENTATION PAGE	READ INSTRUCTIONS BEFORE COMPLETING FORM
1. REPORT NUMBER: 017818-F	2. GOVT ACCESSION NO.: AD-A112 114
3. RECIPIENT'S CATALOG NUMBER:	
4. TITLE (and Subtitle): PN MATCHED FILTERS IN ADAPTIVE ARRAYS	5. TYPE OF REPORT & PERIOD COVERED: Final Report
	6. PERFORMING ORG. REPORT NUMBER:
7. AUTHOR(s): M. P. Ristenbatt, T. G. Birdsall, E. Holland-Moritz	8. CONTRACT OR GRANT NUMBER(s): DAAG29-79-C-0220
9. PERFORMING ORGANIZATION NAME AND ADDRESS: Cooley Electronics Laboratory, University of Michigan, Ann Arbor, Michigan 48109	10. PROGRAM ELEMENT, PROJECT, TASK AREA & WORK UNIT NUMBERS:
11. CONTROLLING OFFICE NAME AND ADDRESS: U. S. Army Research Office, P. O. Box 12211, Research Triangle Park, N. C. 27709	12. REPORT DATE: September 1981 13. NUMBER OF PAGES: 124
14. MONITORING AGENCY NAME & ADDRESS (if different from Controlling Office)	15. SECURITY CLASS. (of this report): Unclassified 15a. DECLASSIFICATION/DOWNGRADING SCHEDULE:

16. DISTRIBUTION STATEMENT (of this Report)

Approved for public release; distribution unlimited.

17. DISTRIBUTION STATEMENT (of the abstract entered in Block 20, if different from Report)

NA

18. SUPPLEMENTARY NOTES

The view, opinions, and/or findings contained in this report are those of the authors and should not be construed as an official department of the Army position, policy, or decision unless so disignated by other documentation.

19. KEY WORDS (Continue on reverse side if necessary and identify by block number)

Spread spectrum
Adaptive array
AJ technique
ECCM

20. ABSTRACT (Continue on reverse side if necessary and identify by block number)

This report describes and evaluates a new way to combine pseudo-noise (PN) spread spectrum and adaptive (antenna) arrays, consisting of multiple matched filters followed by sampled matrix inversion (SMI) array processing. The evaluation of this technique was done by using a 4-element linear array and: 1) straightforward matrix calculations; 2) a computer computation of output signal-to-noise ratio; SNR_o, versus angle when the theoretically correct noise covariance matrix was used; and 3) a computer simulation/demonstration that estimated the

DD FORM 1 JAN 73 1473 EDITION OF 1 NOV 65 IS OBSOLETE S/N 0102-014-6601

SECURITY CLASSIFICATION OF THIS PAGE (When Data Entered)

noise covariance matrix from computer-generated interference samples.

An improved combined processing has been effected which can be viewed as sliding-window in both the time axis and in the spatial domain, due to the use of multiple steering vectors. The results indicate that using the method evolved here, along with the 4 parallel steering vectors, may likely be the best way to combine PN waveform processing and adaptive array processing. It is recommended that this method be further pursued, to further develope and document its advantages.


DAT
FILM